

## INFORMATION TO USERS

This was produced from a copy of a document sent to us for microfilming. While the most advanced technological means to photograph and reproduce this document have been used, the quality is heavily dependent upon the quality of the material submitted.

The following explanation of techniques is provided to help you understand markings or notations which may appear on this reproduction.

1. The sign or "target" for pages apparently lacking from the document photographed is "Missing Page(s)". If it was possible to obtain the missing page(s) or section, they are spliced into the film along with adjacent pages. This may have necessitated cutting through an image and duplicating adjacent pages to assure you of complete continuity.
2. When an image on the film is obliterated with a round black mark it is an indication that the film inspector noticed either blurred copy because of movement during exposure, or duplicate copy. Unless we meant to delete copyrighted materials that should not have been filmed, you will find a good image of the page in the adjacent frame.
3. When a map, drawing or chart, etc., is part of the material being photographed the photographer has followed a definite method in "sectioning" the material. It is customary to begin filming at the upper left hand corner of a large sheet and to continue from left to right in equal sections with small overlaps. If necessary, sectioning is continued again—beginning below the first row and continuing on until complete.
4. For any illustrations that cannot be reproduced satisfactorily by xerography, photographic prints can be purchased at additional cost and tipped into your xerographic copy. Requests can be made to our Dissertations Customer Services Department.
5. Some pages in any document may have indistinct print. In all cases we have filmed the best available copy.

University  
Microfilms  
International

300 N. ZEEB ROAD, ANN ARBOR, MI 48106  
18 BEDFORD ROW, LONDON WC1R 4EJ, ENGLAND

8014953

BASU, AMITABHA

STUDIES IN THE CHEMISTRY OF NITRO AND PHOSPHONIUM  
SUBSTITUTED BIPYRIDINES AND THEIR TRANSITION METAL  
COMPLEXES

*City University of New York*

PH.D.

1980

University  
Microfilms  
International

300 N. Zeeb Road, Ann Arbor, MI 48106

18 Bedford Row, London WC1R 4EJ, England

STUDIES IN THE CHEMISTRY OF NITRO AND PHOSPHONIUM  
SUBSTITUTED BIPYRIDINES AND THEIR TRANSITION  
METAL COMPLEXES

by

AMITABHA BASU

A dissertation submitted to the Graduate Faculty in  
Chemistry in partial fulfillment of the requirements  
for the degree of Doctor of Philosophy, The City University  
of New York.

1980

This manuscript has been read and accepted for the Graduate Faculty in Science in satisfaction of the dissertation requirement for the degree of Doctor of Philosophy.

1/21/80  
date

Michael V. Levin  
Chairman of Examining Committee

January 22, 1980  
date

David C. Locke  
Executive Officer

Juan R. Villa  
Harry D. Gfney  
Supervisory Committee

ABSTRACTSTUDIES IN THE CHEMISTRY OF NITRO AND PHOSPHONIUM  
SUBSTITUTED BIPYRIDINES AND THEIR TRANSITION  
METAL COMPLEXES

Advisor: Professor Michael Weiner

Substituted pyridines and 2,2'-bipyridines with  $\text{NO}_2$  and  $(\text{C}_2\text{H}_5)_3\text{P}^+$  groups para to the ring nitrogens have been prepared, and were used as ligands in complexes with  $\text{Fe}(\text{II})$ ,  $\text{Ru}(\text{II})$ , and  $\text{Co}(\text{II})$ . The  $\text{pK}$  values and reduction potentials of the free ligands were measured, and the results discussed in terms of the nature of the electron withdrawing effect of the two substituents. The information on the free ligands was then used to help interpret the metal  $\rightarrow$  ligand charge transfer data as well as the redox potentials for the complexes. The results obtained in this study were compared with previous attempts to evaluate substituent constants for the  $\text{NO}_2$  and  $\text{R}_3\text{P}^+$  groups. Emission spectra of the different substituted bipyridines were measured at room temperature and  $77^\circ\text{K}$  to obtain information about their energy levels which was then used to interpret the quenching rates of  $\text{Ru}(\text{Bpy})_3^{2+*}$  (Bpy = 2,2'-bipyridine) with the substituted bipyridines. The electron transfer reactions of  $^*\text{Ru}(\text{Bpy})_3^{2+}$  and  $^*\text{Ru}(\text{Et}_3\text{P}^+\text{Bpy})_3^{5+}$  with  $\text{Co}(\text{Bpy})_3^{3+}$  were studied by flash photolysis technique in an attempt to probe the effect of electron withdrawing groups on the excited state

photochemistry of  $\text{Ru}(\text{Epy})_3^{2+}$ .

ACKNOWLEDGEMENTS

I wish to express my appreciation and gratitude to Professor Michael Weiner who supervised this research. Ideas generated from our numerous discussions formed the basis of the entire work. He was always encouraging and understanding and is genuinely one of the finest mentors.

I also wish to express my thanks to Professor Harry Gafney for his kind interest and collaboration for the second part of my thesis which was done in his laboratory under his guidance.

Thanks are also in order to Professor Juan Villa who gave his time to discuss various aspects of this work with me.

## VI

Table of Contents

List of Tables.....	VIII
List of Diagrams.....	X
Part I: Organophosphonium Substituted Pyridines and Bipyridines as Ligands in Transition Metal Complexes.....	1
Introduction.....	2
Background.....	2
Experimental.....	14
Preparation of the Ligands.....	15
Preparation of the Complexes.....	20
Results and Discussion.....	25
Part II: Study of the Photochemistry of Ru(II) Substituted-Bipyridine Complexes by Flash Photolysis Techniques.....	46
Introduction.....	47
Experimental.....	54
Results and Discussion.....	64
Thermal Transformation of $\text{Ru}(\text{NO}_2\text{Bpy})_3^{2+}$ in 95% EtOH.....	74
Quenching of $\text{Ru}(\text{Bpy})_3^{2+}$ by Substituted Bipyridines.....	79
Quenching of $\text{Ru}(\text{Bpy})_3^{2+}$ or $\text{Ru}(\text{Et}_3\text{P}^+\text{Bpy})_3^{5+}$ by Co(III) Complexes of Bipyridines.....	82
Flash Photolysis Experiments.....	84

VII

Flash Photolysis of Substituted Bipyridines..	95
Conclusion.....	104
References.....	110

## VIII

List of Tables

Table I	Absorption Maxima of some Phosphorus Donor Complexes of Co(II).....	7
Table II	Absorption Maxima of some Phosphorus Donor Complexes of Co(II) and Ni(II).....	9
Table III	Absorption Maxima of Co(II) and Ni(II) Complex- es of P <sup>+</sup> Py and P <sup>+</sup> Pic.....	11
Table IV	Elemental Analysis of Complexes.....	23
Table V	pK <sub>a</sub> Values of Substituted Pyridines and Bipyridines.....	25
Table VI	Reduction Potentials of Substituted Bipyridines.....	28
Table VII	Oxidation Potentials of Fe(II) and Ru(II) Complexes.....	33
Table VIII	Reduction Potentials of Fe(II) and Ru(II) Complexes.....	36
Table IX	Charge-Transfer Absorption Energies of Complexes.....	38
Table X	Emission Bands of Substituted Bipyridines....	65
Table XI	Stern Volmer Quenching Constants and Bimolecular Rate Constants for the Quenching of Ru(Bpy) <sub>3</sub> <sup>2+</sup> by Substituted Bipyridines.....	83
Table XII	Stern Volmer Quenching Constants and Bimolecular Rate Constants for the Quenching of Ru(Bpy) <sub>3</sub> <sup>2+</sup> and Ru(Et <sub>3</sub> P <sup>+</sup> Bpy) <sub>3</sub> <sup>5+</sup> by Co(III) Complexes.....	85

Table XIII	Rate Constants for the Thermal Back	
	Reaction.....	94

List of Diagrams

Figure 1	A Diagram of Flash Apparatus.....	56
Figure 2	A Diagram of Flash Cells.....	59
Figure 3	Emission Spectrum of 2,2'-Bipyridine at Room Temperature.....	66
Figure 4	Emission Spectrum of 2,2'-Bipyridine at 77°K.....	67
Figure 5	Emission Spectrum of 4Et <sub>3</sub> P <sup>+</sup> 2,2'-Bipyridine at Room Temperature.....	68
Figure 6	Emission Spectrum of 4Et <sub>3</sub> P <sup>+</sup> 2,2'-Bipyridine at 77°K.....	69
Figure 7	Emission Spectrum of 4,4'-diEt <sub>3</sub> P <sup>+</sup> 2,2'- Bipyridine at Room Temperature.....	70
Figure 8	Emission Spectrum of 4,4'-diEt <sub>3</sub> P <sup>+</sup> 2,2'- Bipyridine at 77°K.....	71
Figure 9	Emission Spectrum of Ru(Bpy) <sub>3</sub> <sup>2+</sup> at Room Temperature and 77°K.....	72
Figure 10	Emission Spectrum of Ru(Et <sub>3</sub> P <sup>+</sup> Bpy) <sub>3</sub> <sup>5+</sup> at Room Temperature and 77°K.....	73
Figure 11	Change in Visible Absorption Spectrum of Ru(NO <sub>2</sub> Bpy) <sub>3</sub> <sup>2+</sup> in 95% EtOH with Time.....	75
Figure 12	Change in UV Absorption Spectrum of Ru(NO <sub>2</sub> Bpy) <sub>3</sub> <sup>2+</sup> in 95% EtOH with Time.....	76
Figure 13	Stern Volmer Plot for the Quenching of Ru(Bpy) <sub>3</sub> <sup>2+</sup> by 4-NO <sub>2</sub> Bpy.....	80

XI

Figure 14	Stern Volmer Plot for the Quenching of Ru(Bpy) <sub>3</sub> <sup>2+</sup> by 4-Et <sub>3</sub> P <sup>+</sup> Bpy.....	81
Figure 15	Stern Volmer Plot for the Quenching of Ru(Bpy) <sub>3</sub> <sup>2+</sup> by Co(Bpy) <sub>3</sub> <sup>3+</sup> .....	86
Figure 16	Stern Volmer Plot for the Quenching of Ru(Bpy) <sub>3</sub> <sup>2+</sup> by Co(NO <sub>2</sub> Bpy) <sub>3</sub> <sup>3+</sup> .....	87
Figure 17	Stern Volmer Plot for the Quenching of Ru(Et <sub>3</sub> P <sup>+</sup> Bpy) <sub>3</sub> <sup>5+</sup> by Co(Bpy) <sub>3</sub> <sup>3+</sup> .....	88
Figure 18	Decay Trace of Ru(III) in Flash Experiments.	90
Figure 19	Agreement of the Transient Spectrum with that of Ru(Bpy) <sub>3</sub> <sup>3+</sup> .....	91
Figure 20	Agreement of the Transient Spectrum with that of Ru(Et <sub>3</sub> P <sup>+</sup> Bpy) <sub>3</sub> <sup>6+</sup> .....	92
Figure 21	Spectral Change in Continuous Photolysis of 4-NO <sub>2</sub> Bpy in 95% EtOH.....	99
Figure 22	Spectral Change in Continuous Photolysis of 4-NO <sub>2</sub> Bpy in 20% EtOH.....	100
Figure 23	Spectral Change in Continuous Photolysis of 2,2'-Bipyridine.....	101
Figure 24	Spectral Change in Continuous Photolysis of 4Et <sub>3</sub> P <sup>+</sup> 2,2'-Bipyridine.....	102
Figure 25	UV Spectrum of Pyridine of N-Oxide.....	103

(1)

Part I

Organophosphonium Substituted Pyridines and Bipyridines  
as Ligands in Transition Metal Complexes

## Introduction

A substituent group which could alter the electronic distribution in the pyridine or the bipyridine ring most significantly (by withdrawing electronic charge most effectively) would be one which is positively charged. For this reason  $R_3P^+$  substituted pyridines and bipyridines were used as ligands in the study of the relationship between the ligand properties and their behavior in various transition metal complexes.

We believe that this study could be the vehicle for answering some fundamental questions about ligand effects, and will provide insight into the mechanism by which substituent effects are transmitted to the ligand metal bonds.

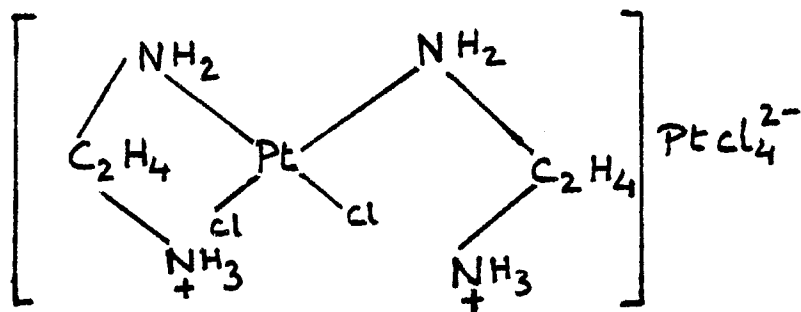
In order to be able to compare the effects of the cationic ligands with those of the analogous neutral ligands of comparable electron withdrawing power, we synthesized pyridines and bipyridines substituted in the 4-position and 4,4'-positions with  $NO_2$  and  $(C_2H_5)_3P^+$  groups. The reason for the choice of the 4-substituted derivatives is that the 4-position is in direct conjugation with the N-donor atoms of the pyridine and bipyridine rings. Previous workers have investigated transition metal complexes containing cationic ligands and have obtained interesting results.

## Background

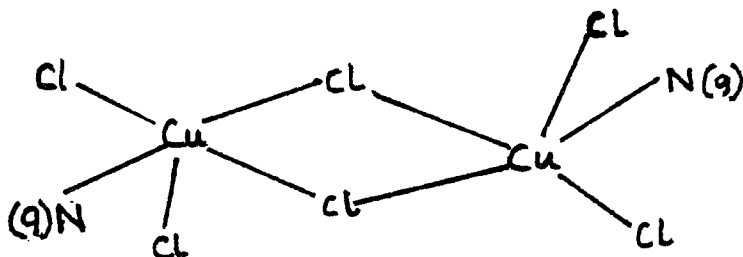
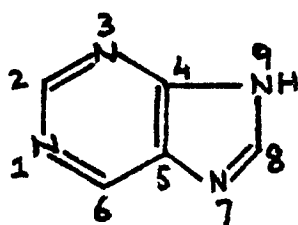
Although the results on complexes of cationic ligands

are not always unequivocally interpreted, the overall conclusion thus far is that the effect of cationic ligands as compared to the analogous neutral ligands is minimal. However the kind of experiments performed and measurements obtained (d-d electronic transition,  $\nu_{C-O}$ ) may not be the ones required to fully exploit the differences in ligancy between the cationic and neutral ligands. In some extreme cases, where the cationic site had some structurally obvious influence on the donor site (eg. hydrazinium ion), the complexes of the cationic ligand were limited.

Some of the systems previously studied are discussed below, together with the experimental evidence (or lack of it) of the diminished ligancy of the cationic ligand. The first reported cationic ligands were prepared by Drew (1). He found that monoprotonated ethylenediamine acts as a ligand toward the platinum ion in the salt:

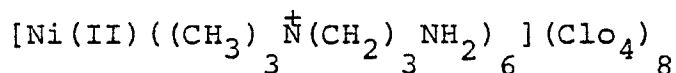


Villa reported the results of a spectral study of trichloroguaninium copper(II) monohydrate (2). The atoms in a purine system are numbered as follows:



This complex exists as a chloride bridged dimer of  $D_{3h}$  symmetry with the three chloride ions in the equatorial plane and one chloride ion and the guaninium ion in the axial position. The guaninium ion is protonated at N(3) and N(7) and is coordinated via N(9). Villa showed that there is somewhat weaker bonding on the axial position, probably caused by the presence of the positively charged guaninium ion.

The first systematic study of the coordinating ability of cationic ligands was reported by Quagliano and Coworkers (3). They prepared metal complexes with monomethylated diamines acting as ligands. They compared the electronic spectrum of the octahedral complex formed between Ni(II) and the  $\beta$ -aminoethyltrimethylammonium cation, (abbreviated as  $\beta\text{-L}^+$ ) with the Ni(II) complexes of the  $\gamma$ -amino propyl-trimethylammonium cation (abbreviated as  $\gamma\text{-L}^+$ ).



The spectra showed an appreciable shift to lower frequencies in the d-d spectrum for the complexes of  $\beta\text{-L}^+$  compared to those of  $\gamma\text{-L}^+$ . The Ni(II) complex of  $\gamma\text{-L}^+$  absorbed at 27,000, 17,000 and 10,000  $\text{cm}^{-1}$ , whereas the  $\beta\text{-L}^+$ -complex absorbed at 26,000, 16,500 and 10,000  $\text{cm}^{-1}$ . Similar shifts to lower frequencies by the  $\beta\text{-L}^+$  complexes were also observed in the octahedral Co(II) complexes as well as the tetrahedral Cu(II) complexes. Absorptions at lower frequencies indicate that the ligand produces a weaker field. Basicity studies of the two cationic ligands

paralleled the spectral measurements. That is to say, the ligand which produced the weaker field ( $\beta\text{-L}^+$ ) was the weaker base. The spectral measurements placed the  $\gamma\text{-L}^+$  ligand very close to methylamine in the spectrochemical series, while the  $\beta\text{-L}^+$  ligand was placed towards the weaker field end, about halfway between methylamine and water. This study showed that a positive charge three methylene groups removed from the donor site does not effect the donor ability of the ligand, whereas a positive charge two methylene groups from the donor site does reduce the donor ability. In this particular case, since no  $\pi$  bonding is involved, the field strengths of these ligands should be directly proportional to its donor ability and its basicity.

In a continuation of the study of the effect of positive charge on the donor ability of ligands, these same workers prepared complexes with the 1,1,1-trimethylhydrazinium cation acting as a ligand (4). In these complexes the site of positive charge is immediately adjacent to the nitrogen donor atom. They found that slow evaporation of an aqueous solution of a nickel(II) halide and the corresponding trimethylhydrazinium halide in a molar ratio of 1:2 gave yellow crystals of the complex  $[\text{NiX}_4((\text{CH}_3)_3\overset{+}{\text{N}}\text{NH}_2)_2]$ . The d-d electronic spectra of these complexes indicate a tetragonally distorted octahedral stereochemistry, with the cationic ligands in the axial position. The spectra were virtually super imposable with those of the complexes  $[\text{NiX}_4(\text{H}_2\text{O})_2]^{2-}$ , indicating that the

field strength of the trimethylhydrazinium cation must be very similar to that of water, and much lower than that of uncharged primary amines. Thus a positive charge adjacent to the donor atom in a ligand considerably lowers the donor ability of the ligand. The trimethylhydrazinium cation has, of course, an extremely low basicity ( $-2.9 \text{ p}K_a$  units) and it is interesting that it would form complexes at all. In fact, only complexes of nickel were isolable and at temperatures near  $100^\circ\text{C}$  they transformed to the blue complex salts  $[\text{NiX}_4^{2-}](2(\text{CH}_3)_3\text{NNH}_2^+)$ , containing the tetrahedral tetrahalonickelate(II) anion. In this case basicity of the ligand does not seem to parallel its field strength as observed in the previous case of ammonium cations, even though no  $\pi$  bonding is involved.

Kotaday, Morris and Taylor reported the results of a study of complexes with cationic ligands in which the effect of the positive site is transmitted to the donor site via an unsaturated organic bridge (5). They prepared Co(II) Zwitterionic complexes of  $C_{2v}$  symmetry with the cationic ligands:

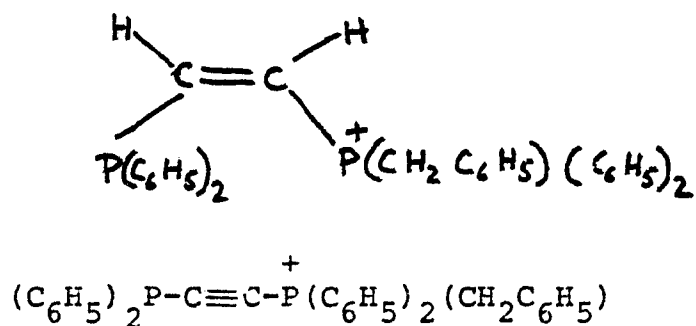


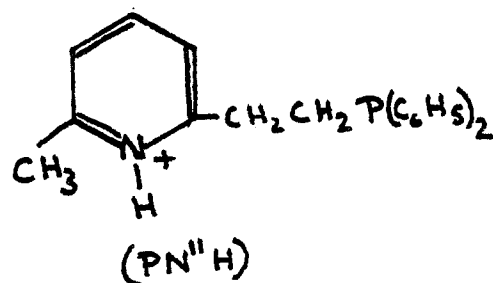
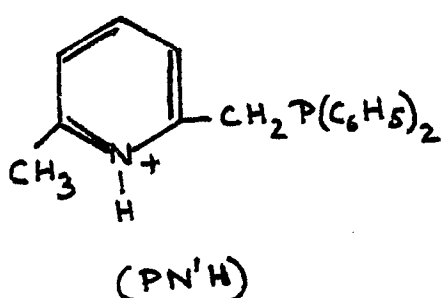
Table I lists the d-d absorption maxima of these complexes.

Table I

Absorption Maxima of Some Phosphorus Donor Complexes of Co(II)

<u>Complex</u>	<u>Electronic Absorption Maxima (cm<sup>-1</sup>)</u>
$[\text{Ph}_2\text{PC}_2\text{H}_2\overset{+}{\text{P}}\text{Ph}_2(\text{CH}_2\text{Ph})\text{CoBr}_3^-]$	14,910
	15,260
	16,270
$(\text{Et}_4\text{N}^+) [\text{CoBr}_3 \text{Ph}_2\text{PC}_2\text{H}_2\text{PPh}_2]$	14,990
	15,100
	16,210
$[\text{Ph}_2\text{PC}_2\overset{+}{\text{P}}\text{Ph}_2(\text{CH}_2\text{Ph})\text{CoBr}_3^-]$	14,650
	15,000
	15,000
	15,200
$(\text{Et}_4\text{N}^+) [\text{CoBr}_3\text{Ph}_2\text{PC}_2\text{PPh}_2]^-$	14,560
	14,950
	16,150

A comparison of the d-d spectra of these complexes with those of analogous neutral ligands illustrates the absence of significant spectral shifts. The absence of a shift led these authors to conclude that the positive site has a negligible effect on the donor capability of the unquarternized phosphorus atom. Nelson and coworkers prepared Co(II) and Ni(II) complexes of the positively charged ligands (6).



The complexes formed between the halide salts of these cations and Co(II) and Ni(II) halides were found to be 1:1 Zwitterionic complexes of C<sub>3v</sub> symmetry. A comparison between the d-d spectra of the complexes of PN'H and PN''H which are listed in Table II showed that the ligand in which the positive charge is closer to the donor phosphorus atom produced a slightly higher average field. These authors concluded that the higher field is a result of a greater degree of metal to phosphorus bonding in complexes of PN'H. The cationic site withdraws electron density from the phosphorus atom to a greater extent in the ligand

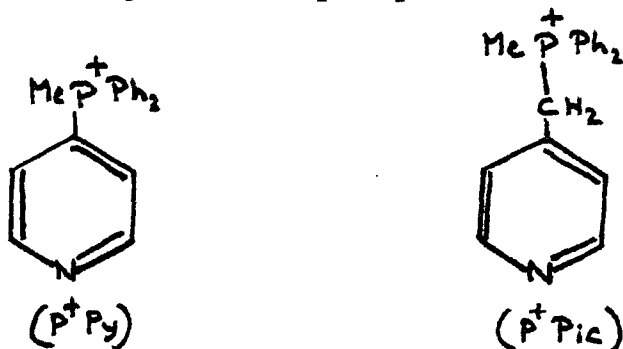
Table II

Absorption Maxima of Some Phosphorus Donor  
Complexes of Co(II) and Ni(II)

<u>Complex</u>	<u>Absorption Maxima (cm<sup>-1</sup>)</u>
Co(PN'H)Cl <sub>3</sub>	18,300
	16,500
	14,700
	8,200
	4,500
Co(PN"H)Cl <sub>3</sub>	18,000
	16,400
	14,000
	8,000
	4,500
Ni(PN'H)Br <sub>3</sub>	16,300
	9,500
	8,600
	5,800
Ni(PN"H)Br <sub>3</sub>	16,000
	9,600
	8,800
	5,600

where the two sites were closer and complex of this ligand would show a greater degree of  $M \rightarrow P$  backbonding.

Recently Weiner and Schwartz reported the preparation and properties of Co(II) and Ni(II) complexes of the methyl-diphenyl-4-pyridylphosphonium ligand ( $P^+PY$ ) in which the positive charge is conjugated to the donor nitrogen atom via the  $\pi$  orbitals of the pyridine ring (7). This was compared with the complex of the methyl diphenyl-4-picolyphonium ligand ( $P^+Pic$ ) in which a  $CH_2$  group is inserted between the ring and the phosphonium moiety.



All the complexes pseudo tetrahedral Zwitterionic complexes of the type  $[M(L^+)X_3^-]$ , as shown from a study of their magnetic moments. From the study of the ligand field bands of these complexes, as listed in Table III, the authors concluded that the cationic site had no large effect on the electronic behavior of the ligands. The slightly higher field for  $P^+py$  presumably indicates some increase in the  $\pi$ -acceptor nature of the pyridyl ring.

It is well established that the C-O stretching frequencies (or the C-O force constants) in substituted metal carbonyls ( $LnM(CO)_m$ ) are a function of the ability of L to place electron density at the metal (8). The greater the

Table III

Absorption Maxima of Co(II) and Ni(II) Complexes of P<sup>+</sup>Py  
and P<sup>+</sup>Pic.

<u>Complex</u>	<u>Absorption Maxima, Cm<sup>-1</sup></u>
<sup>+</sup> Co(PPy)Br <sub>3</sub>	4,720
	7,520
	14,700
	15,300
	16,100
<sup>+</sup> Co(PPic)Br <sub>3</sub>	4,720
	7,400
	14,550
	15,200
	16,200
Et <sub>4</sub> N <sup>+</sup> [Co(C <sub>5</sub> H <sub>5</sub> N)Br <sub>3</sub> ] <sup>-</sup>	4,720
	7,250
	14,600
	15,300
	16,200
<sup>+</sup> Ni(PPy)Br <sub>3</sub>	8,850
	15,500
Ni(P <sup>+</sup> Pic)Br <sub>3</sub>	8,770
	15,400

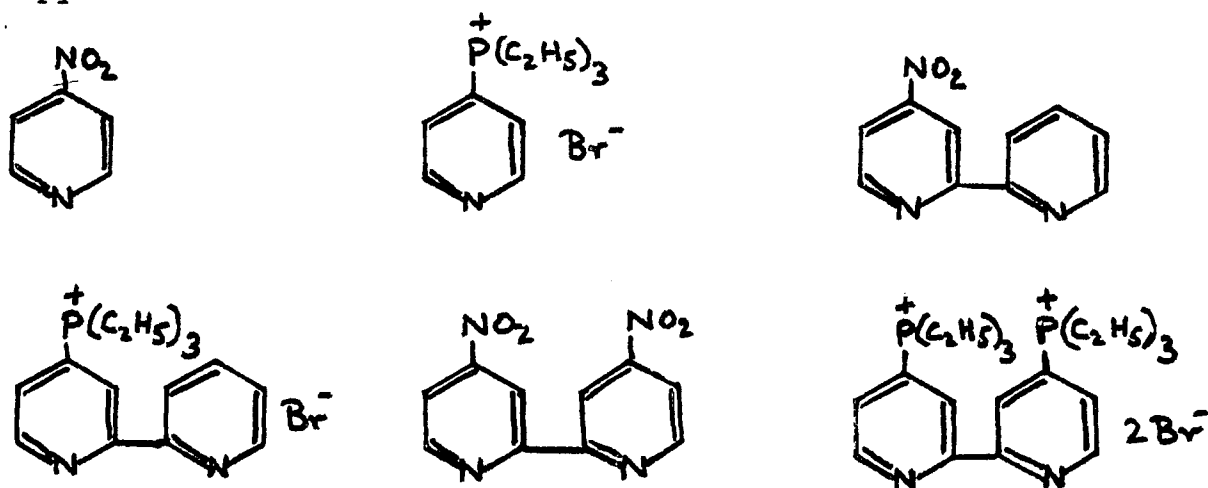
electron density at the metal, the lower the C-O stretching frequency, presumably as a result of an enhanced  $\pi$  bonding between the metal d orbitals and the antibonding orbitals on the carbon monoxide. A recent study related increasing IP of the donor electron pair in a series of uncomplexed ligands (phosphorus donor) with the increasing C-O stretching frequency of their carbonyl complexes (9). It concluded that for a series of ligands in which M  $\rightarrow$  P  $\pi$  bonding is similar, the greater donor IP means less  $\sigma$ -donor ability on the part of the ligand, and less charge transfer to the metal. As the  $\pi$ -acceptor capacity of the phosphine increased, there was an additional loss of electron transfer to the metal and a higher C-O stretching frequency.

Discussions of this effect in  $M(\text{CO})_5\text{L}$  (L includes pyridine and other amines) have been extended to the relative  $\sigma$  vs  $\pi$  influence of L on the electron density at the metal, and it was concluded that pyridine does not exhibit  $\pi$ -interaction with the metal (while 2,2'-bipyridine shows some  $\pi$ -interaction) (10,11,12,13). The above discussion however appears not to agree with work on the C-O stretching frequencies of Cr and W carbonyls of the type  $[M(\text{CO})_5\text{L}^+]\text{X}^-$ , when  $\text{L}^+$  is a cationic ligand with a phosphorus donor.

Here little or no shift was seen for the cationic ligands when compared with the analogous neutral ligands (14,15,16). In one case where the cationic site was one  $\text{CH}_2$  group from the donor site, a slight rise in the C-O stretching frequency was observed. In these cationic ligand systems,

the greater donor electron pair IP, combined with a possibility of greater  $\pi$  acceptor capacity for the phosphorus, should result in a considerably diminished electron transfer to the metal. Thus it appears that the change in IP is not being translated into a bonding effect of the ligand on its complexes.

The question of why the cationic site has shown such a minimal effect, as seen in most of the previous examples, poses an intriguing problem. Does the transmission mechanism for electronic effects in the ligand preclude the influence of the cationic site, so that only ligands such as hydrazinium show a substantial effect, or are just the properties thus far measured unaffected. The present report describes the synthesis and characterization of the following -Nitro and -phosphonium substituted pyridines and bipyridines.



The formation of complexes of these ligands with  $\text{Co(II)}$ ,  $\text{Fe(II)}$  and  $\text{Ru(II)}$  and characterization of these complexes by spectral and electrochemical measurements is discussed.

Experimental

Proton NMR spectra were obtained on a JEOL 100 MHz spectrometer. Resonances are stated in parts per million downfield from sodium 2,2-dimethyl-2-silacyclopentane-5-sulfonate as internal standard. Melting points were obtained with a Thomas Hoover capillary apparatus. All reactions involving organophosphines were carried out under an atmosphere of prepurified nitrogen. All compounds that are reported for the first time were analyzed by Galbraith.. laboratories.

4-Nitro pyridine was obtained by heating 4-nitro pyridine N-oxide with a mixture of concentrated  $H_2SO_4$  and  $HNO_3$  at  $240^\circ C$  for 20 minutes. The mixture was then poured into ice, neutralized with a saturated NaOH solution and extracted with chloroform. The product (M.pt.  $48-49^\circ C$ ) was obtained from the extract after evaporation of the solvent and crystallization from hexane.

4-Bromo pyridine was obtained by adding aqueous KOH to a chilled aqueous solution of the hydrochloride and extracting with ether. The ether was removed just before use.

4-Nitro-2,2'-bipyridine and 4,4'-dinitro-2,2'-bipyridine were prepared by modifications of literature methods described by Jones and Maerker (17,18). Details of these synthesis are described below. 4-Bromo-2,2'-bipyridine and 4,4'-dibromo-2,2'-bipyridine were prepared from the corresponding nitro compounds. The phosphorus trichloride, phosphorus tribromide,

and acetyl bromide used in these syntheses were distilled just before use.

Preparation of 4-Nitro-2,2'-Bipyridine.

Oxidation and Nitration of 2,2'-Bipyridine.

Aqueous 30% hydrogen peroxide (75 cc.) was added to a vigorously stirred solution of 2,2'-bipyridine (15.0 g) in glacial acetic acid (75 cc.) and the mixture was heated at 50°C for 18 hrs. Volatile compounds were removed under vacuum to give a yellow residual oil. The oil was cooled in an ice salt bath and dissolved in concentrated sulphuric acid (40 cc.).

(CAUTION: This reaction is extremely exothermic and should be carried out slowly!). A mixture of 60 cc. of fuming nitric acid and 40 cc. of concentrated sulphuric acid was added over a 15 minute period and the mixture was then heated at 100°C for 4-5 hours. The solution was poured on to ice (200 g) and the pH adjusted to 5.5 with 20% aqueous sodium hydroxide.

The orange brown precipitate obtained was extracted with a small amount of hot ethanol. The ethanol extract was cooled to give yellow needles of 4-nitro-2,2'-bipyridine 1-oxide (4.4 g, 21%) M.pt. 183-185°C. Further extraction of the residue with a larger volume of hot ethanol gave 4,4'-dinitro-2,2'-bipyridine 1,1'-dioxide (2.5 g, 10%) M. pt. 273-274°C.

The aqueous filtrate from the nitration step was neutralized with ammonia and extracted continuously with chloroform. The chloroform extract was dried with magnesium sulphate and evaporated to dryness. The unreacted 2,2'-

bipyridine in the residual solid obtained was removed by extraction with hexane (b.pt. 60-80°C). Recrystallization of the remaining residual solid from ethanol gave 4-nitro-2,2'-bipyridine 1,1'-dioxide (3.2 g, 34%), yellow needle, M.pt. 243°C. - 244°C.

#### 4-Nitro-2,2'-Bipyridine.

Phosphorus trichloride (2 cc.) was added to 4-nitro-2,2'-bipyridine 1,1'-dioxide (1.0 g.) in chloroform (15 cc.) at 0°C. The mixture was refluxed for 1 hr. and then poured onto ice. The solution was made alkaline with aqueous sodium hydroxide, filtered, and the filtrate was extracted with chloroform. Evaporation of the chloroform extract gave the product which was crystallized from ethanol to give white needles of 4-nitro-2,2'-bipyridine, M.pt. 116-118°C.

#### 4-Bromo-2,2'Bipyridine

4-Nitro-2,2'-bipyridine 1,1'-dioxide (1.0 g), acetyl bromide (20 cc) and phosphorus tribromide (5 cc.) were refluxed for 1 hr and poured onto 100 gms of ice. The aqueous solution was neutralized with sodium hydroxide, filtered and extracted with chloroform (3x50 cc.). The chloroform extracts were dried over anhydrous  $MgSO_4$  and evaporated to dryness. The residue was extracted with hexane (40-60°C) and recrystallized from the same solvent to give white needles of 4-bromo-2,2'-bipyridine, M.pt. 50-52°C.

4,4'-Dinitro-2,2'-Bipyridine.

A suspension of 1.5 g (0.0054 mole) of 4,4'-dinitro-2,2'-bipyridine 1,1'-dioxide in 25 ml of anhydrous chloroform was cooled to 0°C and 3 ml (0.034 mole) of phosphorus trichloride was added. The mixture was heated at reflux over a water bath for 1 hr., cooled to room temperature, and poured into a mixture of ice and water. The resulting suspension was made alkaline with aqueous sodium hydroxide and 1.3 gms of unchanged starting material recovered by filtration. The aqueous layer of the filtrate was extracted with several portions of fresh chloroform and discarded. The combined chloroform portions were evaporated to a crystalline residue which was recrystallized first from hexane (40-60°C) and then from 95% ethanol to yield 0.12 gms of white needles M.pt. 188-90°C. Repeated recrystallizations from the same solvents raised the melting point to 192-193°C. Note: Any attempt to improve the yield in this reaction by a longer reaction time led only to more side products like -chloro, nitro compound or the dichloro compound which was very difficult to separate. The purity of the product in this reaction was judged by its mass spectrum. (m/e peaks at 246, 200 and 154 due to ions  $C_{10}N_4H_6O_4$ ,  $C_{10}N_3H_6O_2$  and  $C_{10}N_2H_6$ ).

Preparation of 4,4'-Dibromo-2,2'-Bipyridine.

To a suspension of 1.0 g (0.0036 mole) of 4,4'-dinitro-2,2'-bipyridine 1,1'-dioxide in 15 ml of glacial acetic acid at 60°C was added 7.8 ml of acetyl bromide, and the mixture

(18)

refluxed for two hours on a water-bath. The solution was cooled to room temperature, poured on 150 g of crushed ice and neutralized with 15% sodium carbonate solution, yielding 1.1 gms of dried precipitate.

A suspension of the precipitate in 25 ml of anhydrous chloroform was cooled to  $-3^{\circ}$  and 4.0 ml (0.042 mole) of phosphorus tribromide was added. After the mixture had been allowed to reflux for 75 min., it was cooled and poured into a mixture of ice and water. After separation, the chloroform layer was extracted repeatedly with distilled water, and the aqueous extracts were combined with the water layer from the reaction mixture. Neutralization of the aqueous solution with 25% sodium hydroxide caused separation of a voluminous white precipitate which, after cooling of the mixture, was isolated by filtration and washed thoroughly with water. The crude solid was recrystallized from hexane (b.p.  $60-70^{\circ}$ ) to give white needles M.pt.  $141-142^{\circ}\text{C}$ .

Preparation of Triethyl-4-pyridylphosphonium Bromide (Ppy)<sup>+</sup>Br<sup>-</sup>

Triethylphosphine (4.0 g, 34 mmole) was added to 3.5 gms of 4-bromopyridine (22.4 mmole) under  $\text{N}_2$  and the reaction mixture was left in a sealed tube under  $\text{N}_2$  for 72 hr at  $85^{\circ}\text{C}$ . After washing out the excess phosphine with ether, 2.8g of a purple solid was obtained. Repeated crystallizations with charcoal from an acetone-ether mixture gave 1.8 gms of the product as white needles, m.pt.  $157-158^{\circ}\text{C}$ .

NMR ( $\text{D}_2\text{O}$ ):  $\delta$  8.1-8.3 (M, 2, pyridyl  $\text{H}_\alpha$ ), 7.3-7.5 (M, 2, pyridyl  $\text{H}_\beta$ ); 2.7-2.8 (M, 6,  $\text{CH}_2$ ), 1.1-1.3 (M, 9 ( $\text{CH}_3$ ))

Anal. Calculated for  $C_{11}H_{19}PNBr$ : C, 47.84; H, 6.93.

Found: C, 47.74; H, 7.08

Preparation of Triethyl-4-Bipyridylphosphonium Bromide  
+  
(PBpy)Br.

Triethylphosphine (1.0g, 8.5 mmole) was added to 0.35g of 4-bromo-2,2'-bipyridine (1.5 mmole) and the reaction mixture was left in a sealed tube under  $N_2$  for 120 hr at  $120^\circ C$ . After washing out the excess phosphine with ether, 0.45g of a white solid was obtained. Crystallization from acetone-ether yielded 0.35g of the product, M.p.  $179-180^\circ C$ . NMR ( $D_2O$ ):  $\delta$  7.5-8.9 (M, 7, Bpy H), 2.5-2.8 (M, 6,  $CH_2$ ), 1.0-1.3 (M, 9,  $CH_3$ ).

Anal. Calculated for  $C_{16}H_{22}N_2PBr$ : C, 54.40; H, 6.28.

Found: C, 54.43; H, 6.39.

Preparation of Triethyl-4,4'-Bipyridyldiphosphonium

Dibromide ( $P_2^{+2}Bpy$ )Br<sub>2</sub>.

Triethylphosphine (2.0 g, 17 mmole) was added to 0.43 g of 4,4'-dibromo-2,2'-bipyridine (1.36 mmole), and the reaction mixture was left at  $120^\circ C$  for 100 hr in a sealed tube under  $N_2$ . Only the monophosphonium product was isolated. This product (0.40 g) was mixed with 1.0 g of triethylphosphine and heated for 5 hrs at  $190^\circ C$  in a sealed tube. After washing out the excess phosphine with ether, the isolated solid (0.44 g) was crystallized from ether-acetone to give 0.40 g of the product, m.p.  $320-322^\circ C$ . NMR ( $D_2O$ ):  $\delta$  8.0-9.1 (M, 6, Bpy H), 2.6-3.0 (M, 12,  $CH_2$ ),

1.2-1.5 (M, 18, CH<sub>3</sub>).

Anal. Calculated for C<sub>22</sub>H<sub>36</sub>P<sub>2</sub>N<sub>2</sub>Br: C, 48.02; H, 6.59.

Found: C, 47.98; H, 6.66.

Preparation of Et<sub>4</sub>N<sup>+</sup>[CoBr<sub>3</sub>N<sub>2</sub>C<sub>6</sub>H<sub>4</sub>NO<sub>2</sub>]

Cobalt bromide (109 mg, 0.5 mmole) in 5 ml of ethanol was mixed with a solution of 0.5 mmole (62 mg) of 4-nitropyridine and 0.5 mmole (105 mg) of Et<sub>4</sub>N<sup>+</sup>Br<sup>-</sup> in 3 ml of ethanol under nitrogen. After shaking the solution for five minutes, the green complex that precipitate was filtered to give 170 mg of Et<sub>4</sub>N<sup>+</sup>[CoBr<sub>3</sub>NO<sub>2</sub>Pyr]. M.pt. 195-198°C. Anhydrous conditions were maintained throughout the reaction.

Anal: Calculated for C<sub>13</sub>H<sub>24</sub>N<sub>3</sub>O<sub>2</sub>CoBr<sub>3</sub>: C, 28.23; H, 4.34

Found: C, 28.05; H, 4.38.

Preparation of [CoBr<sub>3</sub>Ppy]<sup>+</sup>

Cobalt bromide (73 mg, 0.33 mmole) dissolved in 3 ml of ethanol was mixed under N<sub>2</sub> with a solution of 92 mg (0.33 mmole) of 4Et<sub>3</sub>Ppy<sup>+</sup>Br<sup>-</sup> in 1 ml of ethanol. The solution was shaken for five minutes and then filtered to give 100 mg of the blue complex.

Anal: Calculated for C<sub>11</sub>H<sub>19</sub>N<sub>2</sub>CoBr<sub>3</sub>: C, 26.69; H, 3.84.

Found: C, 26.52; H, 3.65.

Preparation of Tris(2,2'Bipyridine)iron(II) Perchlorate Complexes.

FeSO<sub>4</sub> (75mg, 0.50 mmoles) is dissolved in 20 ml of hot distilled water and filtered to remove the Fe<sub>2</sub>O<sub>3</sub>·NH<sub>2</sub>O that formed. 0.25 mmole of the appropriate ligand is

dissolved in 5 ml of ethanol and when the two solutions are mixed a deep red or violet color develops. A saturated  $\text{NaClO}_4$  solution is then added to precipitate the perchlorate salt. The precipitate of the perchlorate salt of the different tris( 2,2'-bipyridine) iron compounds was filtered and washed several times with water to remove the excess  $\text{NaClO}_4$ , and then dried under vacuum. The typical yield in these reactions was 50-60%. These complexes were characterized by a strong charge transfer absorption band around 510 nm.

Preparation of Tris( 2,2'-bipyridine)ruthenium (II)

Perchlorate Complexes.

A 25% excess of the appropriate ligand,  $\text{RuCl}_3 \cdot 3\text{H}_2\text{O}$  and half of its molar equivalent of sodium oxalate is heated under reflux for 72 hrs. in 95% EtOH. At the end of this time, the dark colored solution is filtered, evaporated to a smaller volume and 20 mls of a saturated  $\text{NaClO}_4$  solution is added to precipitate the perchlorate salt of the complex. The precipitate is filtered, washed repeatedly with water to remove excess  $\text{NaClO}_4$ , and dried under vacuum. The typical yield in these reactions is 50-60%. These complexes were characterized by a strong charge transfer absorption band around 450 nm.

Preparation of Bis(2,2'-bipyridine)dichloro Ruthenium(II)

Perchlorate Complexes.

The bis complexes of ruthenium(II) were made exactly the same way as the tris complexes described above.

However all attempts to push the reaction to yield the tris complex with these disubstituted bipyridines by using large excess of ligand or longer refluxing time failed to yield the desired result. The formulation of the complexes along with their analyses is given in Table IV.

#### Determination of $pK_a$

The  $pK_a$  values were determined spectrophotometrically. All spectra were taken on a Cary Model 15 spectrophotometer, using matched 1 cm cells. The aqueous (or aqueous alcoholic) solutions were approximately  $10^{-5}$  M. The spectra were obtained in the temperature range 24-28°C. and showed no variation within the limits of this range. The values were calculated using the formula:

$$pK = pH + \log \frac{d - d_n}{d_1 - d}$$

where  $d_1$  is the optical density (O.D.) for the acid form,  $d_n$  is the O.D. for the base form and  $d$  is the O.D. at an intermediate pH. All values of  $d$  apply to the same analytical wavelength in each case. At least three solutions of varying acid-base ratios were used in each determination. The results were reproducible to within  $\pm 0.04$   $pK_a$  units. The pH values were read off directly from a pH meter or in some cases were determined by titration against standardized NaOH. Excited state  $pK_a$  values were estimated using Forster cycle calculations.<sup>19</sup>

Elemental Analysis of Complexes.

<u>Compound</u>	<u>Found (%)</u>			<u>Calculated (%)</u>		
	C	H	Cl	C	H	Cl
$[\text{Fe}(\text{NO}_2\text{Bpy})_3](\text{ClO}_4)_2 \cdot 3\text{H}_2\text{O}$	39.29	2.64		39.49	2.96	
$[\text{Fe}(\text{Et}_3\text{P}^+\text{Bpy})_3](\text{ClO}_4)_5 \cdot 4\text{H}_2\text{O}$	39.71	4.84		39.89	5.12	
$[\text{Fe}(\text{diEt}_3\text{P}^+\text{Bpy})_3](\text{ClO}_4)_8 \cdot 2\text{H}_2\text{O}$	38.58	5.88	13.94	38.50	5.44	13.80
$[\text{Ru}(\text{NO}_2\text{Bpy})_3](\text{ClO}_4)_2$	39.75	2.72	8.35	39.87	2.32	7.85
$[\text{Ru}(\text{Et}_3\text{P}^+\text{Bpy})_3](\text{ClO}_4)_5 \cdot 5\text{H}_2\text{O}$	38.04	4.78	11.25	38.22	5.04	11.75
$[\text{Ru}(\text{diNO}_2\text{Bpy})_2\text{Cl}_2] \cdot \text{H}_2\text{O}$	35.02	2.07	10.61	35.19	2.05	10.41
$[\text{Ru}(\text{diEt}_3\text{P}^+\text{Bpy})_2\text{Cl}_2](\text{ClO}_4)_4 \cdot 5\text{H}_2\text{O}$	36.32	5.12	14.66	36.66	5.69	14.79

(23)

Table IV

Determination of Redox Potential by Cyclic Voltammetry.

A Princeton Applied Research Corp. system consisting of a Model 173 potentiostat and a Model 175 Universal programmer was employed in the cyclic voltammetry measurements. Millimolar solutions of the free ligands and the Fe(II) and Ru(II) complex (as  $\text{ClO}_4^-$  salts) were prepared in a 0.1M acetonitrile solution of tetraethyl ammonium perchlorate. The acetonitrile was dried before using by stirring over calcium hydride and distilling over  $\text{P}_2\text{O}_5$ . The working electrode was platinum and the auxiliary electrode was platinum gauge in the case of the metal complexes. The working electrode in the reduction of the free ligands was a hanging drop electrode (Hg). The reference in all the measurements was a saturated aqueous calomel electrode (SCE). All solutions were handled under nitrogen. The scan rate in all the cyclic voltametric experiments were 100 mv/sec.

Results and Discussion

The ground state and excited state  $pK_a$  values on all the free ligands are listed in Table V.

Table V

$pK_a$  values of Substituted Pyridines and Bipyridines.

<u>Compound</u>	<u><math>pK_a</math></u>	<u><math>pK_a^*</math></u>
4-Nitro Pyridine	1.48 $\pm$ 0.03	
4-Et <sub>3</sub> P <sup>+</sup> Pyridyl Bromide	1.61 $\pm$ 0.02	
2,2'-Bipyridine	4.27	9.21
4-Nitro 2,2'-Bipyridine	3.25 $\pm$ 0.02	5.15
4-Et <sub>3</sub> P <sup>+</sup> 2,2'-Bipyridyl Bromide	2.82 $\pm$ 0.01	6.40
4,4'-Dinitro 2,2'-Bipyridine	0.06 $\pm$ 0.02	3.91
4,4'-DiEt <sub>3</sub> P <sup>+</sup> 2,2'-Bipyridyl Dibromide	0.03 $\pm$ 0.02	5.56

No real differences in  $pK_a$  value between the aqueous and the 20% EtOH solutions were observed in the case of the phosphonium compounds which could be measured in both solvents.

The  $pK_a$  measurements show that the  $NO_2$  and  $Et_3P^+$  substituted bases have approximately equal base strength, both of course diminished considerably from the unsubstituted compounds. In the monosubstituted bipyridines, the values clearly show that protonation occurs on the unsubstituted ring. Thus no real difference appears here between the effect of the  $NO_2$  and the cationic  $Et_3P^+$  substituents. In addition, excited state  $pK_a$  values were estimated using the difference in energy between the  $\pi \rightarrow \pi^*$  transition in the acid and base forms of the molecules (Forster cycle calculation). No direct evaluation of this data was possible since the nitro compounds did not luminesce in water and the luminescence in the other compounds are attributed to the formation of hydrates (20). The enhancement of basicity ( $pK^* - pK$ ) in the excited state of the parent bipyridine is attributable to charge migration toward the nitrogen upon excitation. Although the values in Table V are at times difficult to interpret, one observation seems clear. The  $NO_2$  group shows less basicity enhancement than  $Et_3P^+$ , or apparently less charge migration to the donor nitrogen in the excited state. It therefore exhibits the greater  $\pi$  electron withdrawing nature. The greater basicity enhancement of disubstituted compounds when compared to the mono substituted compounds could be due to a different configuration for the monoprotonated acid of the disubstituted derivative (e.g. instead of the cis or transoid structure, a trans form is possible here) (21).

Reduction of the Free Ligands.

Two successive waves are observed in the reduction of the free ligands. Previous studies by Sagi and Ayagiii have shown that these waves correspond to the first and second reductions into the  $\pi$  system (22). All the reductions were observed to be irreversible with the exception of 4,4'-dinitrobipyridine. This is probably due to chemical reaction of the radical anions produced by the first reduction. This suggestion is supported by the observed second waves, which are otherwise inconsistent with reasonable interpretation, except for the dinitro derivative.

The reduction potentials of all the free ligands are listed in Table VI. The first wave potential of the free ligands are less negative in the order 4,4'-dinitrobipyridine > 4,4'-diEt<sub>3</sub>P<sup>+</sup> bipyridylDibromide > 4-nitrobipyridine > 4-Et<sub>3</sub>P<sup>+</sup> bipyridylBromide > bipyridine.

If the contribution from the solvation energy to the reduction potential is constant for the five ligands, the  $\pi^*$  level in the free ligands decreases in the order bipyridine < 4-Et<sub>3</sub>P<sup>+</sup> bipyridine < 4-nitrobipyridine < 4,4'-diEt<sub>3</sub>P<sup>+</sup> bipyridine < 4,4'-nitrobipyridine. Thus it is seen that although both the NO<sub>2</sub> and Et<sub>3</sub>P<sup>+</sup> groups lower the potential necessary for the reduction of the  $\pi$  system, the NO<sub>2</sub> group shows a stronger effect than the Et<sub>3</sub>P<sup>+</sup> in the monosubstituted compounds. The greater efficiency of the

NO<sub>2</sub> group is even more pronounced in the disubstituted compounds. From the above evidence it is assumed that although

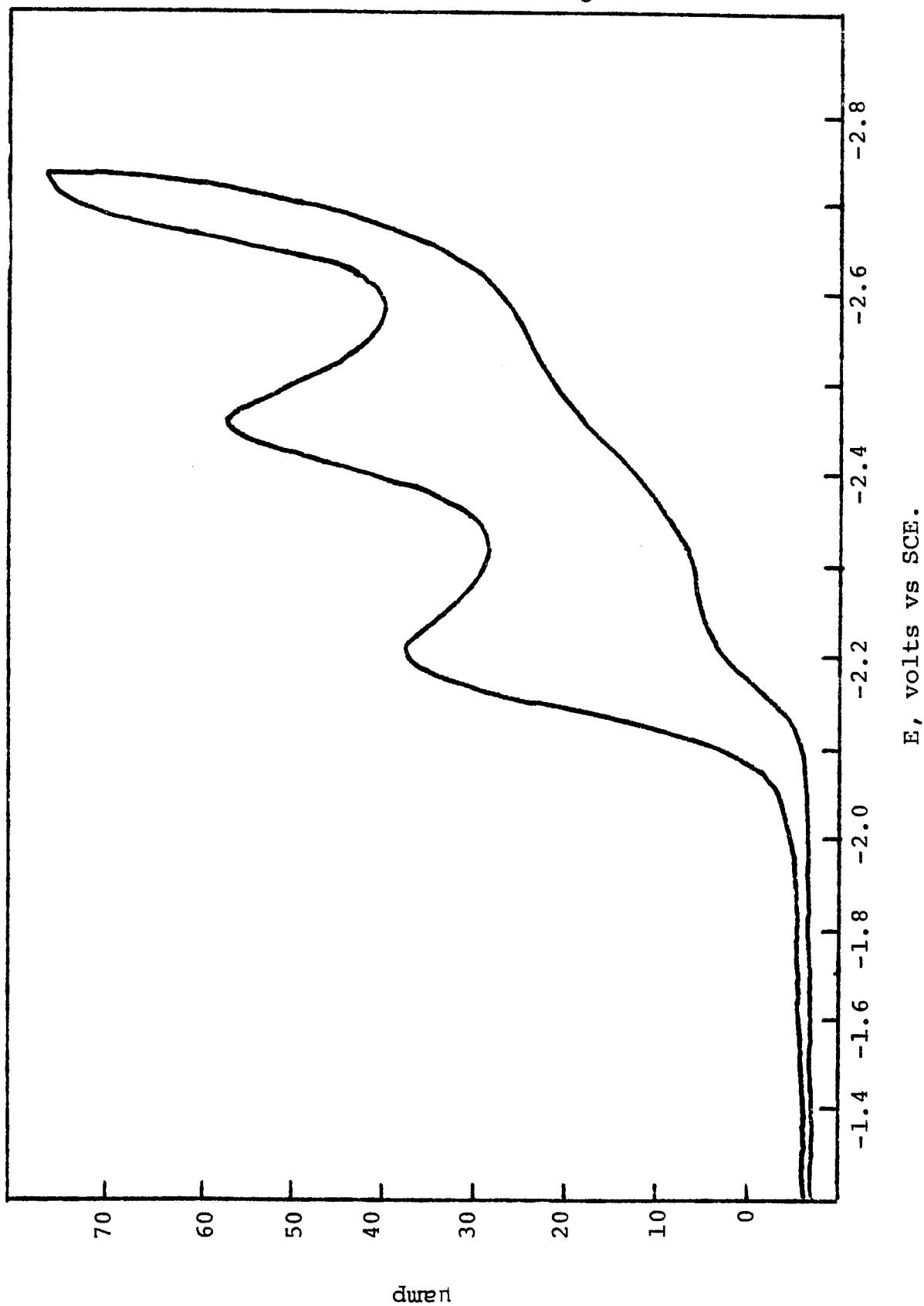
Table VI

Reduction Potential Data via Cyclic Voltammetry (in volts)  
for Free Ligands in  $0.1M Et_4N^+ClO_4^-$  in  $CH_3CN$  (vs SCE)

<u>Compound</u>	<u>1st Wave</u>	<u>2nd Wave</u>
2,2'-bipyridine	-2.21	-2.46
4-Nitro-2,2'-bipyridine	-1.55	-2.38
4- $Et_3P^+$ 2,2'-bipyridyl Bromide	-1.67	-2.22
4,4'-Dinitro-2,2'-bipyridine	-0.80	-0.91
4,4'-di $Et_3P^+$ 2,2'-bipyridyl bromide	-1.43	-2.23

(29)

Cyclic voltammogram for the reduction of  
2,2'-Bipyridine in  $\text{CH}_3\text{CN}$ .



the  $\text{NO}_2$  and  $\text{Et}_3\text{P}^+$  substituents may affect the  $\sigma$  donor ligancy of the pyridyl systems in a nearly equivalent manner, phenomena which directly involve the ring  $\pi$  system of the complexes formed with these pyridyl ligands will show a greater effect by the  $\text{NO}_2$  group.

Properties of the Complexes.

The  $\text{NO}_2$  and  $\text{Et}_3\text{P}^+$  substituted bipyridines showed similar complexing tendencies toward Ru(II) and Fe(II). The tris complexes were readily obtained from the mono-substituted ligands, using the same method employed for the corresponding unsubstituted bipyridine complexes. Repeated attempts to complex Ru(II) with either of the disubstituted ligands produced only the bis complexes. The tris complex of Fe(II) with the disubstituted  $\text{Et}_3\text{P}^+$  ligand was formed, but the dinitro ligand failed to yield a definable complex. The Co(II) complexes formed were of the  $\text{CoBr}_3\text{L}$  type.

Oxidation Potentials of the Complexes

Only one wave is observed in the oxidation of these complexes. Previous studies by Bard (1973) have clearly shown that oxidation involves removal of an electron from the metal  $t_{2g}$  level and produces a species which is paramagnetic. Our results are entirely consistent with this. The oxidation potentials of the different complexes are listed in Table VII. All the oxidations are found to be reversible or quasireversible as evident from the peak separation of the cathodic and anodic curves. The  $E_{1/2}$  values are obtained by taking the average of the anodic and cathodic peak potentials.

(32)

Typical cyclic voltammogram for the oxidation of

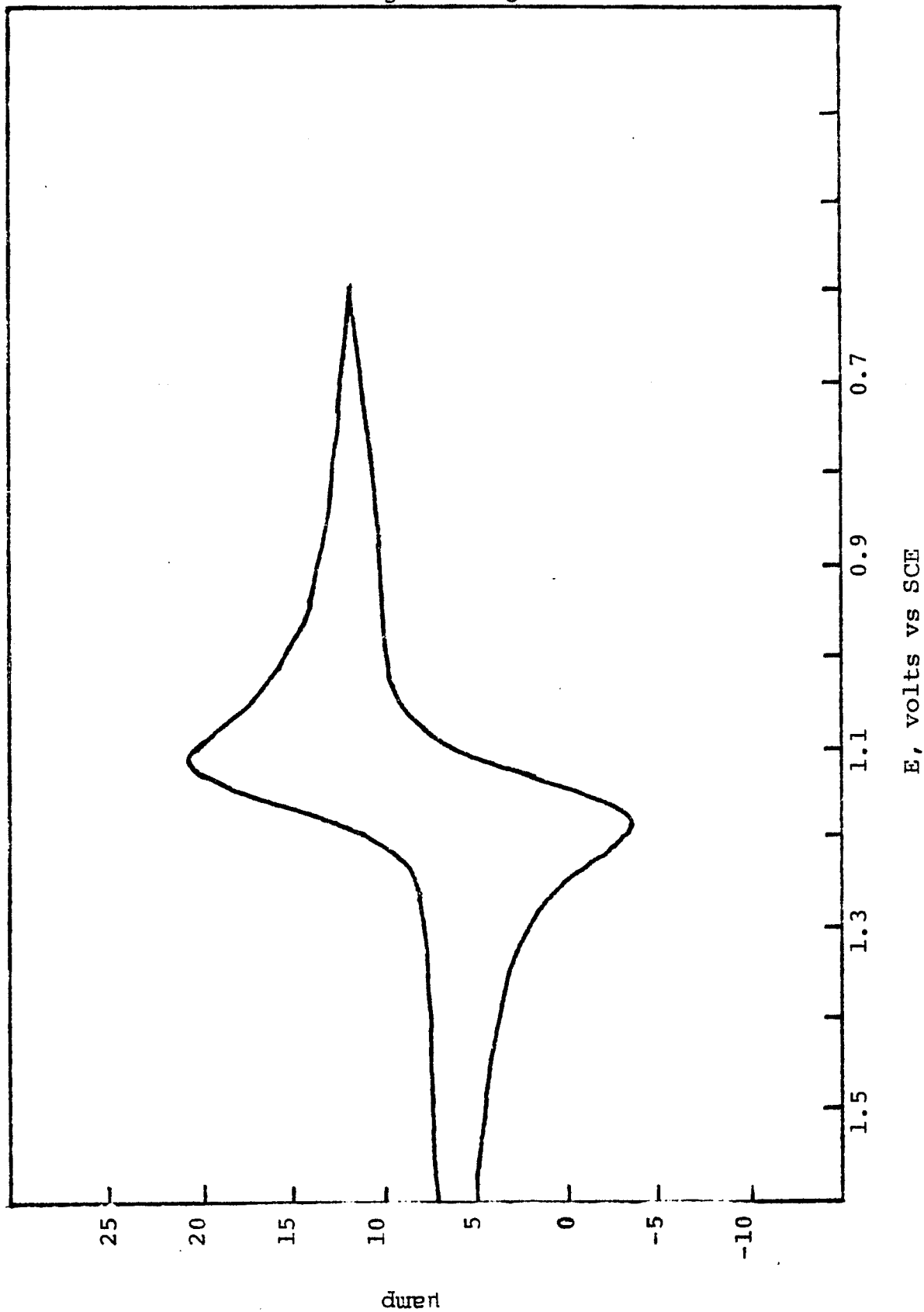
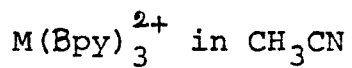


Table VII

Oxidation Potentials (via cyclic voltammetry) of Fe(II) and Ru(II) Complexes in 0.1M Tetraethylammonium Perchlorate in CH<sub>3</sub>CN.

<u>Compound</u>	<u>E<sub>1/2</sub></u>	<u>ΔE<sub>p</sub><sup>*</sup></u>
Fe(Bpy) <sub>3</sub> <sup>2+</sup>	1.06	60
Fe(NO <sub>2</sub> Bpy) <sub>3</sub> <sup>2+</sup>	1.33	70
Fe(4Et <sub>3</sub> P <sup>+</sup> Bpy) <sub>3</sub> <sup>5+</sup>	1.31	100
Fe(4,4'-diEt <sub>3</sub> P <sup>+</sup> Bpy) <sub>3</sub> <sup>8+</sup>	1.52	80
Ru(Bpy) <sub>3</sub> <sup>2+</sup>	1.29	70
Ru(NO <sub>2</sub> Bpy) <sub>3</sub> <sup>2+</sup>	1.54	80
Ru(4Et <sub>3</sub> P <sup>+</sup> Bpy) <sub>3</sub> <sup>5+</sup>	1.52	60
Ru(Bpy) <sub>2</sub> Cl <sub>2</sub>	0.35	70
Ru(4,4'-DiNO <sub>2</sub> Bpy) <sub>2</sub> Cl <sub>2</sub>	0.85	70
[Ru(4,4'-DiEt <sub>3</sub> P <sup>+</sup> Bpy) <sub>2</sub> Cl <sub>2</sub> ] <sup>4+</sup>	0.75	120

\*ΔE<sub>p</sub> = Peak separation of cathodic and anodic waves in mv.

Reduction Potentials of the Complexes.

The three waves observed in the reduction of the metal complexes are attributed to three successive reductions  $M(\text{Bpy})_3^{2+} | M(\text{Bpy})_3^+$ ,  $M(\text{Bpy})_3^+ | M(\text{Bpy})_3^0$  and  $M(\text{Bpy})_3^0 | M(\text{Bpy})_3^-$ . Previous studies by Sagi and Meyer have clearly shown that each added electron occupies a ligand  $\pi$  orbital (22,23). The reduction potential of the different complexes are listed in Table VIII. The reduction of all the complexes except those of 4-NO<sub>2</sub>-bipy were found to be reversible. In the reduction of both the NO<sub>2</sub>-bipy complexes, a desorption spike was observed in the anodic sweep. The above behavior indicates that  $ML_3^+$ , or  $ML_3^0$  species in these complexes is absorbed on platinum.

Table VIII shows that the half-wave potential difference between successive waves for every complex studied is rather small when compared with the difference between two waves in which metal d electrons are added, as reported by Dubois, Iwamoto and Kleinberg (24). This is quite reasonable if one imagines that the electron transferred in the former case occupies a ligand orbital. To a first approximation, the lowest  $\pi^*$ -orbitals in the bipyridine complexes are triply degenerate and localized in the bipyridine system. In the first three reduction waves for bipyridine complexes, each added electron may occupy one of these vacant localized  $\pi^*$ -orbitals. Electronic repulsion between the added electron can be expected to be much smaller than that

(35)

Typical cyclic voltammogram for the reduction of  
 $M(\text{Bpy})_3^{2+}$  in  $\text{CH}_3\text{CN}$

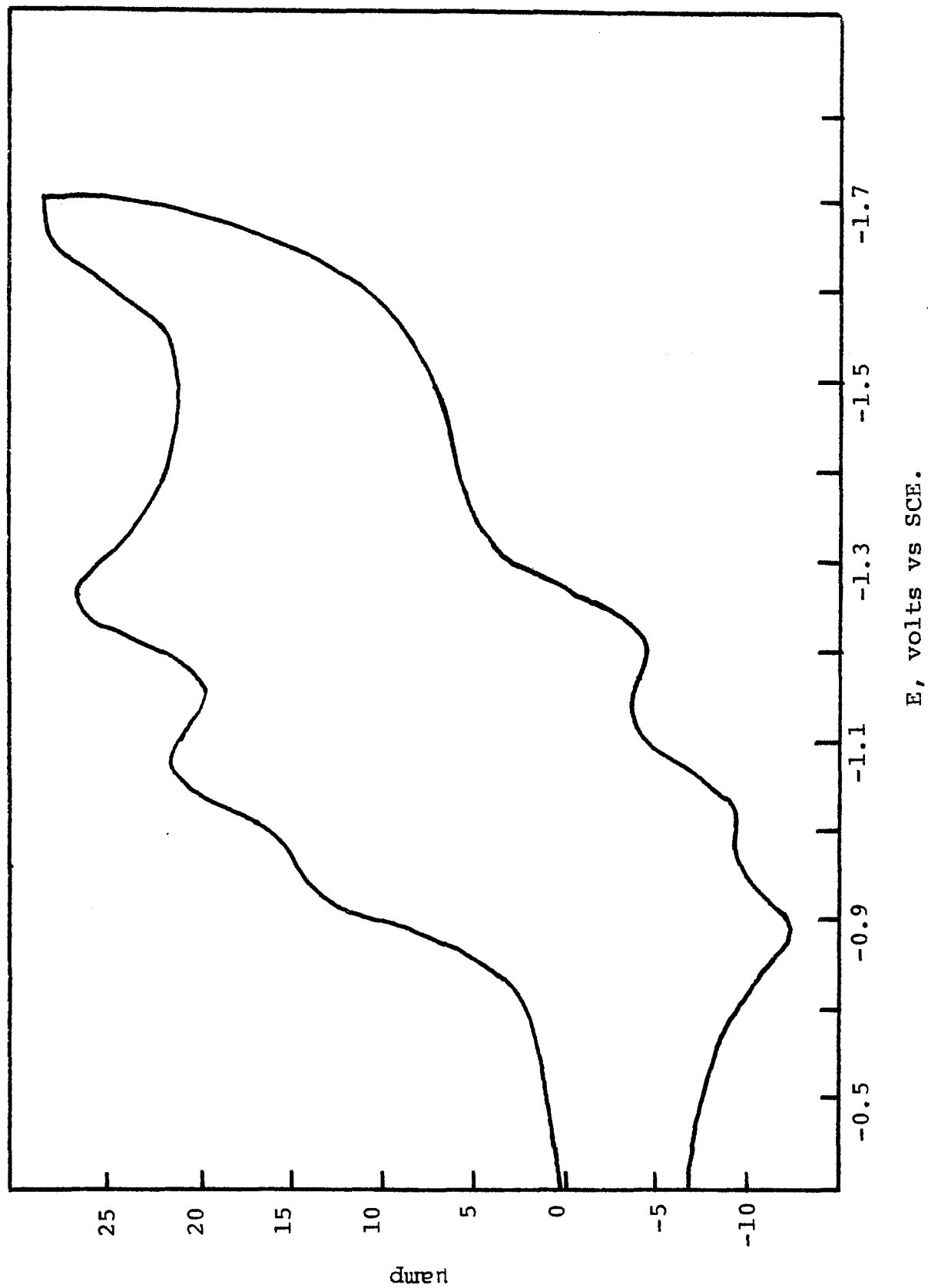


Table VIII

Reduction Potentials of Fe(II) and Ru(II) Complexes in 0.1M Tetraethylammonium Perchlorate in CH<sub>3</sub>CN.

A) Half wave potential in volts vs SCE.<sup>a)</sup>

B) Peak separation in mv

<u>Compound</u>	<u>1st Wave</u>		<u>2nd Wave</u>		<u>3rd Wave</u>	
	<u>A</u>	<u>B</u>	<u>A</u>	<u>B</u>	<u>A</u>	<u>B</u>
Fe(Bpy) <sub>3</sub> <sup>2+</sup>	-1.40	65	-1.59	60	-1.89	80
Fe(NO <sub>2</sub> Bpy) <sub>3</sub> <sup>2+</sup> b)	-0.64		-0.93			
Fe(4Et <sub>3</sub> P <sup>+</sup> Bpy) <sub>3</sub> <sup>5+</sup>	-0.96	80	-1.07	65	-1.25	65
Fe(4,4'-DiEt <sub>3</sub> P <sup>+</sup> Bpy) <sub>3</sub> <sup>8+</sup>	-0.74	70	-0.84	70	-0.98	60
Ru(Bpy) <sub>3</sub> <sup>2+</sup>	-1.40	70	-1.58	60	-1.83	70
Ru(NO <sub>2</sub> Bpy) <sub>3</sub> <sup>2+</sup> b)	-0.63		-1.33			
Ru(4Et <sub>3</sub> P <sup>+</sup> Bpy) <sub>3</sub> <sup>5+</sup>	-0.96	70	-1.07	70	-1.27	60

a) Half wave potentials obtained by taking average of anodic and cathodic peak potentials.

b) These couples are electrochemically irreversible.

between electrons in partially filled  $t_{2g}$  orbitals. This conclusion is supported to a certain extent by spectroscopic investigations by Reynolds on the complexes  $\text{Fe}(\text{Bpy})_3$  and  $\text{Fe}(\text{Bpy})_3^-$  (25,26).

### Spectra

Table IX lists the energies of the common metal  $\rightarrow$  ligand charge transfer transitions. The lowest energy or most familiar transition occurs around  $20,000 \text{ cm}^{-1}$  and is assigned to  $\pi^*(1) \leftarrow t_2$  by Bryant and Lytle (27,28). It is characterized by  $\log \epsilon$  values in the range 3.9-4.0 for the  $(\text{Bpy})_3\text{Fe}(\text{II})$  complexes and 4.1-4.25 for the  $(\text{Bpy})_3\text{Ru}(\text{II})$  complexes. Moreover the high energy shoulder which is observed for the unsubstituted bipyridyl complex is present in the other substituted tris (bipyridyl) spectra as well, though barely discernible in some cases. The transition energies in the tris(bipyridyl) spectra show little effect of changing solvent, while the spectra of the bis(bipyridyl) ruthenium(II) complexes show a substantial solvent shift, in agreement with previous observations made by Meyer and Fergusson (29,30). The tris complexes of  $\text{Ru}(\text{II})$  show larger transition energies than the corresponding  $\text{Fe}(\text{II})$  complexes, which is accounted for by the lower energy of the  $\text{Ru}(\text{II})t_2$  orbitals, presumably due to more substantial metal-ligand  $\pi$  interaction as noted previously by Bryant and Bard (27,31).

Table IX

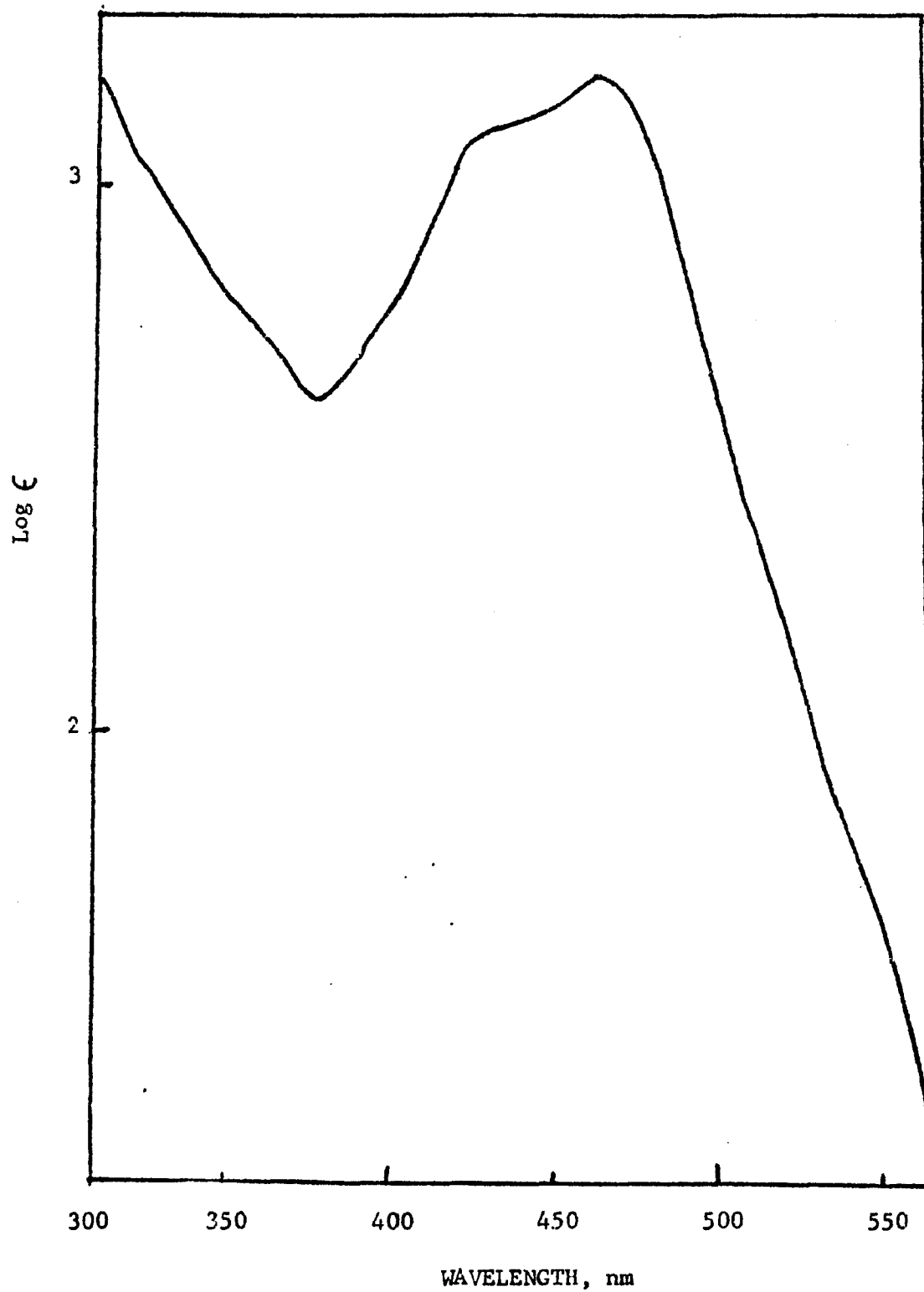
Charge-Transfer Absorption Energies of the Complexes in water and CH<sub>3</sub>CN at 25°C.

Complex	$\lambda_{\max}$ in $\text{cm}^{-1}$ in	$\lambda_{\max}$ in $\text{cm}^{-1}$ in
	$\text{H}_2\text{O} (10^{-3}\epsilon, \text{M}^{-1}\text{cm}^{-1})^a$	$\text{CH}_3\text{CN} (10^{-3}\epsilon, \text{M}^{-1}\text{cm}^{-1})^a$
$\text{Fe}(\text{Bpy})_3^{2+}$	19,120(9.0), 28,571(8.0)	19,267(9.0), 28,571(8.2)
$\text{Fe}(\text{NO}_2\text{Bpy})_3^{2+}$	17,605(4.2)	17,762(9.4)
$\text{Fe}(\text{4Et}_3\text{P}^+\text{Bpy})_3^{5+}$	18,484(10.5)	18,518(8.0)
$[\text{Fe}(4,4'\text{-DiEt}_3\text{P}^+\text{Bpy})_3]^{8+}$	18,450(7.0), 26,316(6.5)	18,382(5.5), 26,316(6.2)
$\text{Ru}(\text{Bpy})_3^{2+}$	22,321(13.2)	22,272(12.06)
$\text{Ru}(\text{NO}_2\text{Bpy})_3^{2+}$	20,576(15.0)	20,661(16.4)
$\text{Ru}(\text{4Et}_3\text{P}^+\text{Bpy})_3^{5+}$	21,459(18.25)	21,505(18.0)
$\text{Ru}(\text{Bpy})_2\text{Cl}_2$	20,492(3.1), 29,439(2.95)	18,116(5.8), 26,666(6.4)
$\text{Ru}(4,4'\text{-DiNO}_2\text{Bpy})_2\text{Cl}_2$	17,452(5.3), 21,978(4.8)	16,234(7.6), 20,618(6.4)
$[\text{Ru}(4,4'\text{-DiEt}_3\text{P}^+\text{Bpy})_2\text{Cl}_2]^{4+}$	18,182(15.5), 25,125(14.7)	16,806(17.1), 23,529(14.6)
$\text{Et}_4\text{N}^+[\text{CoBr}_3\text{NO}_2\text{Pyr}]$	26,315 <sup>b</sup>	
$\text{CoBr}_3(\text{Et}_3\text{P}^+\text{Pyr})$	28,653 <sup>b</sup>	

a) + 10%, + 2 nm    b) Obtained with a Cary Model 14 spectrophotometer as Nujol mulls spread on filter paper.

(39)

Absorption spectrum of  $\text{Ru}(\text{Bpy})_3^{2+}$  in EtOH.



A second, less familiar transition is observed in the 27,000  $\text{cm}^{-1}$  region of the spectra of some Fe(II) complexes (some structure is discernible in this area in the other Fe(II) spectra, but with a much lower intensity). The inconsistency in appearance of this band, plus the inability to observe it in the tris(bipyridyl) ruthenium spectra, make the origin of the transition ambiguous, but it had been assigned to a charge transfer from the metal  $t_2$  orbital into the second ring  $\pi^*$  orbital by Bryant and Lytle (27,28).

The bis complexes show both bands clearly as reported previously by Meyer and Fegusson, and this observation was useful in the present work as evidence for the formulation of these complexes as bis(bipyridyls) (29,30).

It is most important for our work to note the effect of the various substituents on the electronic data. In the tris complexes of both metals, the  $\text{NO}_2$  substituent shows twice the effect of the  $\text{Et}_3\text{P}^+$  in lowering the energy of the charge transfer, despite the positive charge on the latter. (This effect is smaller in the bis complexes). Thus the  $\text{NO}_2$  exhibits the greater withdrawing effect on the ring  $\pi$  system, resulting in a lowering of the  $\pi^*$  orbital energy beyond that shown by  $\text{Et}_3\text{P}^+$ .

As noted in the previous study by Weiner & Schwartz on the  $[\text{CoBr}_3\text{L}^-]$  system, the  $\text{Et}_3\text{P}^+$  substituted pyridine complex of Co(II) showed an absorption at 28,650  $\text{cm}^{-1}$ , which was assigned as before to a metal  $\rightarrow$  pyridine charge transfer transition (7). This band was missing in  $\text{Et}_4\text{N}^+[\text{Co}(\text{C}_5\text{H}_5\text{N})^-]$

$\text{Br}_3]^-$ , and was assumed to be obscured by the  $\text{Br} \rightarrow \text{Co}$  transitions at  $34,000\text{-}37,000 \text{ cm}^{-1}$ . In the present work, the  $\text{NO}_2$  substituted pyridine complex clearly showed this transition, at  $26,320 \text{ cm}^{-1}$ . Thus in this pyridyl system, the  $\text{NO}_2$  group again is more effective in lowering the metal-ligand charge transfer (MLCT) energy.

P. Ford et al. have measured substituent effects on MLCT energies in systems such as  $\text{Ru(II)(NH}_3)_5\text{L}$  and Peterson has performed similar measurements in systems like  $\text{Fe(II)-(CN)}_5\text{L}$ , where the ligands L were various cationic pyridine and pyrazine systems (ie. the pyrazinium ion,  $\text{PyH}^+$ , the N-methylpyrazinium ion, and the 4-pyridylpyridinium ion) (32,33). The lowering in MLCT energy for these complexes from the complexes of the corresponding unsubstituted ligands appears to be somewhat greater than the shifts found in the present study. This may be attributable to the pentamine and pentacyano moieties, where a greater amount of charge is donated to the central metal, raising the metal donor orbital energy and making the MLCT energy more susceptible to changes at the acceptor pyridyl ligand. A recent measurement of the MLCT energy for the  $\text{Ru(Py)}_6^{2+}$  ion ( $29,300 \text{ cm}^{-1}$ ) by Tempteton allows a comparison with the lower value of  $24,500 \text{ cm}^{-1}$   $\text{Ru(NH}_3)_5\text{Py}^{2+}$  reported by Ford, indicating the raised donor orbital energy in the latter complex (34,35). The effect of ligand substituents and of varying the central metal on the MLCT energies is further explained by considering

the redox energies of the complexes (Tables VII and VIII). Our results are consistent with previous studies which have clearly shown that oxidation of these complexes takes place at the metal, while the two lowest energy reductions take place into  $\pi$  orbitals largely centered on the rings. The reduction potentials listed are substituent dependent, but independent of whether the central ion is Fe(II) or Ru(II). Furthermore, the order of the first wave reduction potentials parallels the order of the charge transfer energies for the complexes of a given metal. Thus, while both electron withdrawing substituents lower the potential for reduction of the rings (lower the energy of the LUMO), the effect of  $\text{NO}_2$  is approximately double that of  $\text{PR}_3^+$ . On the other hand, while both substituents raise the potential necessary for oxidation, because of their electron withdrawing effect on the metal, there is no difference between the two substituents. This relates to the comparable  $\text{pK}'\text{s}$  of the bipyridine bases containing the two substituents. The nature of the central metal does effect the oxidation potential however, since the differing metal  $\rightarrow$  ligand  $\pi$  bonding tendencies result in the lowering of the energy of the Ru(II) filled d orbitals more than the Fe(II), and if oxidation takes place at the metal, then this serves to raise the potential necessary for oxidation of the Ru(II). Note that the bis complexes have substantially lower oxidation potentials, showing the effect of reducing the positive charge on the metal by replacing a neutral

bipyridyl ligand with  $\text{Cl}^-$ . (Although direct comparisons of the charge transfer energies for bis and tris bipyridyl complexes are difficult, the former seem to have generally lower MLCT energy values as a consequence of the reduced positive charge on the metal.)

The total picture presented in this work is quite self consistent, and provides an insight into the effect of cationic substituents that has been puzzling us for sometime. The cationic phosphonium substituent reduces the ligancy of the pyridyl bases, but not to any greater extent than electron withdrawing neutral substituents. Therefore it shows no greater influence on those characteristics of the complex which depend on the ligancy of the base. On the other hand, the neutral  $\text{NO}_2$  substituent, which exerts a greater withdrawing effect on the ring  $\pi$  system, lowers the LUMO of the complexes more than  $\text{R}_3\text{P}^+$ , and therefore has a greater influence on the properties which depend on the energy of the LUMO.

Eaborn has suggested that the difference between the electron withdrawing effect of the two substituents on an attached aryl system becomes more exaggerated in favor of  $\text{NO}_2$  as the availability of negative charge to the aryl-system is increased (36). For example, in the acid desilylation of  $\text{P-XC}_6\text{H}_4\text{SiMe}_3$ , the  $\text{Me}_3\text{P}^+$  substituent is more deactivating via electron withdrawal than  $\text{NO}_2$ , while in the cleavage of  $\text{P-XC}_6\text{H}_4\text{CH}_2\text{SiMe}_3$  with base, deactivation by the  $\text{NO}_2$  group is substantially greater. The latter reaction

involves the formation of the benzyl carbanion,  $P-XC_6H_4CH_2^-$ , which can be stabilized to a greater extent by the  $NO_2$  substituent. In the MLCT and reduction potential measurements obtained in the present study, negative charge is introduced directly into the ring, perhaps providing a situation with an even greater  $\pi$  electron availability than is found in the usual experiments on substituent effects.

A real comparison of substituent  $\sigma$  values is difficult to make in this case because of the differing reaction conditions used in their measurement, and different values are often quoted from different sources. From  $^{19}F$  NMR measurements on substituted fluorobenzenes in dimethylsulfoxide as reported by Taft, Johnson and Jones,  $\sigma_i$  (inductive) constants were obtained as 0.43 and 0.53 for  $Me_3P^+$  and  $NO_2$  respectively (37a,b,38). Values of  $\sigma_R$  (conjugative) were obtained as 0.20 and 0.24 for  $Me_3P^+$  and  $NO_2$  respectively. Summing these values yields  $\sigma_p$  constants of 0.63 and 0.77 for the two substituents. From measurements of the ionization constants of substituted phenols or anilines, values of  $\sigma^-$  (substituent constant in the presence of enhanced electron availability) were obtained as 1.02 (phenol) or 0.95 (dimethylaniline) for the  $Me_3P^+$  substituents, and 1.27 for  $NO_2$  (39,40,41). Thus, the small difference in  $\sigma_p$  values between the two substituents (0.14) is increased to 0.28 when  $\sigma^-$  is used as the criterion for electron withdrawing behavior.

It is therefore suggested that this difference is even further exaggerated when considering the MLCT energies and reduction potentials presented in this work.

The use of substituents on ligand positions remote from the coordination site allows one to examine a series of complexes displaying wide variations in the ligand properties (i.e.  $\sigma$ -donor ability,  $\pi$  acceptor/ $\pi$  donor character etc.) yet having the same stereochemical environment at the coordination site. Such perturbations of ligand properties not only may lead to systematic variations of metal-ligand bonding in the ground and excited states but also in some cases can be used to tune excited state energies (42a,b).

Part II

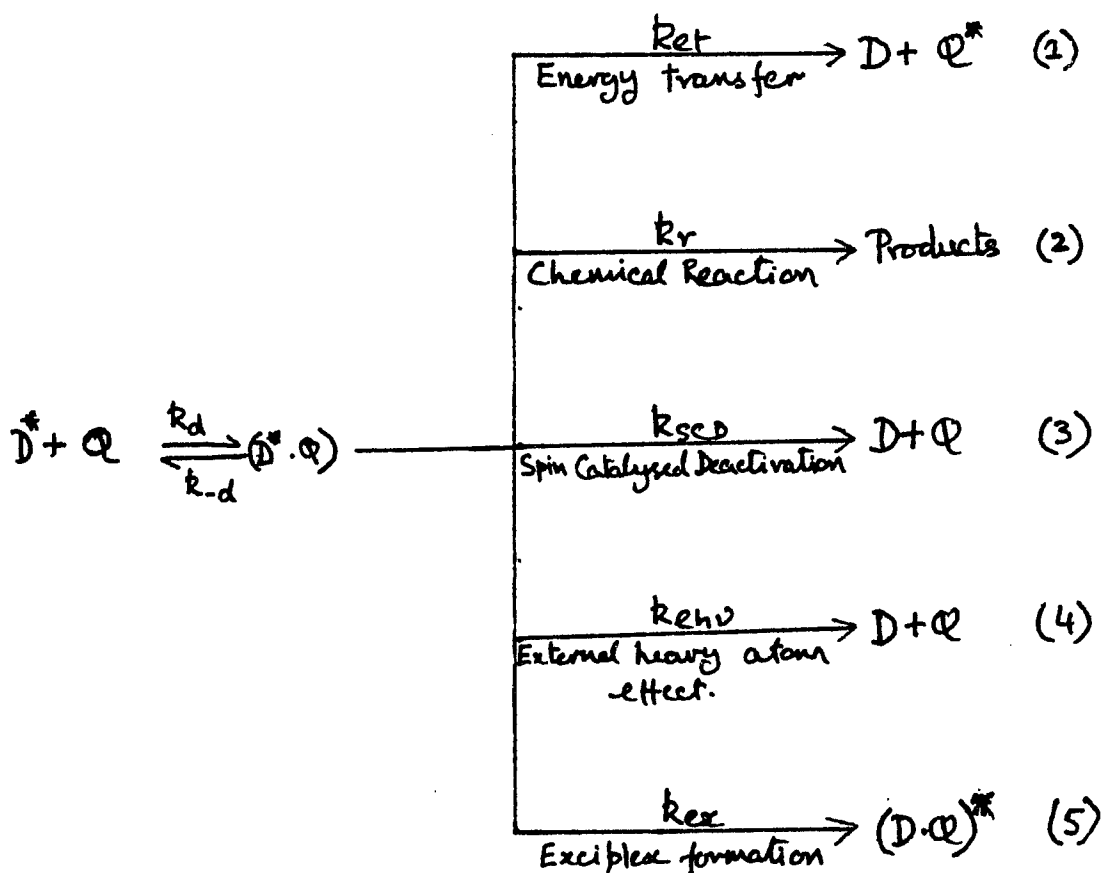
Study of the Photochemistry of Ru(II) Substituted-  
Bipyridine Complexes by Flash Photolysis Techniques

### Introduction

Pressed by the dwindling fossil fuel reserves, and spurred by the fascination with the role of radiant energy on the environment, an extraordinary interest in the photophysical and photochemical processes of a wide variety of compounds has developed. In recent years, this surge of interest and activity has led to some progress in the understanding of the chemistry of the excited state. The development and continued growth of this understanding arises from a detailed knowledge of not only those states which are observed in the absorption spectrum, but also those states where direct population by absorption of light energy is forbidden by various selection rules. In the field of organic chemistry sensitization and quenching techniques have been shown to be powerful tools in obtaining information on these excited states (43). Recently these techniques have been introduced with some success as probes of the interesting, but varied photophysical and photochemical behavior of transition metal complexes (44).

In fluid solution, sensitization or quenching reaction takes place by two basic mechanisms: 1) dynamic quenching (diffusional quenching) where the donor and quencher diffuse to within a reaction volume, or 2) static quenching (associative quenching) where the donor and quencher form a nonluminescent pair dictated by a thermal equilibrium. A dynamic quenching process is a bimolecular interaction

between an electronic excited state of a donor and a ground state quencher, in which the donor is deactivated or converted into a different compound. As indicated by equation 1 through 5, the quenching of an excited molecule may take place by several distinct mechanisms, the most important of which are: 1) electronic energy transfer (2) chemical reaction (3) spin-catalyzed deactivation, (4) external heavy-atom effect, and (5) complex (excimer and exciplex) formation.



$\text{D}^*$  represents an excited donor and  $\text{Q}$  represents a quencher. The rate constants  $k_d$  and  $k-d$  describe the formation and dissociation of an encounter pair indicated by the brackets. The brackets are not intended to imply

composition or structure but simply imply that  $D^*$  and  $Q$  exist within an effective reaction volume or solvent cage for some finite period of time.

1) Electronic Energy Transfer.

In fluid solutions, electronic energy transfer, equation 1, may occur by means of coulombic (dipole-dipole) or by exchange interaction. A coulombic interaction can take place over an intermolecular distance much larger than the molecular diameter. It is important, however, only in the case in which the transitions in the donor and acceptor are spin allowed. The exchange interaction, on the other hand, can only take place over distances of the order of the collision diameters. Its magnitude, however, is not related to the oscillator strength of the transition in either the donor or the acceptor. The low energy ligand-field absorption bands of transition metal complexes are Laport forbidden. It has been suggested that coulombic interactions would play a small role in an energy transfer process. Therefore, with most transition metal complexes, energy transfer occurs by an exchange interaction requiring a collisional mechanism.

The results available show that transition metal complexes can participate in the energy transfer processes as both donors and acceptors (45,56,47). Excitation of  $Ru(Bpy)_3^{2+}$  in the presence of  $Cr(CN)_6^{3-}$  results in emission characteristic of the Cr(III) complex (48). This sensitized

emission establishes an energy transfer process.

## 2) Chemical Reaction

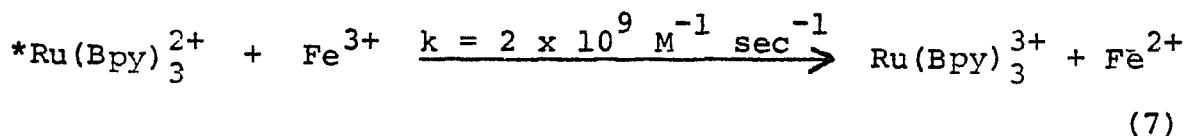
Unlike the complex radical reactions which occur with organic donors and acceptors, sensitization of transition metal complexes induces ligand substitution, isomerization and redox reaction modes. Although postulated in a number of systems, quenching via a chemical mechanism has been unambiguously established in relatively few cases.

For example, the luminescent charge transfer state of  $\text{Ru}(\text{Bpy})_3^{2+}$  is efficiently quenched by  $\text{Tl}^{3+}$  (49). The emission spectrum of  $\text{Ru}(\text{Bpy})_3^{2+}$  establishes that the luminescent charge-transfer state lies at energies  $\leq 19$  kK. Since the excited states of  $\text{Tl}^{3+}$  have energies  $\leq 30$  kK an energy transfer process would be extremely endothermic and can be ruled out. The appearance of the electron transfer products,  $\text{Ru}(\text{Bpy})_3^{3+}$  and  $\text{Tl}^{2+}$ , however, led to the suggestion that quenching occurs via a redox mechanism, equation 6.

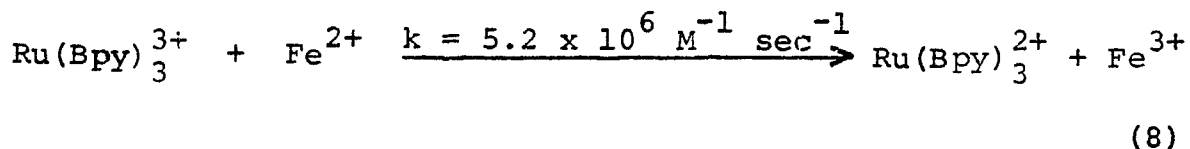


$\text{Tl}^{2+}$  is unstable and rapidly disproportionates to  $\text{Tl}^{3+}$  and  $\text{Tl}^{+1}$ . With many systems, quenching via an electron transfer mechanism can not be established simply by the reaction stoichiometry. For example, photolysis of  $\text{Ru}(\text{Bpy})_3^{2+}$  in the presence of  $\text{Fe}^{3+}$  leads to no net chemical change (50). Flash photolysis experiments, however, show an efficient electron transfer quenching reaction, equation 7

(51)

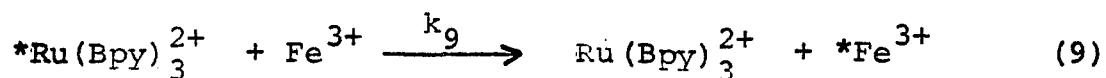


followed by a rapid reverse reaction equation 8 (51).

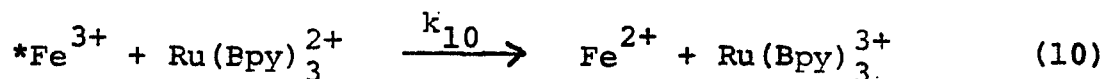


Thus, the absence of electron transfer products does not necessarily negate, the occurrence of an electron transfer process.

Unfortunately, the observation of electron transfer products does not in itself unambiguously establish the quenching mechanism. An energy transfer mechanism might be postulated where the first step would be energy transfer from  $*Ru(Bpy)_3^{2+}$  to  $Fe^{3+}$ , equation 9.



A suitable acceptor state in  $Fe^{3+}$  lies at an energy of 12.3 kK. If one further assumes that  $*Fe^{3+}$  is a strong oxidant, equation 9 could be followed by an electron transfer reaction, equation 10.

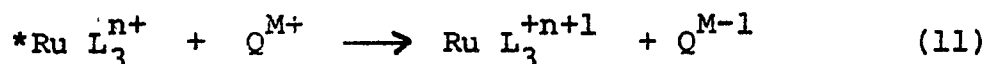


The products are the same in both quenching schemes, but the dynamics of the two schemes are different. In the first scheme, equation 7, the oxidation of the  $*Ru(Bpy)_3^{2+}$  would take place at the same rate as the quenching reaction. In the second scheme, however, if  $k_{10} < k_9$ , the rate of

oxidation of  $*\text{Ru}(\text{Bpy})_3^{2+}$  would be less than the quenching rate. Thus, kinetically the reaction mechanisms can be distinguished. Of course, if  $k_{10} > k_9$ , an experimental distinction between the two schemes would not be possible. Lin and Sutin, however, have used an ingenious series of steady state experiments which provide strong evidence for the first scheme. It was suggested by these investigators that most (if not all) of the quenching events result in electron transfer from the excited ruthenium(II) to the iron(III) (52).

The other three methods of energy transfer play very little role in the case of the transition metal complexes and hence are not discussed here.

In this section, the results of experiments in which the quenching of  $\text{Ru}(\text{Bpy})_3^{2+}$  and  $\text{Ru}(\text{Et}_3\text{P}^+\text{Bpy})_3^{5+}$  by the uncomplexed ligands and various Co(III) complexes are described. Transient Ru(III) complexes observed in flash photolysis experiments characterized the quenching mechanism as a photo induced redox reaction 11,



The asterisk denotes the MLCT state of the complex, L denotes bpy and  $\text{Et}_3\text{P}^+\text{Bpy}$ , and Q denotes the quencher. Similar experiments were attempted with  $\text{Ru}(\text{NO}_2 \text{Bpy})_3^{2+}$ , but unlike the nitro-substituted phenanthroline complexes of Ru(II), the observed emission spectrum was found to be solvent dependent. A series of experiments in various

EtOH-H<sub>2</sub>O mixtures indicate that Ru(NO<sub>2</sub> Bpy)<sub>3</sub><sup>2+</sup> is not luminescent. Rather, the luminescence which is observed when the complex is dissolved in 95% EtOH is due to the solvolysis product Ru(EtO Bpy)<sub>3</sub><sup>2+</sup>.

## Experimental

### Instrumentation and Photochemical Apparatus

#### A. Physical Measurements

Ultraviolet and visible spectra were recorded on a Cary 14 spectrophotometer. Luminescence measurements were recorded on a Perkin-Elmer Hitachi MPF-2A fluorescence spectrophotometer equipped with either a Hamamatsu R 106 or a red sensitive Hamamatsu R 818 photomultiplier. For low temperature luminescence measurements, the sample holder was adjusted to hold a small Dewar flask and the sample was placed in a 3 mm glass tube and inserted in the Dewar containing liquid N<sub>2</sub>. At room temperature, 10x10x40 mm, fused quartz cells, were used in the luminescence measurements. The cells were equipped with a 14/20 ground glass joint and could be fitted to pyrex upper sections. The pyrex upper section had a vacuum stopcock and a 10 ml side-arm for degassing the solution by freeze-thaw techniques. The cell was connected through a 10/30 ground glass joint to a vacuum line. The vacuum line was equipped with an oil diffusion pump, and could be pumped down to a pressure of  $\leq 10^{-5}$  torr. Often times, the solutions were deaerated by bubbling N<sub>2</sub>.

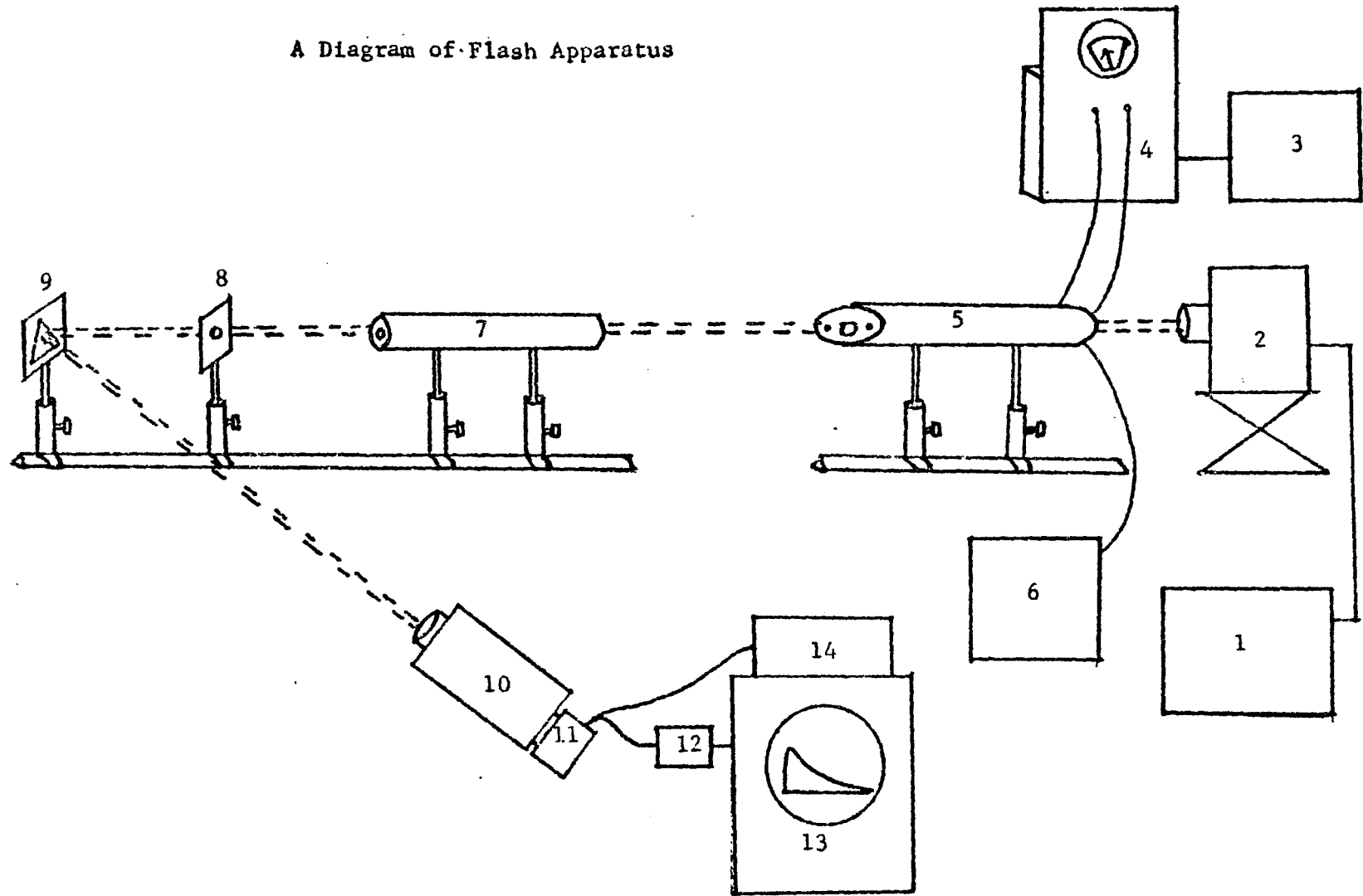
#### B. Flash Experiments

The flash apparatus used in these experiments is of the general design described by Porter and Linchitz and used in a kinetic-spectrophotometric mode (53,54). A diagram of

the flash apparatus is shown in figure 1. The two flash lamps, Xenon Corp. Model FP-100C, are connected in series and across a Sangamo 10  $\mu$ f capacitor by five inch cables to minimize circuit inductance. The capacitor is charged by a Spellman Model RG 10 regulated high voltage power supply. The voltage applied to the capacitor could be varied to dissipate 100- to 500-J per flash. The photolyzing flash, triggered externally with a Xenon Corp. Model C trigger module, has a rise time of 5  $\mu$ sec, a half peak duration of 10  $\mu$ sec, and a total duration of 25 to 30  $\mu$ sec. Following the flash, the chemical change is detected by monitoring the change in intensity of a collimated beam of light from a 100-W high pressure Xe lamp powered by a sola filtered DC power supply. The light beam from the Xe lamp is passed through the center of the reaction cell, a light baffle and on to a mirror which reflects the beam onto the entrance slit of a Bausch and Lomb Model 33-86-76 grating monochromator. The change in intensity of the analyzing beam at a given wavelength is then monitored by an RCA 31034 or Hamamatsu R 818 photomultiplier tube powered by a Pacific Photometric Instruments Model 203 regulated negative high voltage power supply. The photomultiplier current is dropped across a 150 k $\Omega$  resistor and the change in voltage as a function of time is displayed on a Hewlett-Packard Model 175A oscilloscope. The oscilloscope sweep is triggered by inductive coupling with the photolyzing flash. Although the RC time constant of the detection circuit is 3.2  $\mu$ sec,

Figure 1

A Diagram of Flash Apparatus



1. Lamp power supply
2. High pressure Xe lamp
3. High voltage power supply
4. Capacitor
5. Sample holder and flash lamps
6. Trigger module
7. Light baffle
8. Shutter
9. Reflecting mirror
10. Monochromator
11. Photomultiplier
12. 150 k $\Omega$  resistor
13. Oscilloscope
14. Photomultiplier power supply

the time resolution of the apparatus is Ca. 25  $\mu$ sec because of the flash duration. For precise kinetic measurements, however, the time resolution is longer due to a tail in the flash profile.

The solution to be flashed is contained in a fused quartz cell, figure 2. The inner cylindrical sample compartment is 17 cm x 1.2 cm diameter and surrounded by an outer annulus which is 20 cm x 30 cm diameter. The flash cell is connected through a 10/30 joint to an upper section having a side-arm and vacuum stopcock.

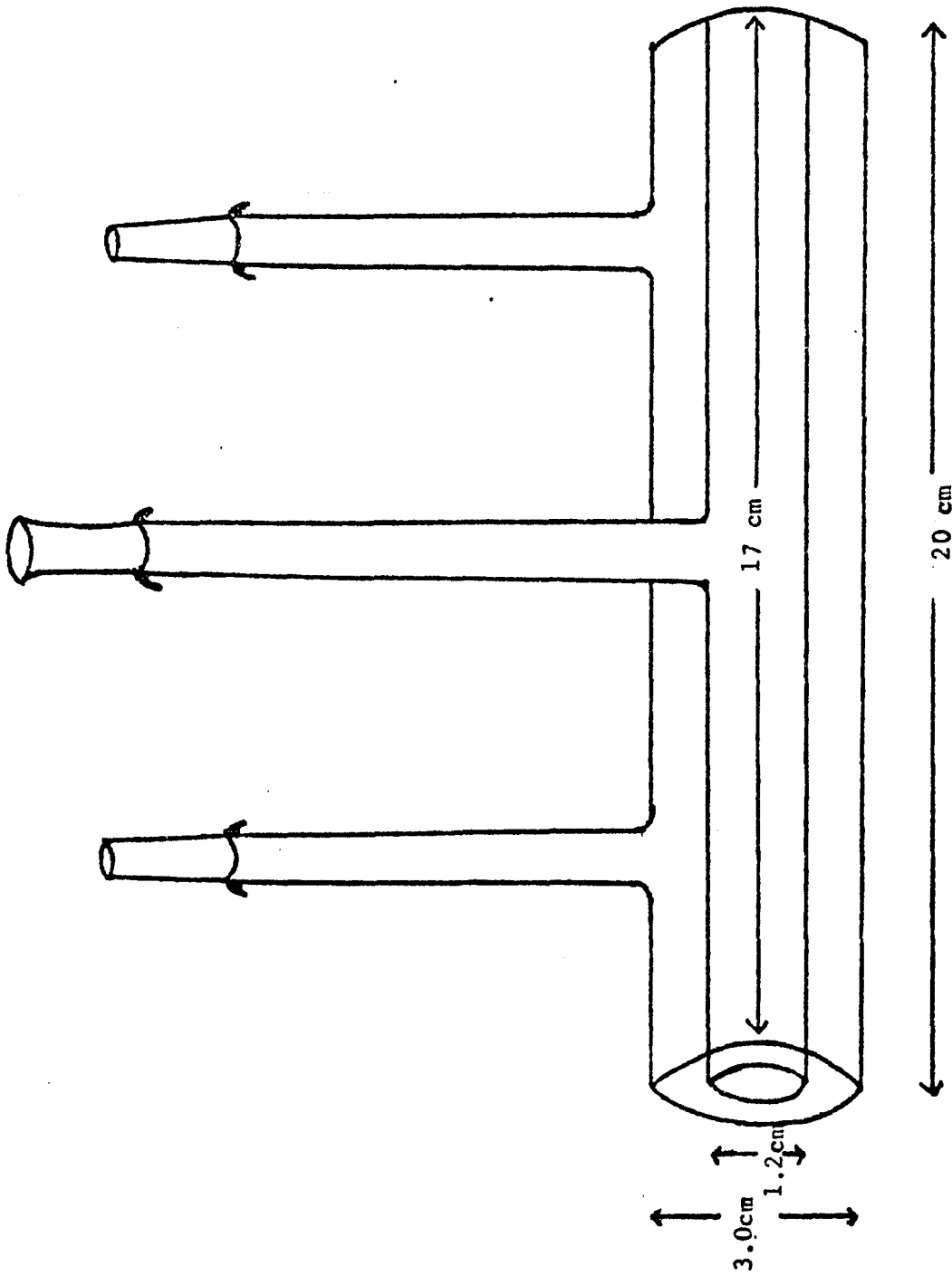
#### C. Continuous Photolysis

The light from a 350-W Illumination Industries high pressure Xenon-Mercury arc lamp was focussed on to the photolysis cell, mounted in an aluminium block. The 10x10x40 fused quartz cells used in the luminescence measurements and described in Part A, were also used as the photochemical reaction cells.

(59)

Figure 2

A Diagram of Flash Cell



Procedure

A. Quenching of  $\text{Ru}(\text{Bpy})_3^{2+}$  and  $\text{Ru}(\text{Et}_3\text{P}^+\text{Bpy})_3^{5+}$  by substituted bipyridines and  $\text{Co}(\text{Bpy})_3^{3+}$ .

In the luminescence quenching study, stock solutions containing  $3 \times 10^{-4}\text{M}$   $\text{Ru}(\text{Bpy})_3\text{Cl}_2 \cdot 6\text{H}_2\text{O}$  or  $\text{Ru}(\text{Et}_3\text{P}^+\text{Bpy})_3(\text{ClO}_4)_5 \cdot 5\text{H}_2\text{O}$  in a buffer of 0.33M aqueous  $\text{Na}_2\text{SO}_4/0.0275\text{M}$  aqueous  $\text{NaHSO}_4$  were used. Due to the limited solubility of 4- $\text{NO}_2$ Bipyridine in water, quenching experiments with this compound were done using 0.33M  $\text{Na}_2\text{SO}_4$  and 0.0275M  $\text{NaHSO}_4$  in 20% EtOH. From these stock solutions, a series of solutions,  $3 \times 10^{-5}\text{M}$  in the Ru(II) complexes and varying concentrations of the quencher, were prepared by diluting the appropriate aliquots with the solvent buffer. The maximum quencher concentrations used in these experiments were  $\sim 10^{-2}\text{M}$ . These concentrations were chosen such that at least 80% of the exciting light was absorbed by donor. Fused quartz cells equipped with degassing bulbs were used. The solutions were deaerated by passing He or  $\text{N}_2$  for about 15 minutes. To minimize the uncertainty associated with the transmission characteristics of the different cells, as well as various pairs of cell faces, all emission intensity measurements were made with a specific pair of faces of a particular cell.

Samples containing  $\text{Ru}(\text{Bpy})_3^{2+}$  were excited at 452 nm and the emission intensity monitored at 588 nm. With  $\text{Ru}(\text{Et}_3\text{P}^+\text{Bpy})_3^{5+}$  the samples were excited at 466 nm and the

(61)

emission monitored at 640 nm. The observed emission intensities were corrected for trivial absorption of the exciting and emitted light using equation 12 (55).

$$\left(\frac{I_0}{I}\right)_{\text{corr}} = \left(\frac{I_0}{I}\right)_{\text{app}} \times \frac{A_D}{A_D + A_Q} \times \frac{1 - 10^{-(A_D + A_Q)}}{1 - 10^{-A_D}} \times 10^{-0.5 A'_Q} \quad (12)$$

where  $I_0$  represents the emission intensity in the absence of the quencher and  $I$  represents the emission intensity in the presence of the quencher.  $(I_0/I)_{\text{corr}}$  is the corrected ratio of  $I_0$  and  $I$  and  $(I_0/I)_{\text{app}}$  is the measured ratio of  $I_0$  and  $I$ . The other variables in the equation represent the absorption of the donor at the exciting wavelength,  $A_D$ , and the absorption of the quencher (assuming 1 cm path length) at the exciting and emitting wavelengths,  $A_Q$  and  $A'_Q$  respectively.

### Photochemical Experiments

Since the luminescent charge transfer states of these Ru(II) complexes are known to be strong reducing agents, a number of photochemical experiments were carried out to determine if the quenching reaction leads to the formation of electron transfer products (56,57,58). An unusual aspect of an excited state electron transfer reaction of these Ru(II) complexes is that the strong reductant,  $*\text{Ru}(\text{Bpy})_3^{2+}$  is converted on electron transfer to a strong oxidant,  $\text{Ru}(\text{Bpy})_3^{3+}$  (56). (The reduction potential of  $\text{Ru}(\text{Bpy})_3^{3+}$  is 1.24v in 1M acid (59)). Thus, as discussed in the

Introduction, quenching via electron transfer may be followed by a rapid reverse reaction which leads to no net chemical change. To explore this possibility, a number of flash photolysis experiments were carried out. The flashed solutions were analyzed at 675 nm, the absorption maximum of  $\text{Ru}(\text{Bpy})_3^{3+}$ . Various parameters, such as photomultiplier voltage, slit width, and alignment of the analyzing beam, were optimized to obtain a full scale deflection on the oscilloscope graticle. The flash was then triggered and the oscilloscope trace was photographed with a Polaroid oscilloscope camera, (see Fig. 1 for flash apparatus). The kinetic data were obtained from the Polaroid photograph of the decay of the 675 nm absorption of Ru(III).

#### Preparation of $\text{Ru}(\text{Et}_3\text{P}^+\text{Bpy})_3^{6+}$

$\text{Ru}(\text{Et}_3\text{P}^+\text{Bpy})_3^{6+}$  was prepared in situ by chlorine oxidation of the corresponding Ru(II) complex. However, to prevent additional reactions such as an irreversible oxidation of the ligand, aqueous solutions of  $\text{Ru}(\text{Et}_3\text{P}^+\text{Bpy})_3^{5+}$ ,  $\sim 10^{-5}\text{M}$ , were only partially oxidized. A partial oxidation procedure was adopted because complete oxidation by extensive chlorine bubbling led to a Ru(III) complex which, on addition of  $\text{NaNO}_2$ , could not be completely reduced to the original  $\text{Ru}(\text{Et}_3\text{P}^+\text{Bpy})_3^{5+}$ . Absorption spectra of fully oxidized solutions which were then reduced with excess  $\text{NaNO}_2$  indicated irreversible chemical changes of the coordinated ligands. The extinction coefficient of

$\text{Ru}(\text{Et}_3\text{P}^+\text{Bpy})_3^{6+}$  was determined by partially oxidizing a known concentration of Ru(II) complex with  $\text{Cl}_2$ , and calculating the amount of Ru(II) oxidized from the change in absorbance at 466 nm. The absorbance at any wavelength due to a known amount of  $\text{Ru}(\text{Et}_3\text{P}^+\text{Bpy})_3^{6+}$  could then be calculated.

Preparation of  $[\text{Co}(\text{NO}_2\text{Bpy})_3](\text{ClO}_4)_3$ .

$[\text{Co}(\text{NO}_2\text{Bpy})_3](\text{ClO}_4)_3$  was prepared by procedures described in the literature for  $[\text{Co}(\text{Bpy})_3](\text{ClO}_4)_3$ , but we, like others, have found it difficult to obtain pure samples of  $\text{Co}(\text{NO}_2\text{Bpy})_3^{3+}$ . Because of the relatively low solubilities of these complexes and the similarity of the absorption spectra of these Co(II) and Co(III) complexes (60), it was difficult to spectrally characterize the oxidation state of the complex. In one preparation of the  $\text{Co}(\text{NO}_2\text{Bpy})_3^{3+}$ , 238 mg of  $\text{CoCl}_2 \cdot 6\text{H}_2\text{O}$  and 700 mg of 4- $\text{NO}_2$  bipyridine were dissolved in warm (ca. 60°C) 95% EtOH and treated with 1 ml of 30%  $\text{H}_2\text{O}_2$ . Following the effervescence, a saturated solution of  $\text{NaClO}_4$  was added and on cooling a yellowish brown precipitate was obtained. This precipitate was analyzed by the thiocyanate procedure (61) and found to have 25%  $\text{Co}(\text{NO}_2\text{Bpy})_3^{2+}$  in it. So the sample was recrystallized from water to which 5 ml of 30%  $\text{H}_2\text{O}_2$  was added. Thiocyanate analysis of this recrystallized sample indicate that the amount of  $\text{Co}(\text{NO}_2\text{Bpy})_3^{2+}$  had been reduced to <2%, and this sample was then used for all quenching studies.

Results and Discussion

The excitation and emission spectra of the substituted bipyridines were recorded at room temperature as well as liquid N<sub>2</sub> temperature. The emission spectra of all the bipyridines at room temperature and 77°K are shown in figures 3 through 8 and are listed in Table X. At 77°K, the emission spectra of these substituted bipyridines in ethanol-methanol (4:1 v/v) glass consists of a broad band with a vibrational progression. At room temperature, the energies of the emissions are somewhat different and also the vibrational fine structure is lost. For the nitro-substituted bipyridines, no emission is observed even at 77°K. In the case of bipyridine and Et<sub>3</sub>P<sup>+</sup> bipyridine, the room temperature emission is not quenched by oxygen and is attributed to fluorescence. The detailed assignment of the emission bands were not possible.

The visible absorption spectra of Ru(Bpy)<sub>3</sub><sup>2+</sup> and Ru(4Et<sub>3</sub>P<sup>+</sup>Bpy)<sub>3</sub><sup>5+</sup> are dominated by intense metal to ligand charge transfer, MLCT, transitions at 452 nm and 466 nm respectively. Figures 9 and 10 show the room temperature and liquid N<sub>2</sub> temperature emission spectra of these Ru(II) complexes. Recent studies have interpreted the luminescence as arising from three closely spaced electronic states of the unsubstituted tris(bipyridine) complex (62) (A<sub>1</sub>, E, and A<sub>2</sub> in D<sub>3</sub> symmetry). The energy spacing between these states is less than 100 cm<sup>-1</sup>.

Table X

## Emission Bands of Substituted Bipyridines

<u>Compound</u>	<u><math>\lambda</math>, nm. a)</u>	<u><math>\lambda</math>, nm. b)</u>
2,2'-Bipyridine	432	434 <sup>c)</sup>
	460	
	480	
4-Et <sub>3</sub> P <sup>+</sup> Bipyridine	439	445 <sup>d)</sup>
	469	
	488	
4,4'-diEt <sub>3</sub> P <sup>+</sup> Bipyridine	446	430 <sup>e)</sup>
	470	
	492 ( h)	

a) At liq. N<sub>2</sub> in 4:1 EtOH-MeOH glass      b) At room temp in  
 0.33M NaSO<sub>4</sub> and 0.0275M NaHSO<sub>4</sub> in H<sub>2</sub>O.      c) excitation at  
 340 nm      d) excitation at 350 nm.      e) excitation at 340  
 nm.

Emission spectrum of 2,2'-Bipyridine in aqueous

0.33M Na<sub>2</sub>SO<sub>4</sub>/0.0275M NaHSO<sub>4</sub>

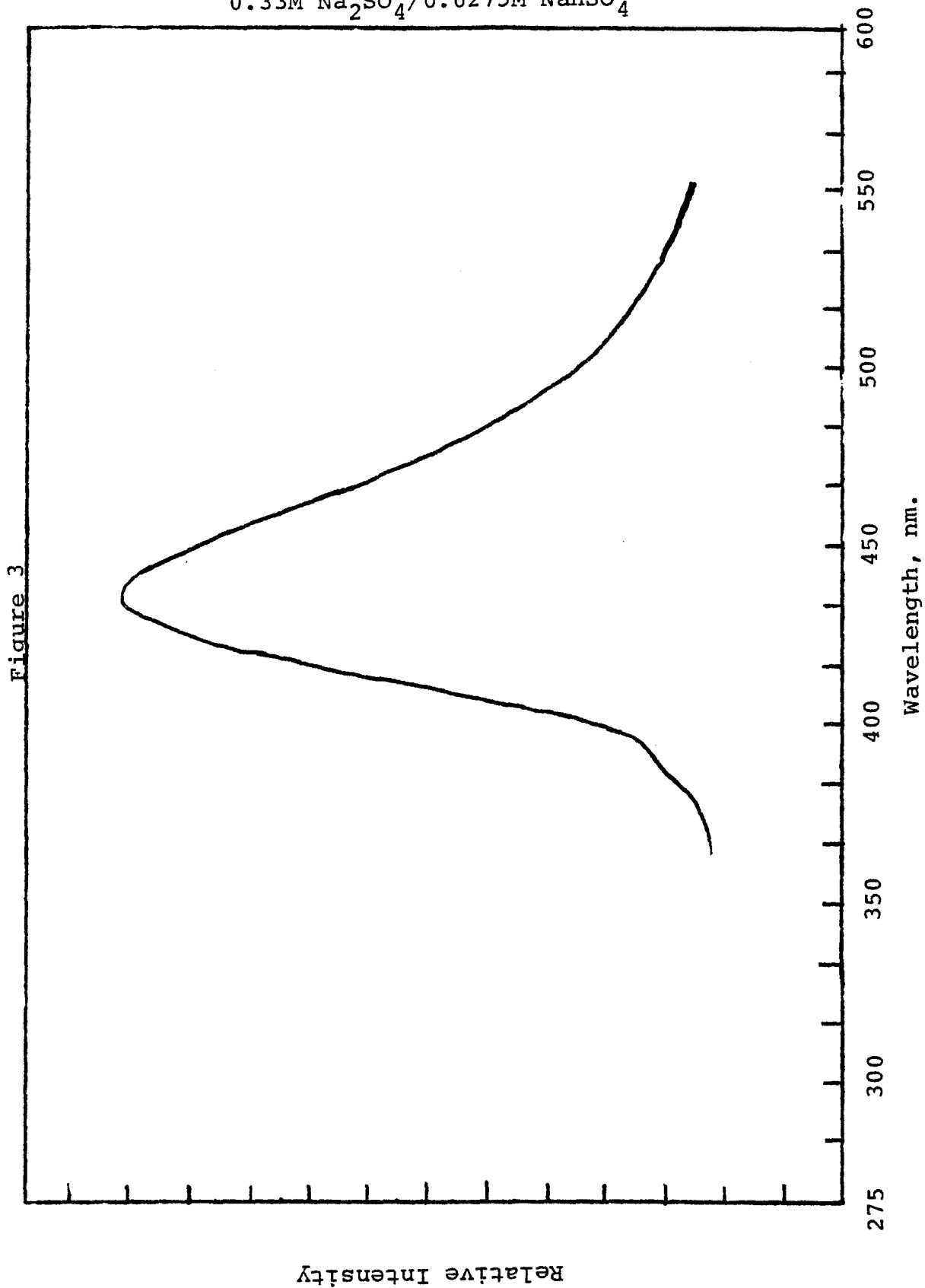
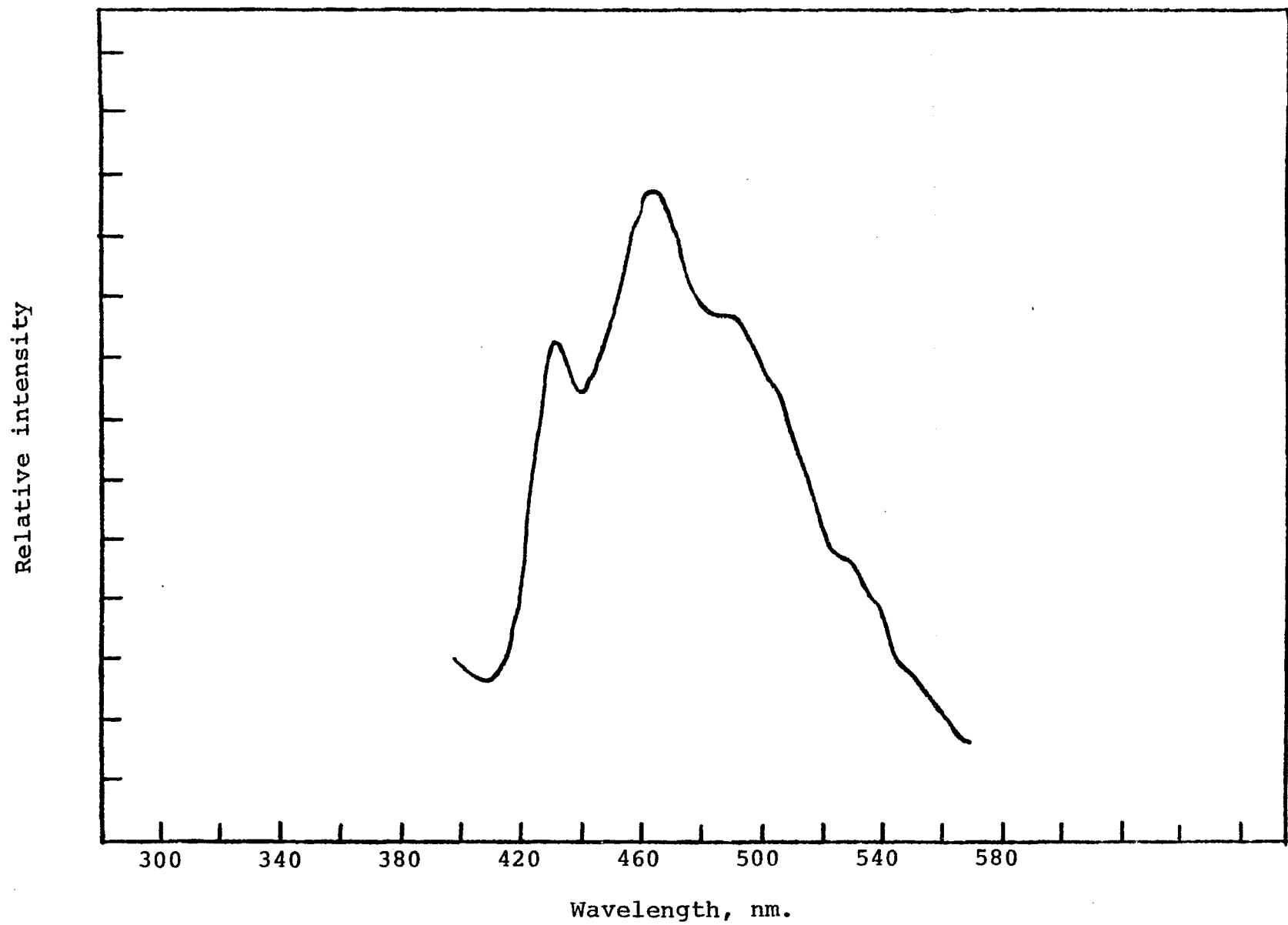


Figure 3

Figure 4



Emission spectrum of 2,2'-Bipyridine at 77°K in  
4:1 EtOH-MeOH glass

Figure 5

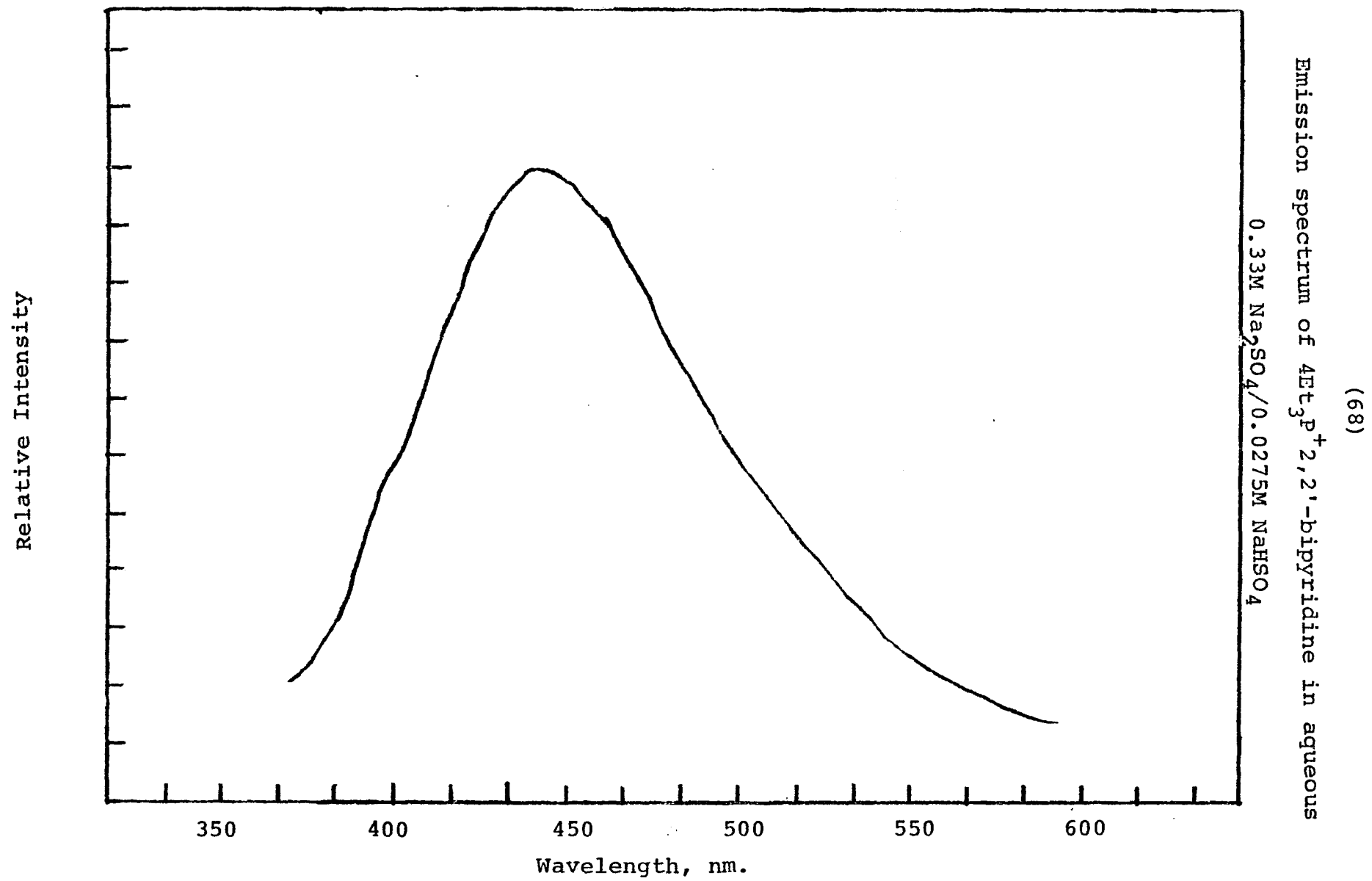
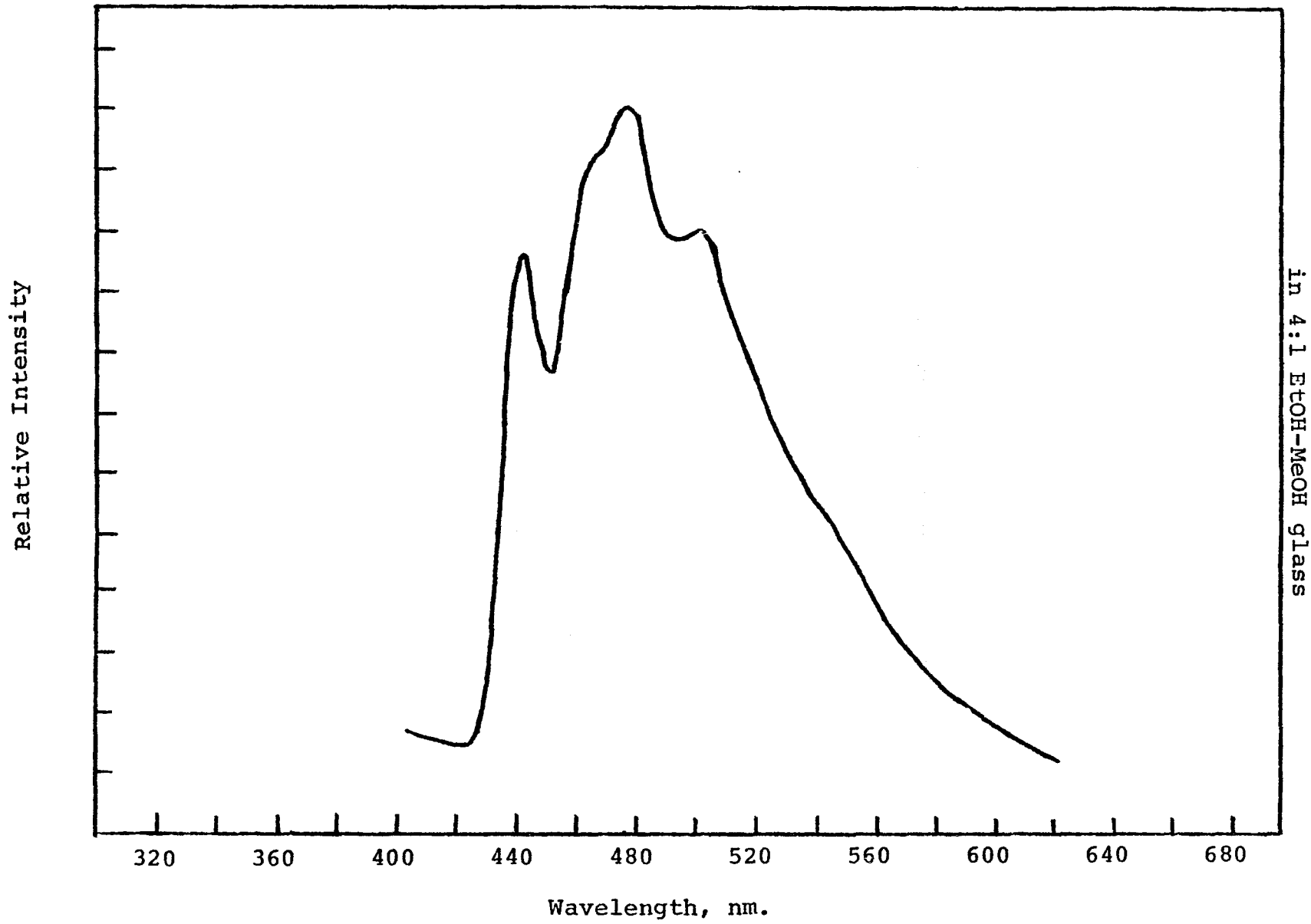


Figure 6



Emission spectrum of 4Et<sub>3</sub>P<sup>+</sup>2,2'-Bipyridine at 77°K  
in 4:1 EtOH-MeOH glass

Figure 7

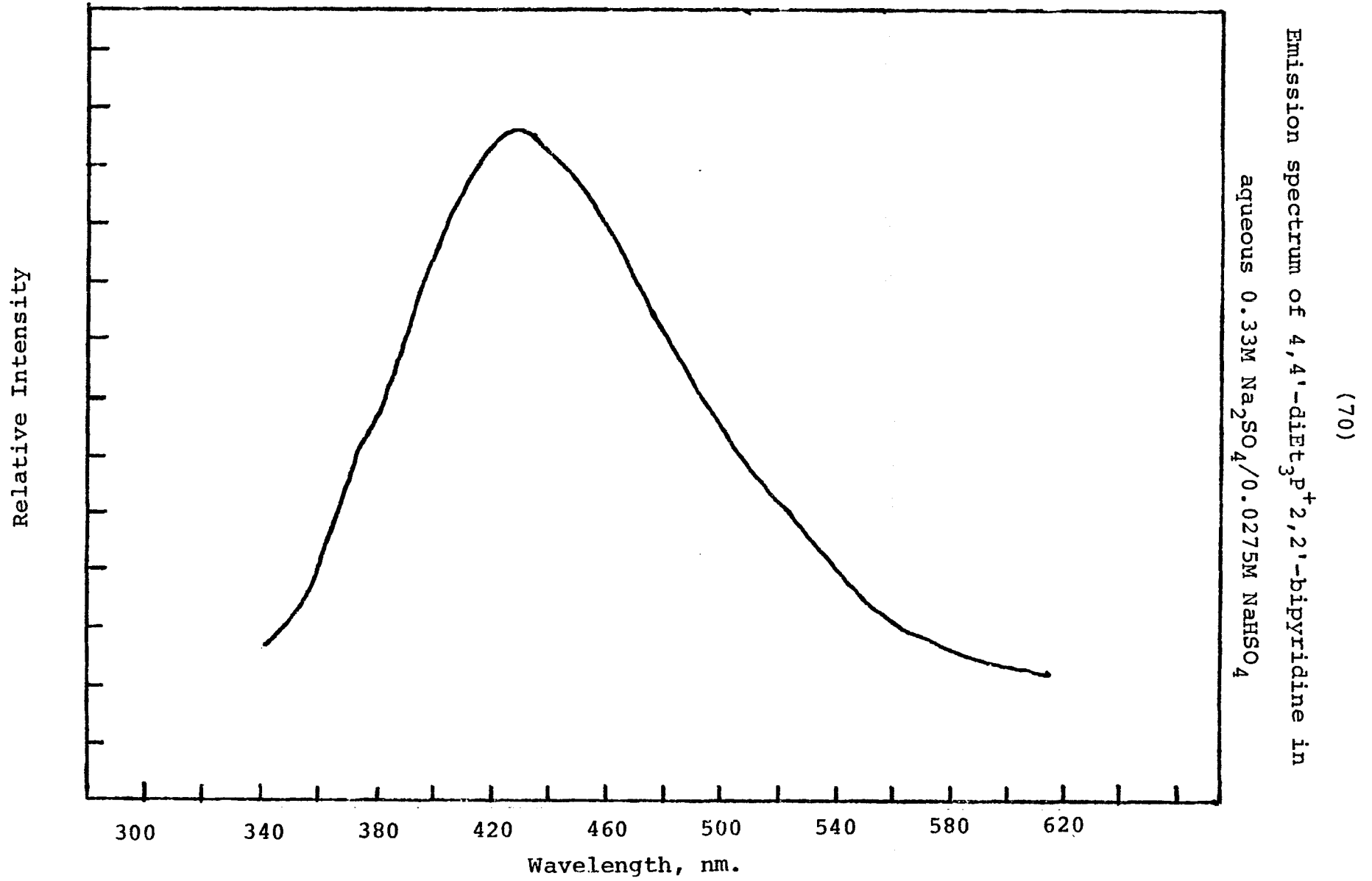
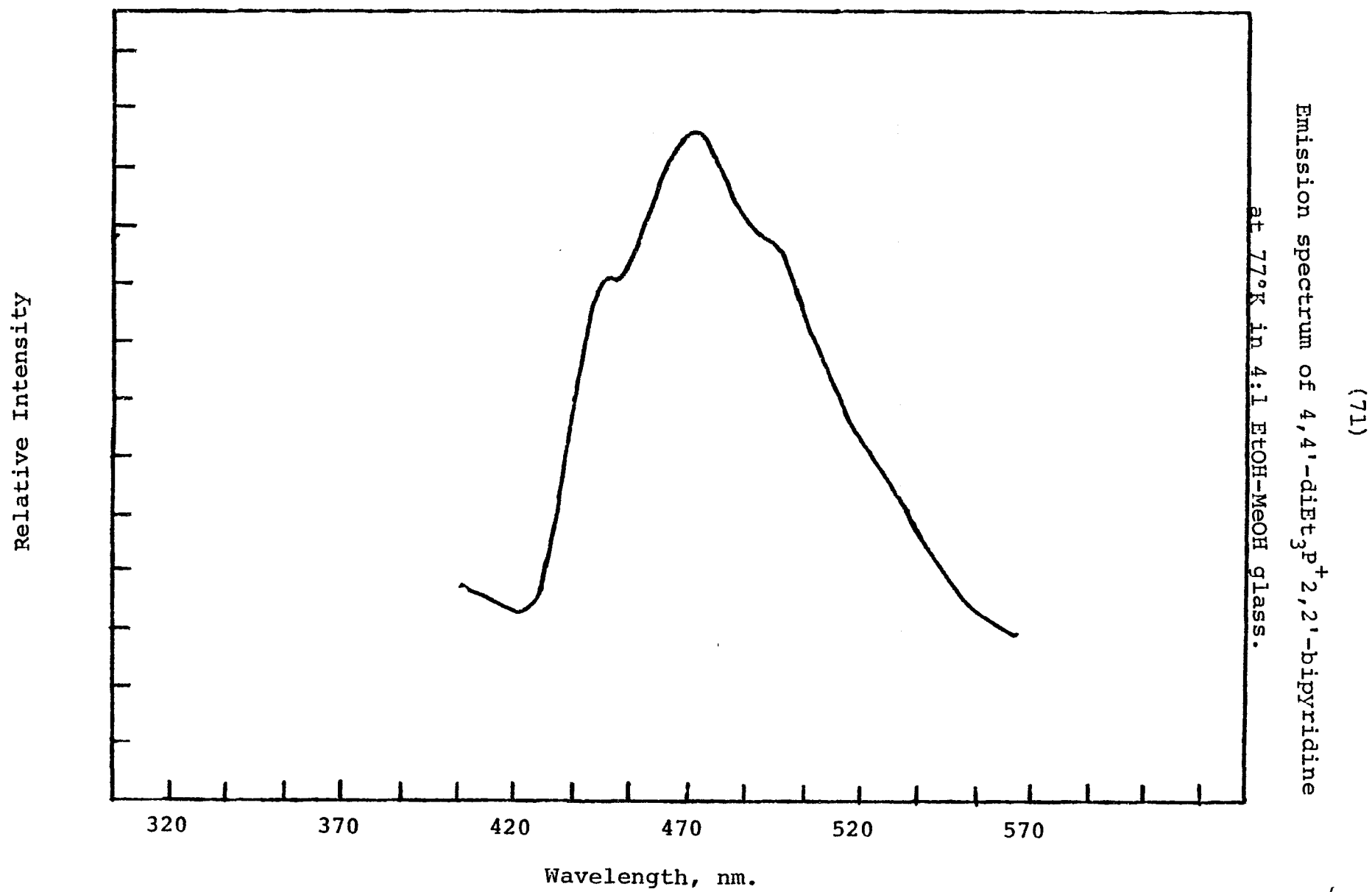


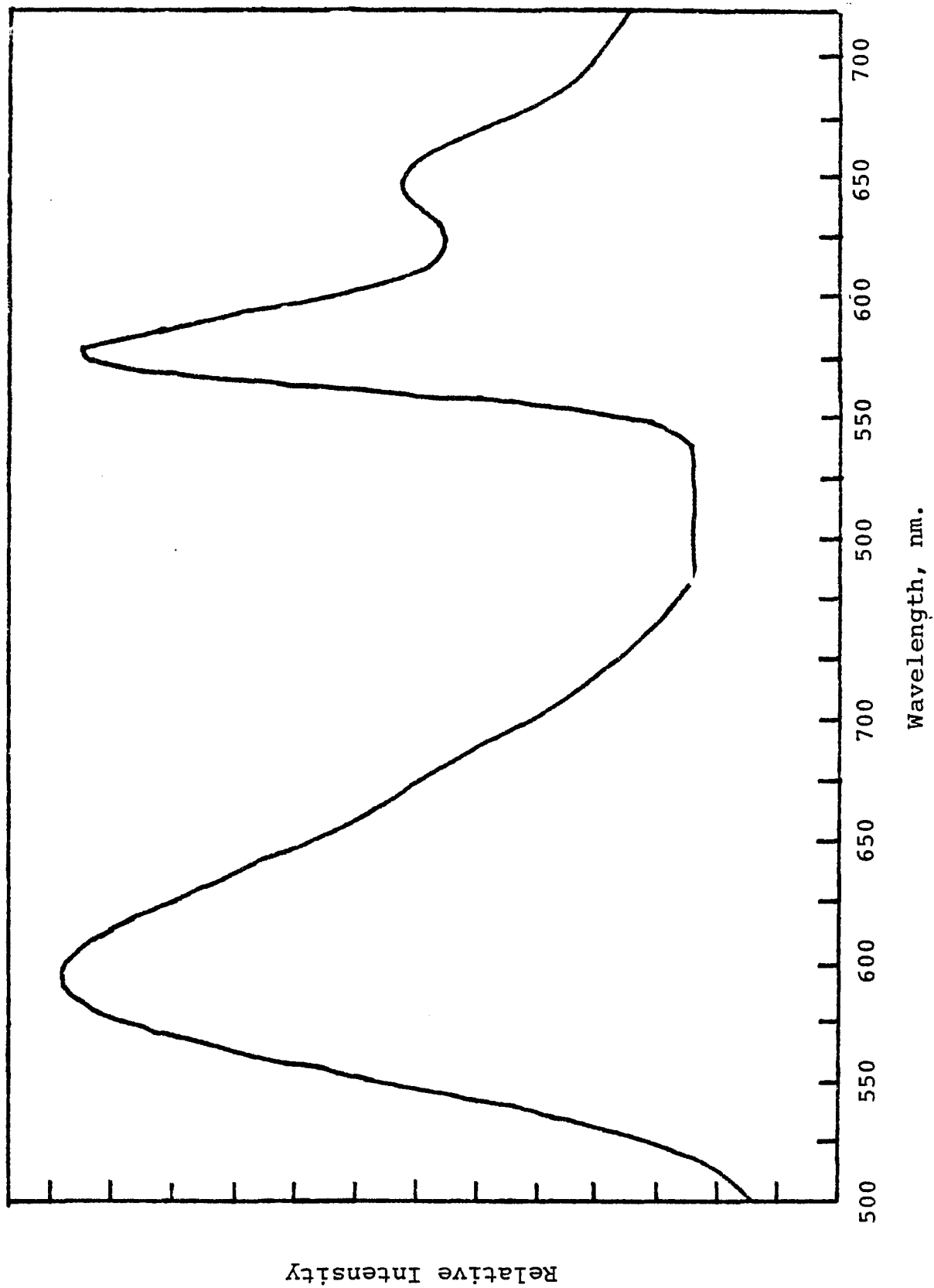
Figure 8



(72)

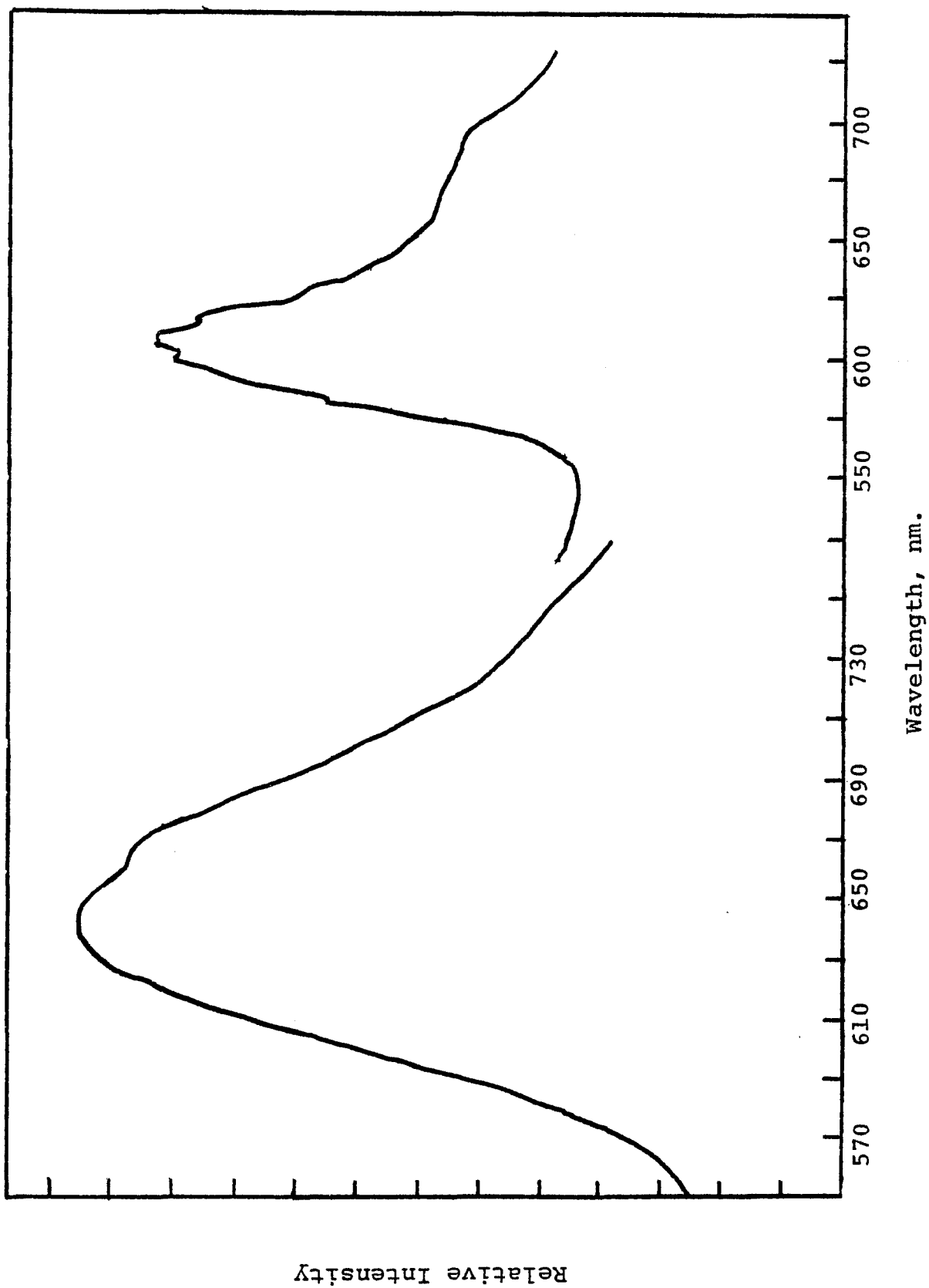
Emission spectrum of  $\text{Ru}(\text{Bpy})_3^{2+}$  at room temperature and  $77^\circ\text{K}$   
in 4:1 EtOH-MeOH mixture

Figure 9



Emission spectrum of  $\text{Ru}(\text{Et}_3\text{P}^+\text{Bpy})_3^{5+}$  at room temperature  
and 77°K in 4:1 EtOH-MeOH mixture

Figure 10



Therefore at room temperature, the states are in rapid thermal equilibrium. Furthermore, due to the high atomic number of the metal ion,  $Z = 44$ , the spin orbit coupling is sufficiently large to render meaningless a singlet or triplet classification (63). For convenience, however, we will refer to these states as triplet states which contains some singlet character. The above reservations, however, should be kept in mind.

The Ru(II) bis-complexes or the Fe(II) complexes were found to be nonluminescent even at liq  $N_2$  temperature.

Thermal Transformation of  $Ru(NO_2Bpy)_3^{2+}$  in 95% EtOH

The  $Ru(NO_2Bpy)_3^{2+}$  complex has a strong charge transfer absorption band at 488 nm in  $H_2O$  or 20% EtOH- $H_2O$  mixture. The complex is very stable in these solvents as the absorption spectrum does not change on storing the solution for days. The complex is also nonluminescent in these solvents. In 95% EtOH, a fresh solution of  $Ru(NO_2Bpy)_3^{2+}$  has exactly the same absorption band at 488 nm but the absorption spectrum is time dependent. The spectral changes shown in figures 11 and 12 are found to be the same in the dark and in the presence of light and hence are not light induced. After 1 hour, the spectrum shows absorption peaks at 498 nm, with a shoulder at 450 nm, which continues to change. After leaving the solution overnight, the final spectrum has a peak at 460 nm with a shoulder at 440 nm. which does not change any further.

Figure 11

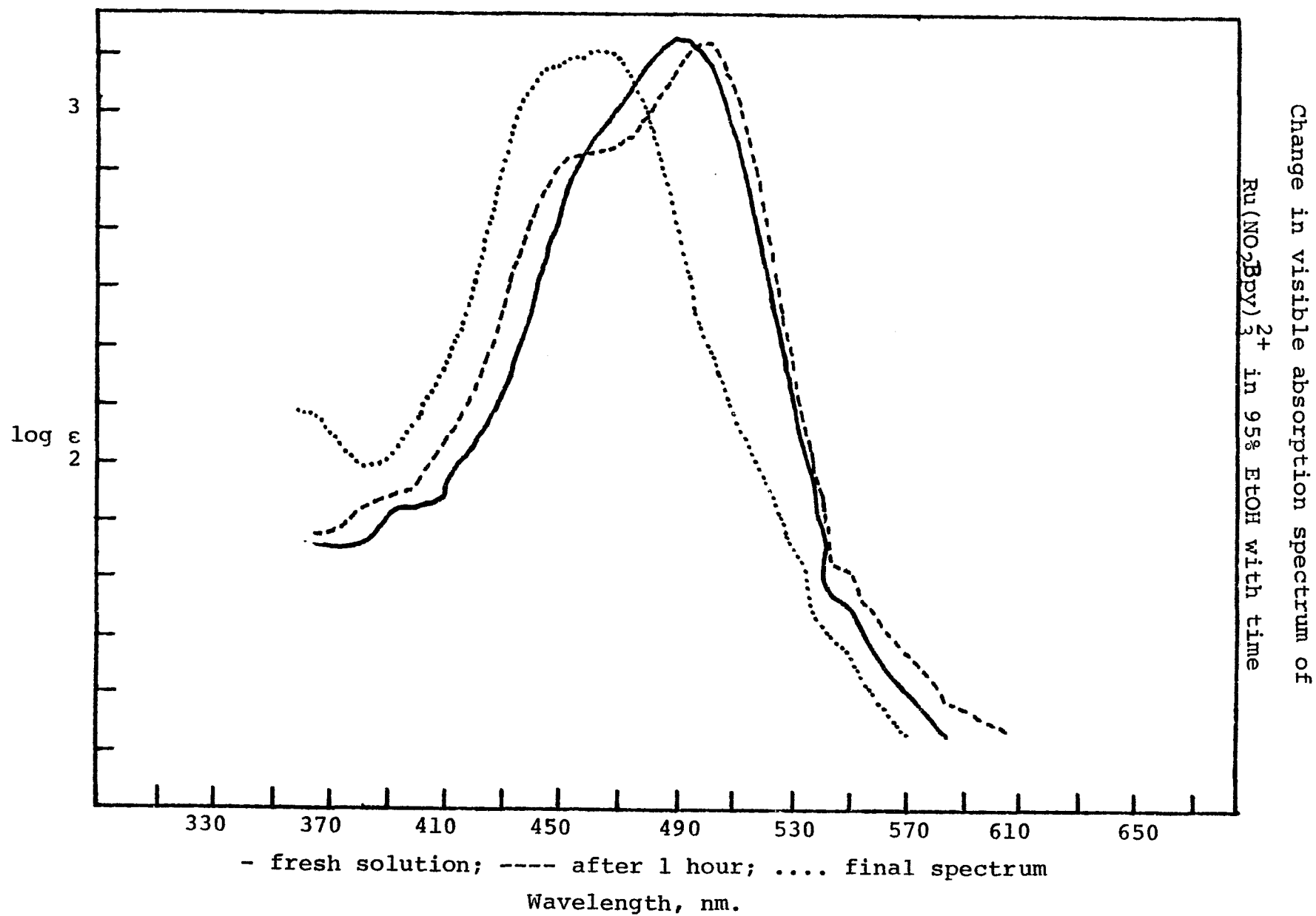
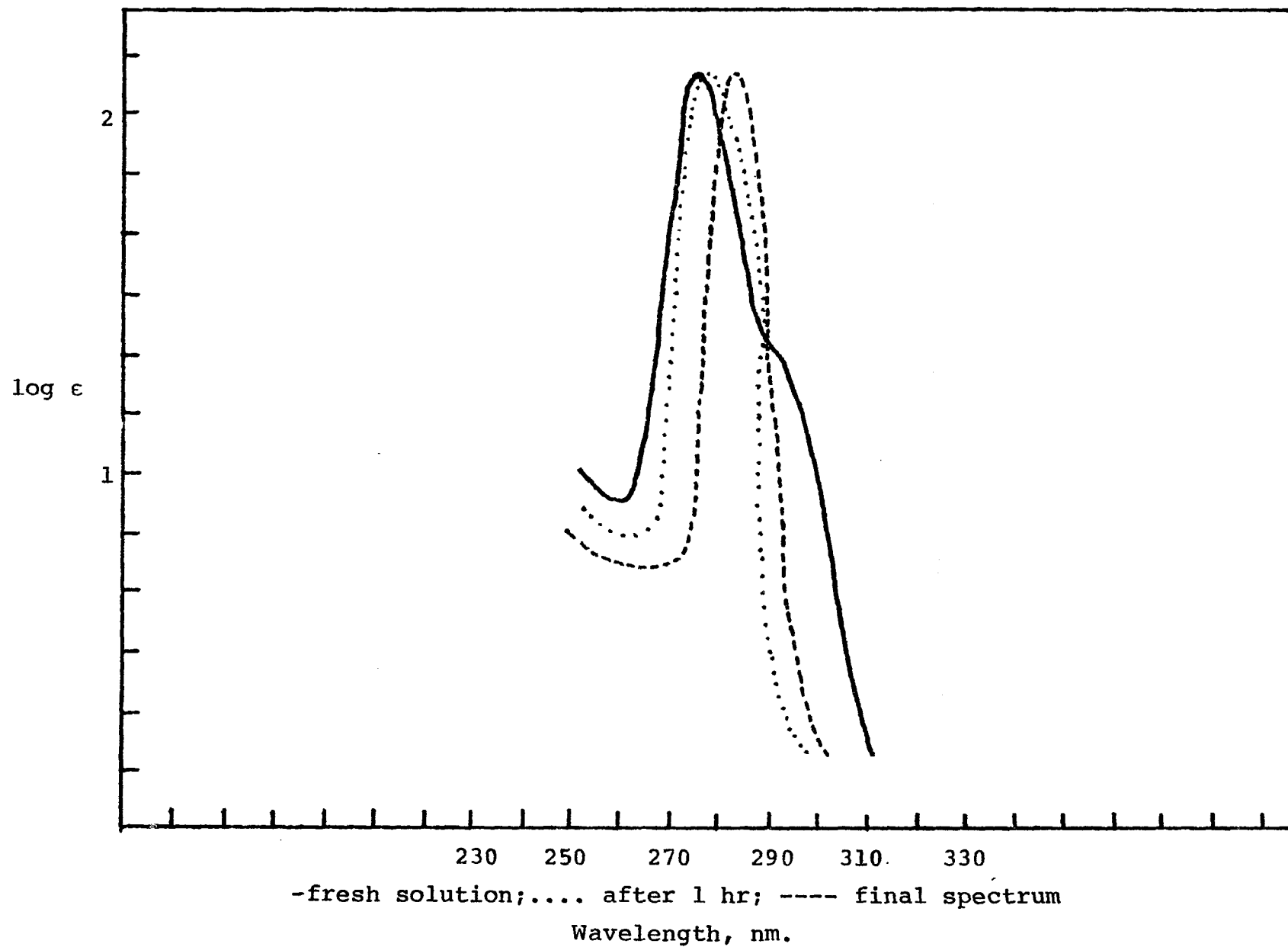


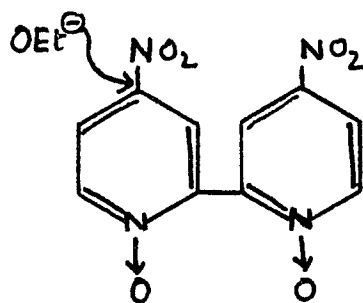
Figure 12



Change in UV. absorption spectrum of  $\text{Ru}(\text{NO}_2\text{Bpy})_3^{2+}$  in  
95% EtOH with time

A similar change is observed in the UV spectrum of the complex in 95% EtOH. A fresh solution of the complex has a spectrum very similar to that in H<sub>2</sub>O with a peak at 274 nm and a shoulder at 308 nm. On storing the solution for 1 hour, the shoulder at 308 nm completely disappears and the peak shifts to 279 nm. The final spectrum, obtained after keeping the solution overnight, has a peak at 284 nm. The disappearance of the 308 nm shoulder, which is characteristic of  $n \rightarrow \pi^*$  transition within the NO<sub>2</sub> group indicates that the NO<sub>2</sub> group in the complex is undergoing substitution. The existence of strong charge transfer peaks in the final spectrum shows that the substitution is not taking place on the metal, and the tris complex of Ru(II) remains unchanged. However, the peak shifts in both the visible and the UV spectrum indicate that a substitution is taking place on the periphery of the bound ligand. Presumably, the NO<sub>2</sub> group is a much stronger electron withdrawing substituent, when compared to OEt, the blue shift of the MLCT transition is consistent with a displacement of NO<sub>2</sub> by OEt. This appears likely because Maerker and Case point out that in 4,4'-dinitro-2,2'-bipyridine 1,1'-dioxide, it is possible to substitute the NO<sub>2</sub> group directly with OEt by reaction with sodium ethoxide in excess EtOH (18). This reaction is probably a nucleophilic displacement of NO<sub>2</sub> group in the 4,4'-dinitro-2,2'-bipyridine 1,1'-dioxide due to an attack

by  $\text{OEt}^-$  group.



Such a nucleophilic displacement reaction is facilitated in the dioxide because the electron withdrawal by the oxygen atom in the N-oxide moiety makes the position para to it electron deficient and more susceptible to attack by a nucleophile like  $\text{OEt}^-$ . Since the positive charge on the Ru(II) ion would exert an effect similar to the N-oxide moiety, we propose that the metal ion labilizes the  $\text{NO}_2$  group. When compared to N-oxide, however, the Ru(II) ion would appear to exert a stronger labilizing effect, since the reaction occurs with a much weaker base, EtOH, as compared to  $\text{OEt}^-$ . An attempt to characterize the product with N.M.R. failed because the complex was not sufficiently soluble to give a good N.M.R. spectrum.

A fresh solution of  $\text{Ru}(\text{NO}_2\text{Bpy})_3^{2+}$  in 95% EtOH does not luminesce. However on storing the solution, the luminescence intensity starts growing and the final solution is strongly luminescent with a peak at 650 nm. This shows that although the starting complex is non-luminescent, the product (presumably  $\text{Ru}(\text{OEt-Bpy})_3^{2+}$ ) is strongly luminescent, as is any other tris bipyridine

complex of Ru(II). An attempt to measure the kinetics of the transformation has been made by following the change in luminescence intensity at 650 nm with time. This yields a first order rate constant  $k = 13.6 \times 10^{-2} \text{ min}^{-1}$ .

Intensity Quenching of Ru(Bpy)<sub>3</sub><sup>2+</sup> by Substituted Bipyridines.

In a simplified form, a bimolecular quenching reaction can be written as



where  $D^*$  represents a luminescent donor and  $Q$  the quencher. Steady state analysis of a reaction sequence including excitation, radiative and nonradiative relaxation, and bimolecular quenching, equation 13, leads to the Stern-Volmer expression

$$I_0/I = 1 + K_{sv}[Q] \quad (14)$$

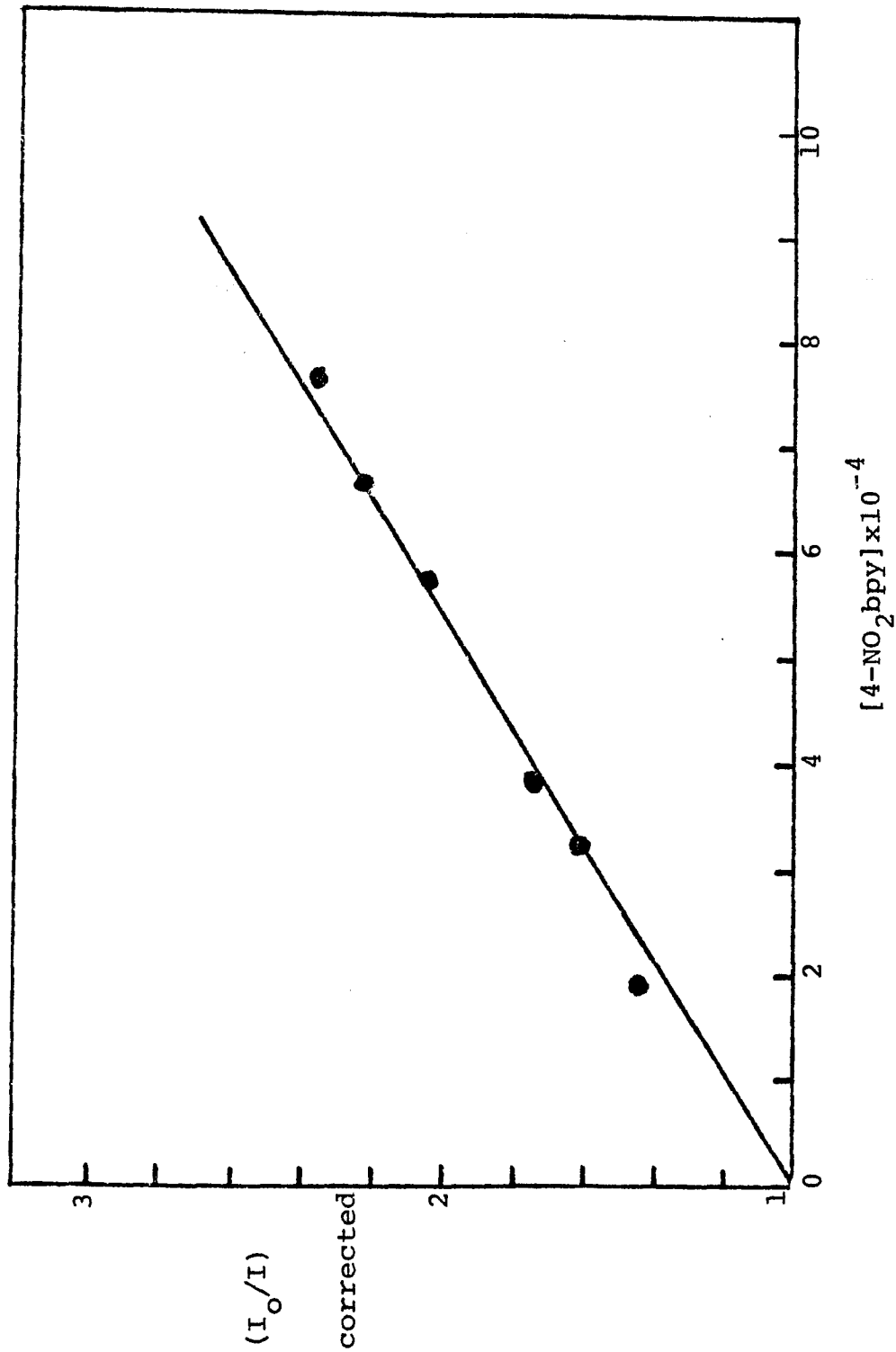
where  $K_{sv}$  represents the Stern-Volmer quenching constant and is related to  $k_q$ , the biomolecular quenching rate constant, by

$$K_{sv} = k_q \tau_0 \quad (15)$$

where  $\tau_0$  is the radiative lifetime measured in the absence of the quencher (64). The values of  $K_{sv}$  summarized in Table XI were obtained by plotting  $(I_0/I)$  corrected versus the concentration of the quencher,  $[Q]$ . These plots for the various substituted bipyridines (Figures 13 and 14) were

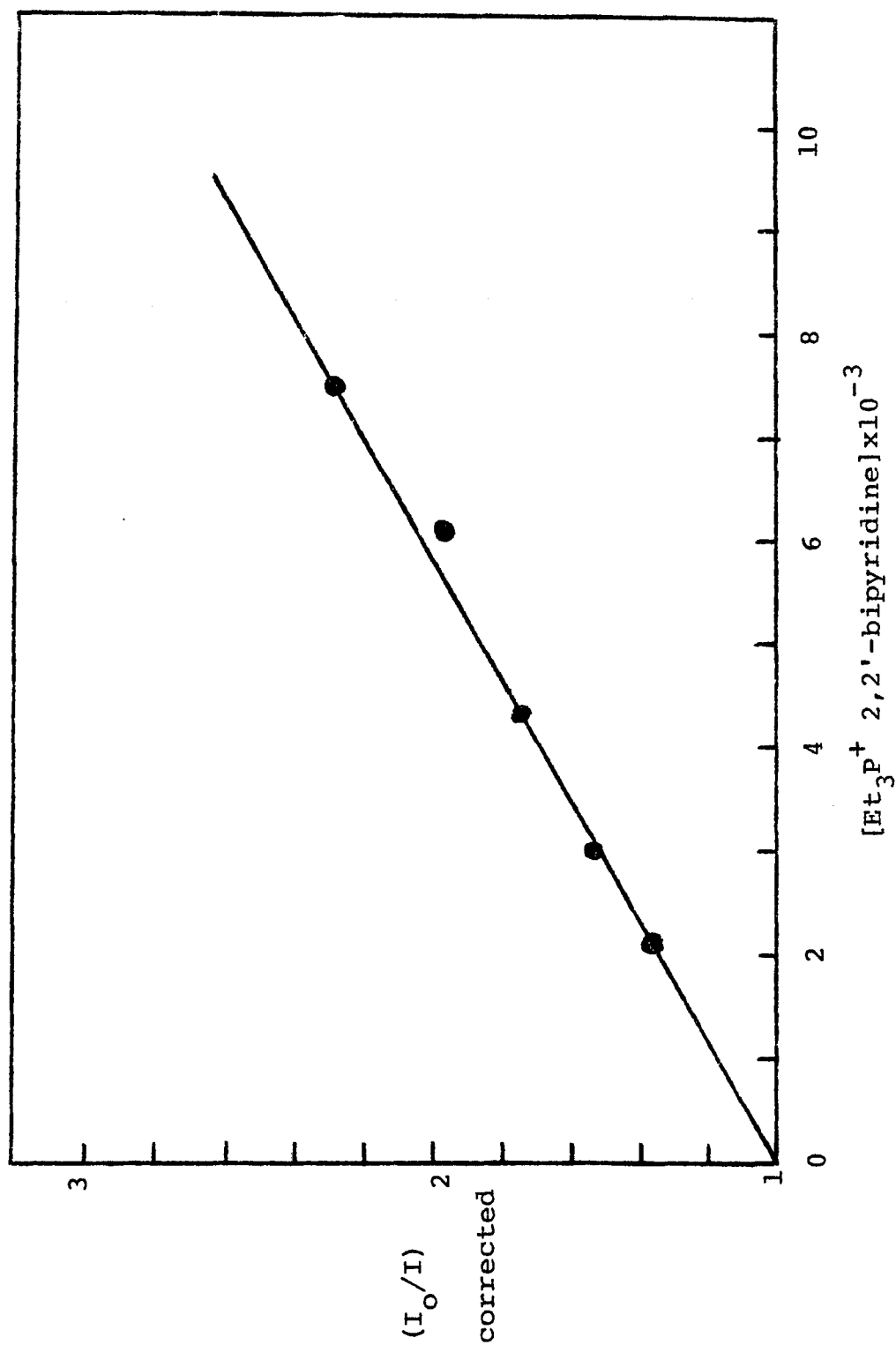
Stern Volmer Plot for the quenching of  $\text{Ru}(\text{Bpy})_3^{2+}$  by  
4- $\text{NO}_2\text{bpy}$  in 20% EtOH (by volume) containing  
0.33M  $\text{Na}_2\text{SO}_4$ /0.275M  $\text{NaHSO}_4$

Figure 13



Stern-Volmer Plot for the Quenching of  $\text{Ru}(\text{Bpy})_3^{2+}$  by  
 $4\text{Et}_3\text{P}^+$  2,2'-bipyridine in aqueous  
 $0.33\text{M Na}_2\text{SO}_4/0.0275\text{M NaHSO}_4$

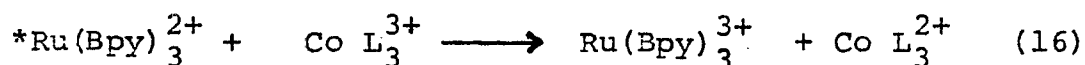
Figure 14



found to be linear through ca. 70% quenching. Since a static mechanism, ie. a thermal equilibrium to form a nonluminescent donor-quencher pair, generally causes a distinct upward curvature to the plots, the linearity of the plots indicates that quenching occurs by a dynamic mechanism. The bimolecular rate constants,  $k_q$ , for the quenching of  $*Ru(Bpy)_3^{2+}$  (Table XI) were calculated from equation 15, where  $\tau_0$  is the radiative lifetime of  $Ru(Bpy)_3^{2+}$  in deaerated 0.33M  $Na_2SO_4/0.0275M NaHSO_4$  buffer, ( $600 \pm 20$  nsec) (55).

Quenching of  $Ru(Bpy)_3^{2+}$  or  $Ru(Et_3P^+Bpy)_3^{5+}$  by Co(III) Complexes of Bipyridines.

Recent luminescence quenching and flash photolysis studies have shown that the luminescent charge transfer state of  $Ru(Bpy)_3^{2+}$ , designated as  $*Ru(Bpy)_3^{2+}$ , is a strong reductant and can be very efficiently quenched by  $Co(phen)_3^{3+}$  or  $Co(Bpy)_3^{3+}$  according to the equation



where L denotes bipyridine or phenanthroline. The quenching reaction is relatively exothermic,  $\Delta G \sim 1.2$  ev, but no spectral evidence for a Co(II) intermediate with a coordinated radical anion has been obtained. (ie. no evidence for electron transfer to the ligand ring). The Stern Volmer quenching constants and the bimolecular rate constants for quenching by the Co(III) complexes are listed

Table XI

Stern Volmer Quenching Constants and Bimolecular Rate Constants for the Quenching of  $\text{Ru}(\text{Bpy})_3^{2+}$  by Substituted Bipyridines.<sup>a</sup>

<u>Complex</u>	<u><math>K_{\text{sv}} \times 10^{-2}, \text{M}^{-1}</math></u> <sup>b,c</sup>	<u><math>K_{\text{q}} \times 10^{-8} \text{M}^{-1} \text{sec}^{-1}</math></u> <sup>d</sup>
2,2'-Bipyridine	$\leq 0.275$	$\leq 0.46$
4-Et <sub>3</sub> P <sup>+</sup> Bipyridine	$1.37 \pm 0.02$	$2.25 \pm 0.03$
4-NO <sub>2</sub> -Bipyridine	$15.7 \pm 0.5$	$25.8 \pm 1.2$

a)  $\mu = 1.0\text{M}$ ;  $T = 25^\circ\text{C}$ .

b) Determined in solutions containing  $3 \times 10^{-5} \text{M}$   $\text{Ru}(\text{Bpy})_3^{2+}$

c) Samples excited with 452 nm radiation and emission monitored at 588 nm.

d) Calculated assuming  $\tau_0 = 600 \pm 20$  nsec.

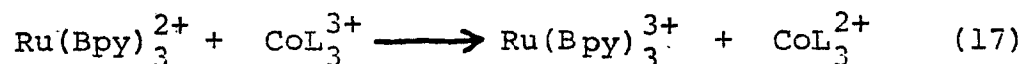
e) Measured in a 20% (by volume) EtOH-H<sub>2</sub>O solution

in Table XII. The values of  $K_{sv}$  were obtained by plotting  $(I_o/I)_{corr}$  versus the concentration of the quencher [Q], as shown in figures 15 through 17.

### Flash Photolysis Experiments

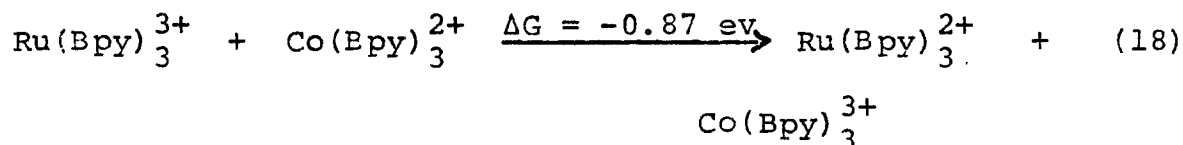
Often quenching experiments per se do not distinguish various quenching mechanisms. Because of this, a number of flash photolysis experiments were carried out in an attempt to elucidate the quenching mechanism.

Flash photolysis of solutions containing  $Ru(Bpy)_3^{2+}$  and  $Co(Bpy)_3^{3+}$  or  $Co(NO_2Bpy)_3^{3+}$  induces a photochemical reaction which produces the corresponding  $Ru(III)$  and  $Co(II)$  complexes in relatively high yield. The photochemical reaction is then followed by a rapid exothermic, thermal reaction ( $\Delta G \sim 0.8$  ev) yielding an overall reaction scheme of



where L denotes bipyridine or 4-nitrobipyridine. As pointed out by Meyer and coworkers, the formation of electron transfer products during the flash duration allows the use of the flash photolysis technique as one in which very rapid electron transfer reactions can be studied (65).

For example, the driving force for the back reaction



is large and favorable, and yields reaction rates beyond the

Table XII

Stern Volmer Quenching Constants and Bimolecular Rate

Constants for the Quenching of  $\text{Ru}(\text{Bpy})_3^{2+}$  and  $\text{Ru}(\text{Et}_3\text{P}^+\text{Bpy})_3^{5+}$   
by Co(III) Complexes.<sup>a</sup>

Reactants	$K_{\text{sv}} \times 10^{-3}, \text{M}^{-1}$ <sup>b,c</sup>	$K_{\text{q}} \times 10^{-9} \text{M}^{-1} \text{sec}^{-1}$ <sup>d</sup>
$\text{Ru}(\text{Bpy})_3^{2+} - \text{Co}(\text{Bpy})_3^{3+}$	$1.15 \pm 0.01$	$1.92 \pm 0.15$
$\text{Ru}(\text{Bpy})_3^{2+} - \text{Co}(\text{NO}_2\text{Bpy})_3^{3+}$	$0.54 \pm 0.15$	$0.90 \pm 0.20$
$\text{Ru}(\text{Et}_3\text{P}^+ \text{bpy})_3^{5+} - \text{Co}(\text{Bpy})_3^{3+}$	$0.14 \pm 0.14$	

a)  $\mu = 1.0\text{M}$ ;  $T = 25^\circ\text{C}$ b) Determined in solutions containing  $3 \times 10^{-5} \text{M}$   $\text{Ru}(\text{Bpy})_3^{2+}$ 

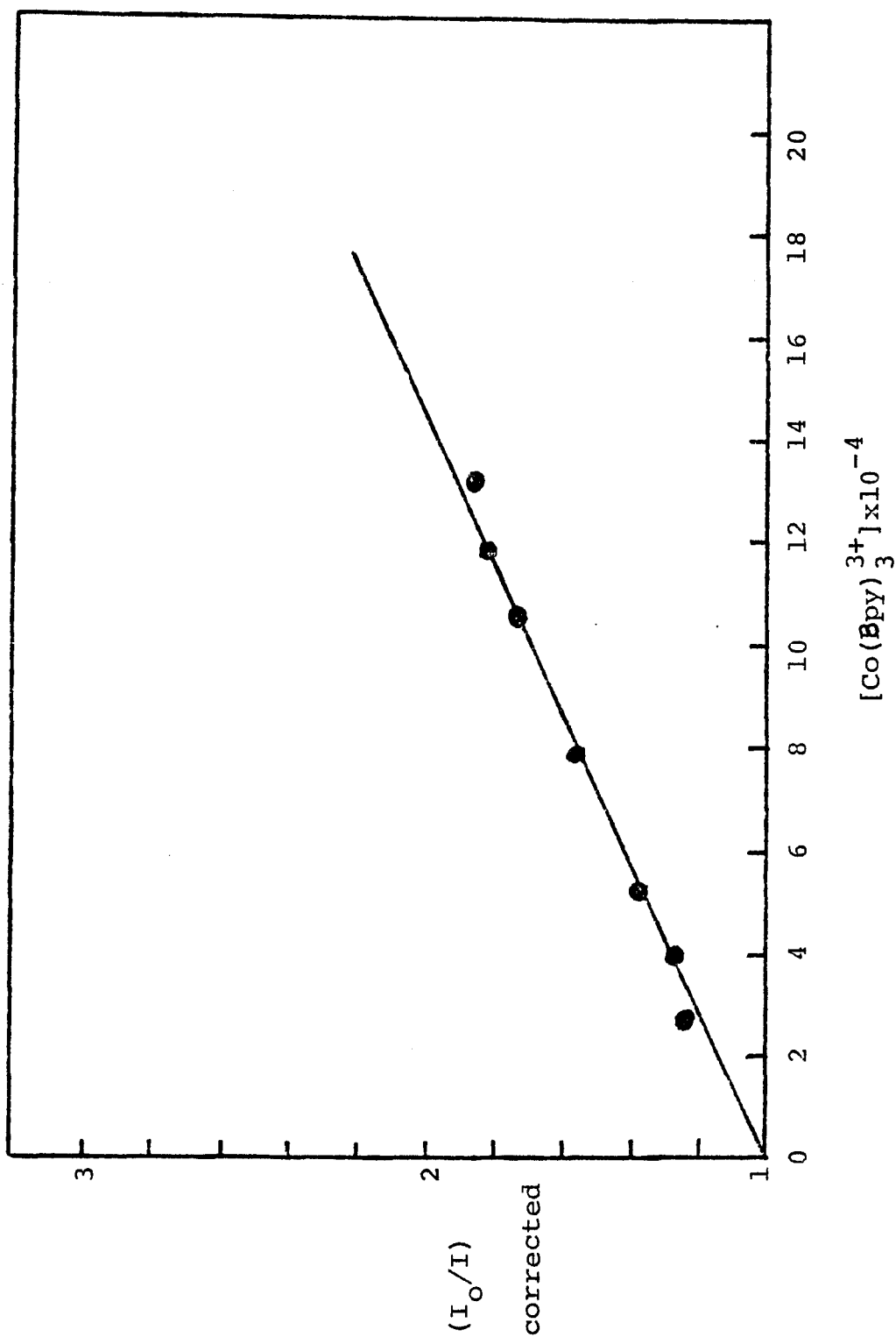
c) Samples excited with 452 nm radiation and emission monitored at 588 nm.

d) Calculated assuming  $\tau_0 = 600 \pm 20$  nsec.e) Obtained for the quenching of  $\text{Ru}(\text{Et}_3\text{P}^+\text{Bpy})_3^{5+}$ 

f) Samples excited with 466 nm radiation and emission monitored at 640 nm.

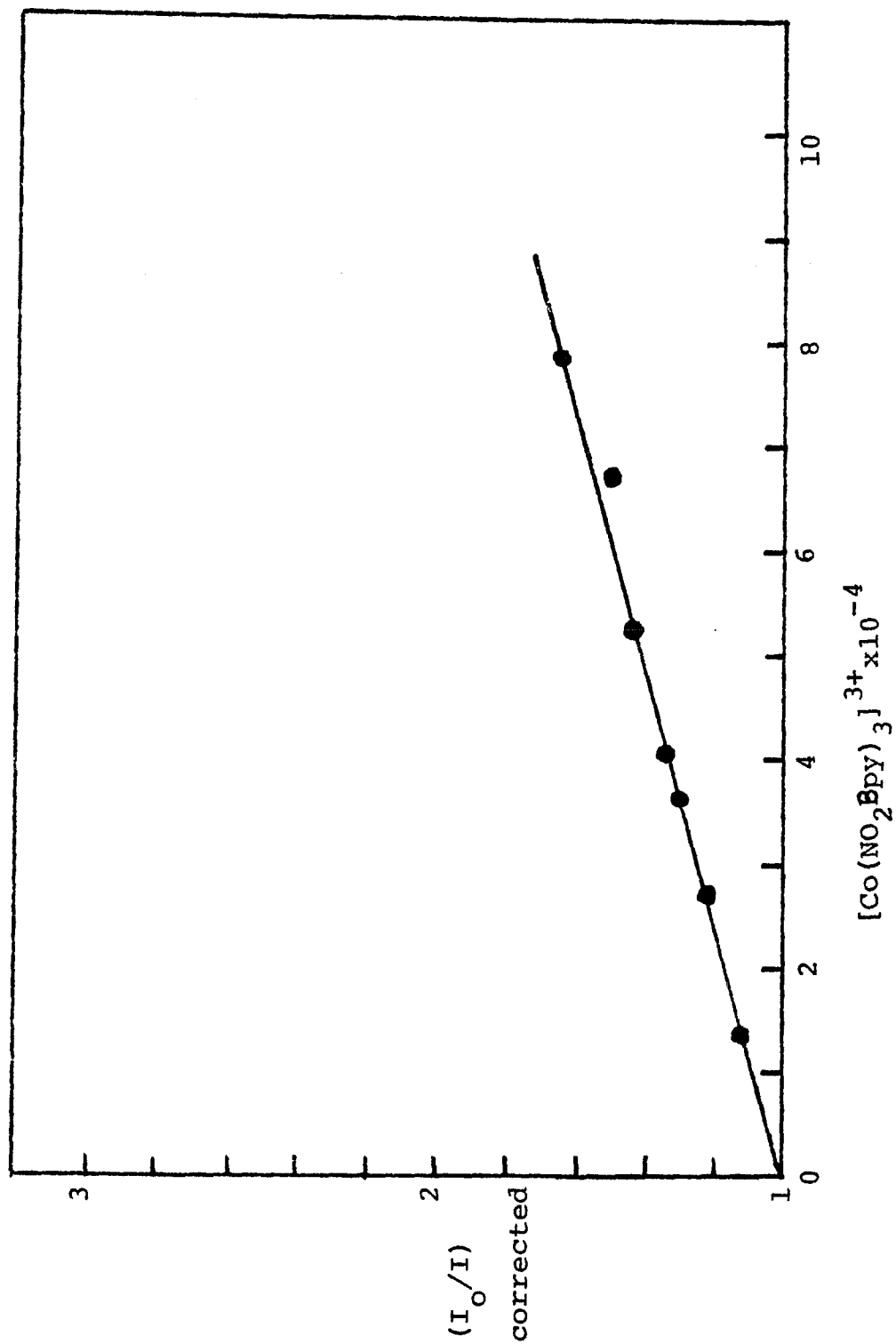
Stern-Volmer Plot for the Quenching of  $\text{Ru}(\text{Bpy})_3^{2+}$  by  
 $\text{Co}(\text{Bpy})_3^{3+}$  in aqueous  $0.33\text{M Na}_2\text{SO}_4/0.0275\text{M NaHSO}_4$

Figure 15



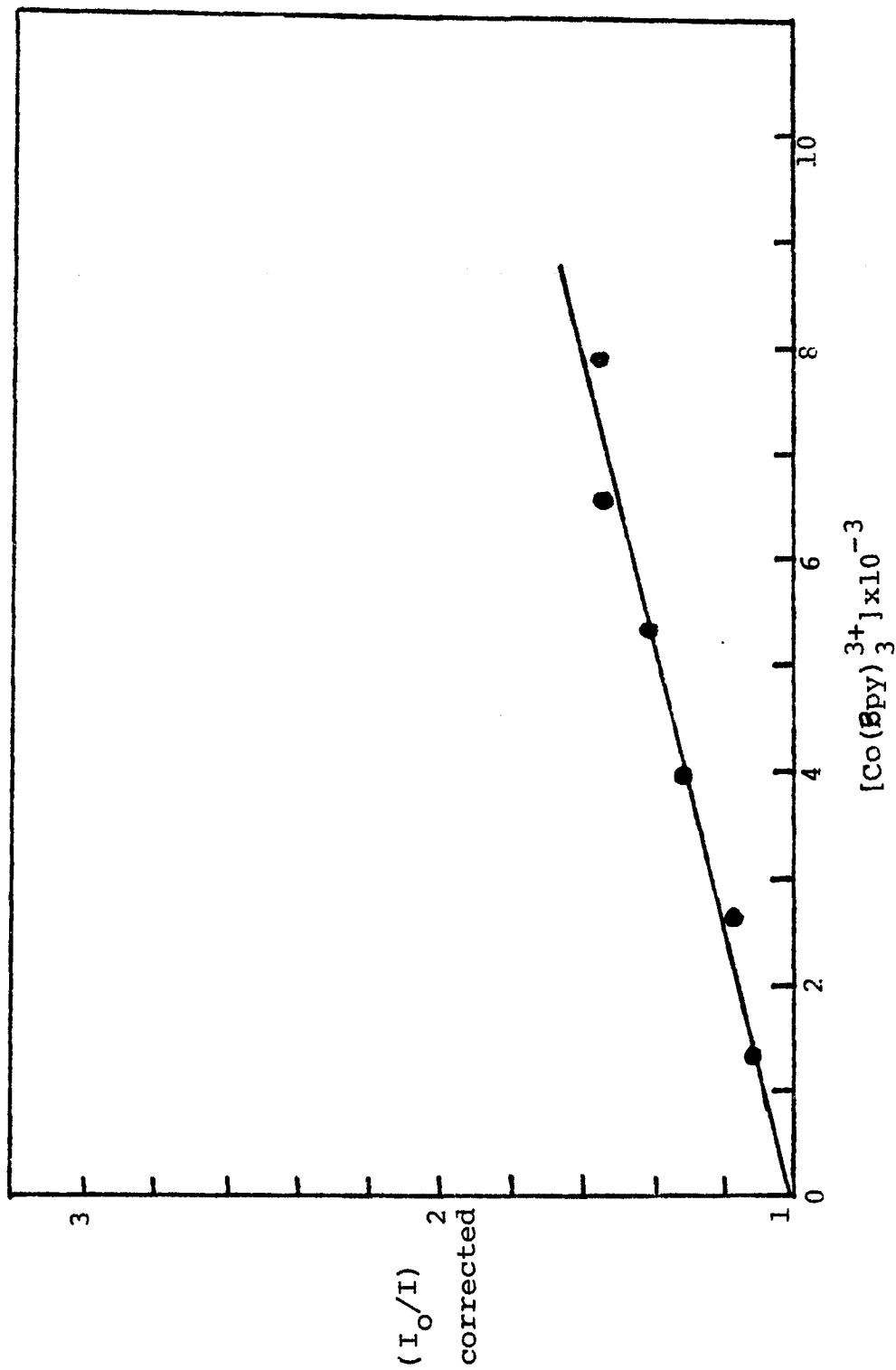
Stern Volmer Plot for the Quenching of  $\text{Ru}(\text{Bpy})_3^{2+}$  by  
 $\text{Co}(\text{NO}_2\text{Bpy})_3^{3+}$  in aqueous  $0.33\text{M Na}_2\text{SO}_4/0.0275\text{M NaHSO}_4$

Figure 16



Stern Volmer Plot for the Quenching of  $\text{Ru}(\text{Et}_3\text{P}^+\text{Bpy})^{5+}$  by  $\text{Co}(\text{Bpy})_3^{3+}$  in aqueous  $0.33\text{M Na}_2\text{SO}_4/0.0275\text{M NaHSO}_4$

Figure 17



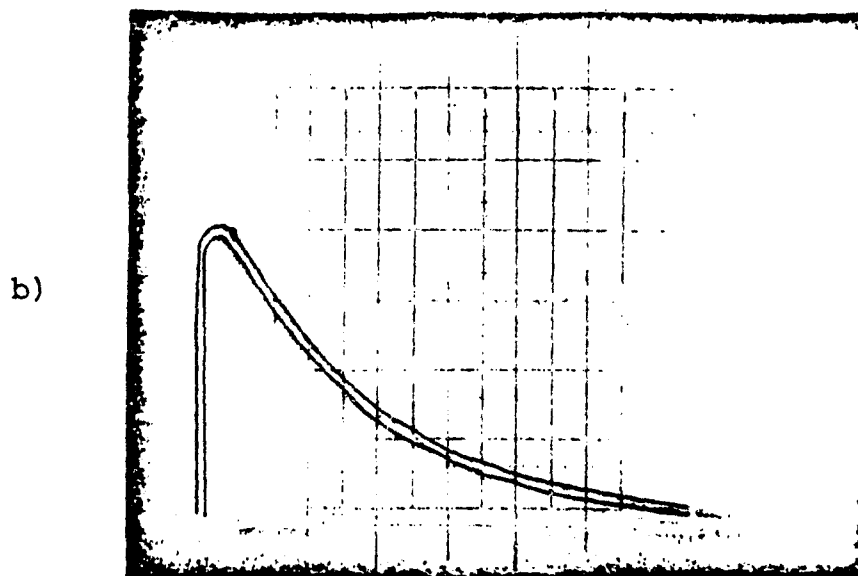
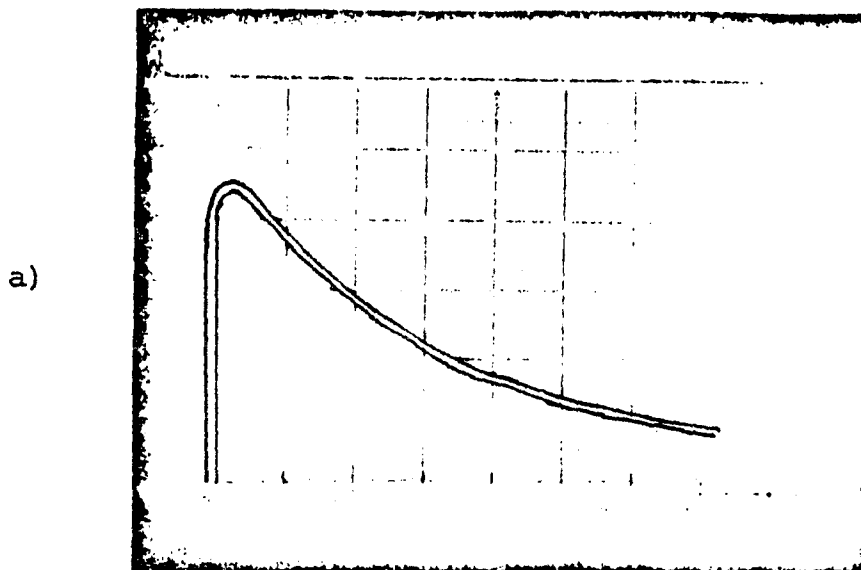
range of conventional stopped-flow techniques.

A series of flash photolysis experiments were performed to establish photoredox quenching and to measure the rates of the exothermic back reactions. In these flash photolysis experiments, the concentration of the quencher used is such that 60-70% quenching is obtained. The concentration of  $\text{Ru}(\text{Bpy})_3^{2+}$  used was  $7.5 \times 10^{-5} \text{ M}$  in order to obtain a uniform cross-sectional absorbance.

Typical oscilloscope traces monitoring the decay of the  $\text{Ru}(\text{III})$  complexes are shown in Figure 18. Following the flash, the solutions were analyzed at various wavelengths from 560 to 850 nm. The absorbance of the transient  $\text{Ru}(\text{III})$ ,  $A_0$ , was obtained by extrapolating plots of  $1/A$  versus time to  $t = 0$ . At each wavelength, the plots were linear and yielded rate constants which were identical within experimental error. The values of  $A_0$  determined at the various wavelengths relative to that determined at 675 nm differed by less than 3% from similar ratios calculated from the extinction co-efficients of  $\text{Ru}(\text{Bpy})_3^{3+}$  or  $\text{Ru}(\text{Et}_3\text{P}^+\text{Bpy})_3^{6+}$  (see experimental section above). As indicated in figures 19 and 20, the spectrum of the transient is in excellent agreement with the spectrum of  $\text{Ru}(\text{Bpy})_3^{3+}$  or  $\text{Ru}(\text{Et}_3\text{P}^+\text{Bpy})_3^{6+}$  and established  $\text{Ru}(\text{III})$  as a product of the reaction. Polaroid photographs of the oscilloscope traces, were analyzed according to second-order kinetics for equimolar concentrations of the  $\text{Ru}(\text{III})$  and  $\text{Co}(\text{II})$  complexes. Plots of  $1/A$  versus time were linear

Figure 18

The decay trace of Ru(III) in flash experiments



$7 \times 10^{-5} \text{ M Ru(Bpy)}_3^{2+}$  and  $1 \times 10^{-3} \text{ M Co(Bpy)}_3^{3+}$ , 200  $\mu\text{sec}$  per division.

a) Anal. Wavelength, 675 nm b) Anal wavelength 650 nm.

Figure 19  
Agreement of the transient spectrum with that of Ru(Bpy)<sub>3</sub><sup>3+</sup>

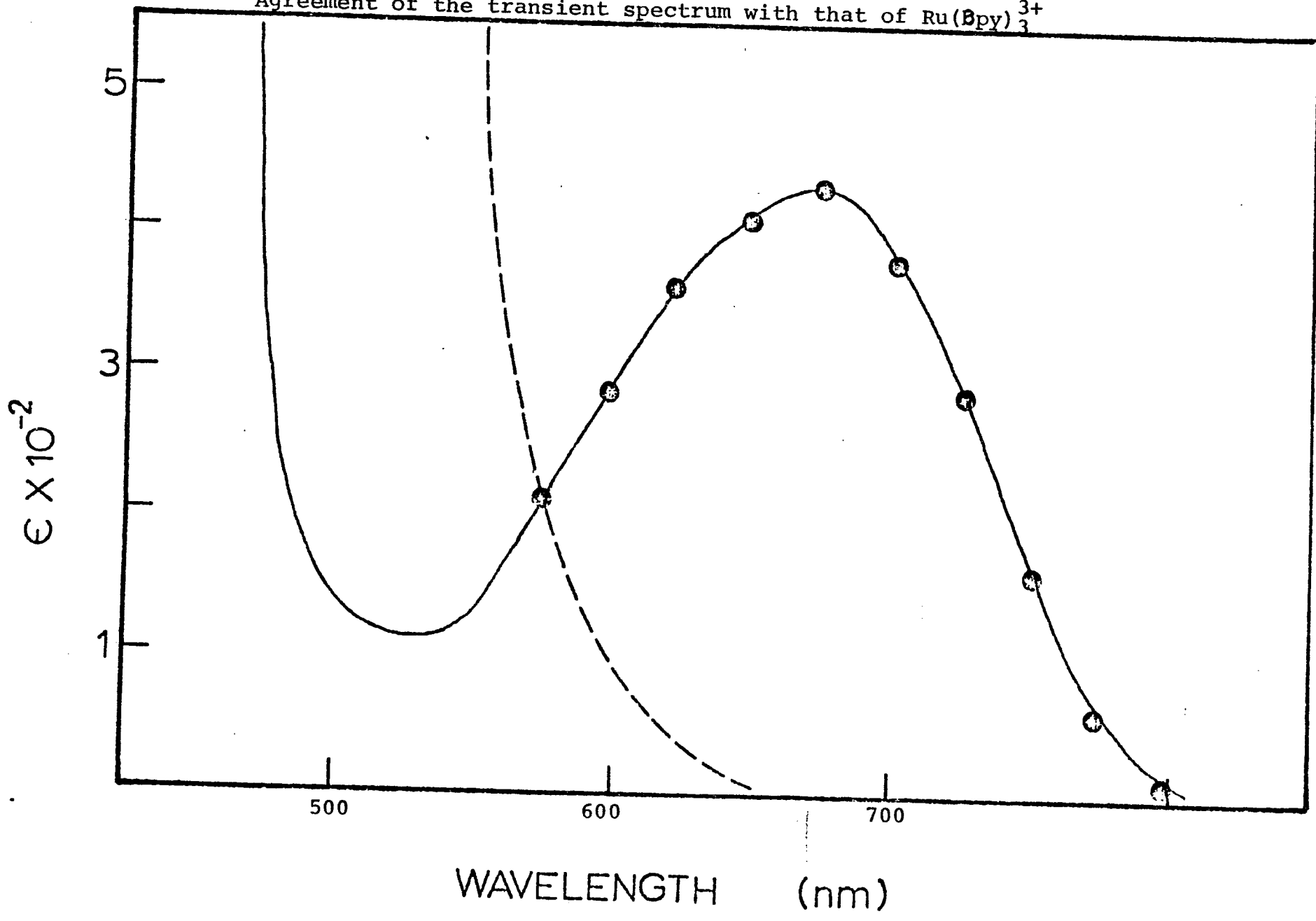
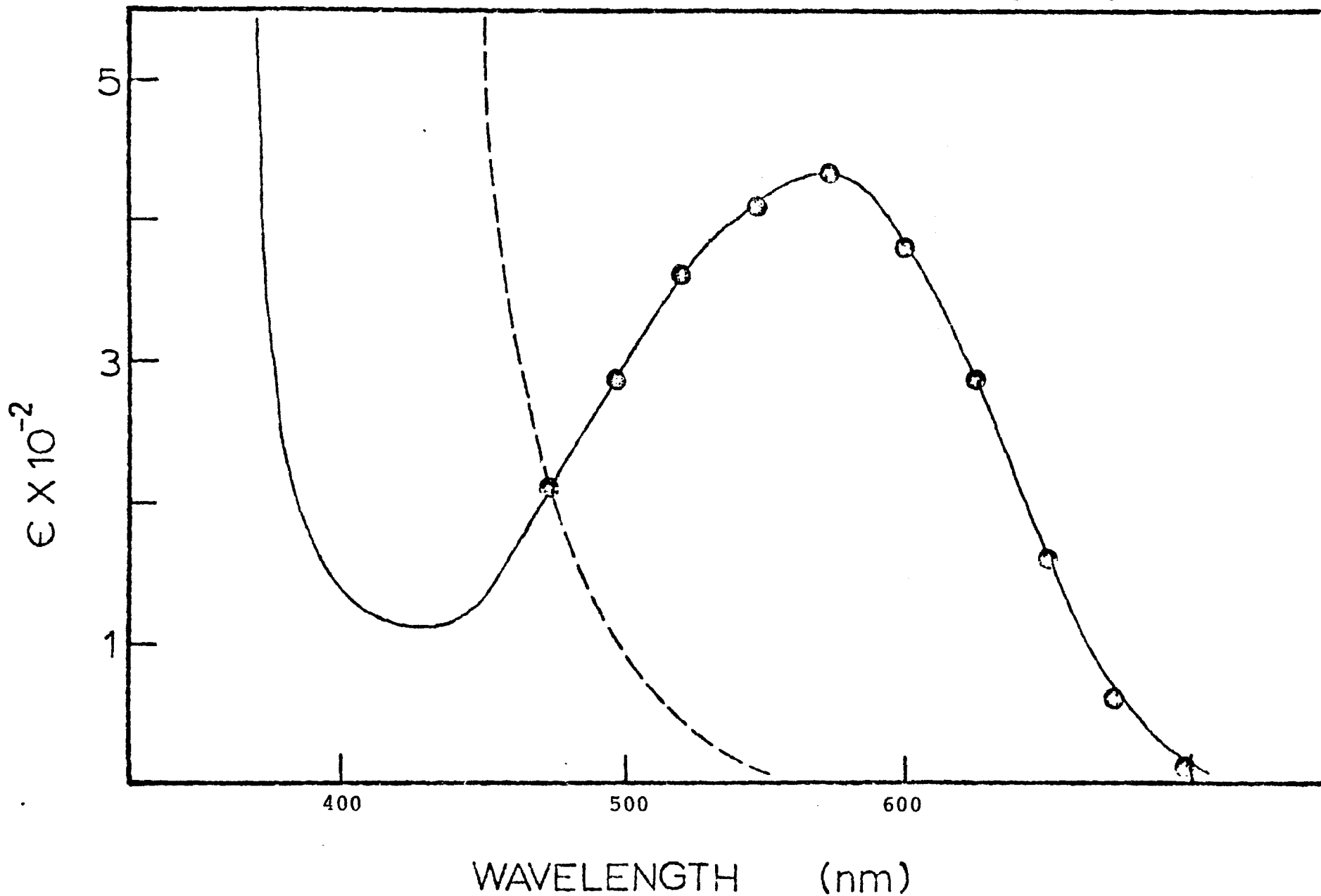


Figure 20  
Agreement of the transient spectrum with that of  $\text{Ru}(\text{Et}_3\text{P}^+\text{Bpy})_3^{6+}$



and the rate constants obtained from these plots are summarized in Table XIII.

The flash photolysis experiment with  $\text{Ru}(\text{Bpy})_3^{2+}$  and  $\text{Co}(\text{NO}_2\text{Bpy})_3^{3+}$  failed to give any transient signal. Although the quenching rate constant is similar to that found with the other compounds, the complex absorbs a larger fraction of the excitation pulse. Consequently the amount of reaction induced, under conditions where the Ru(II) complex is the dominant absorbing species, is small and beyond the detection limit of the flash photolysis equipment. In the flash photolysis experiments with  $\text{Ru}(\text{Bpy})_3^{2+}$  and 4- $\text{NO}_2^-$  bipyridine or 4- $\text{Et}_3\text{P}^+$  bipyridine, no transients having life times longer than 50  $\mu\text{sec}$  could be detected. An energy transfer quenching is ruled out in these reactions, because the singlet state energy of these free ligands, as obtained from their emission spectra at liq  $\text{N}_2$  temperature, is much higher in energy than the charge transfer emitting state of  $\text{Ru}(\text{Bpy})_3^{2+}$ . The lack of free ion formation with these free ligands as quenchers in an electron transfer process is not surprising since the immediate product is most probably an ion pair. With Co(III) complexes, the quenching products are both positively charged and the escape probability from the ion pair is very large. For the combination,  $\text{Ru}(\text{Bpy})_3^{2+} \dots \text{Q}^-$ , the escape probability is very low and therefore the concentration of free ions produced is probably undetectable. The other possibility for the absence of a transient absorbance is that the rate constant

Table XIII

Rate Constants for the Thermal Back Reactions

<u>Reactants</u>		<u><math>k^a</math> avg x <math>10^{-8} \text{ M}^{-1} \text{ sec}^{-1}</math></u>
$\text{Ru}(\text{Bpy})_3^{3+}$	$\text{Co}(\text{Bpy})_3^{2+}$	$1.33 \pm 0.27 (3)$
$\text{Ru}(\text{Et}_3\text{P}^+\text{Bpy})_3^{6+}$	$\text{Co}(\text{Bpy})_3^{2+}$	$2.15 \pm 0.15 (3)$

a)  $\mu = 1.0\text{M}$   $T = 25^\circ\text{C}$ ; number in parentheses indicates number of measurements.

of the reverse reaction is greater than  $5 \times 10^8 \text{ M}^{-1} \text{ sec}^{-1}$ . This estimate is based on flash photolysis experiments where the reaction between  $\text{Ru}(\text{Bpy})_3^{3+}$  and tris(1,10 phenanthroline)cobalt (II) is monitored at 675 nm, the absorption maximum of  $\text{Ru}(\text{Bpy})_3^{3+}$ . These experiments yield a rate constant of  $1.08 \times 10^8 \text{ M}^{-1} \text{ sec}^{-1}$ . Assuming a minimum signal to noise ratio of 2:1 and the same extinction coefficient at 675 nm for  $\text{Ru}(\text{Bpy})_3^{3+}$  in 20% EtOH, a lower limit of  $5 \times 10^{-8} \text{ M}^{-1} \text{ sec}^{-1}$  is calculated.

Our observations are consistent with that of Meyer and coworkers who observed a similar lack of transient absorbance in flash photolysis studies of  $\text{Ru}(\text{Bpy})_3^{2+}$  with a series of nitro aromatics (66).

#### Flash Photolysis of Substituted Bipyridines.

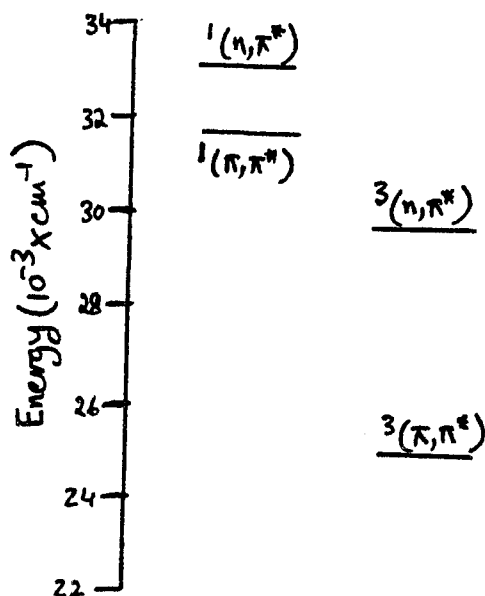
Flash photolysis of  $1 \times 10^{-4} \text{ M}$  2,2'-bipyridine in  $0.33 \text{ M Na}_2\text{SO}_4/0.0275 \text{ M NaHSO}_4$  shows a strong triplet absorption spectrum with a maximum at 350 nm which decays with a first order rate constant of  $k = 22 \pm 5 \times 10^2 \text{ sec}^{-1}$ . In the presence of triplet quenchers like oxygen, the triplet absorption spectrum is not seen at all, in agreement with the work of Harriman (67).

Flash photolysis of  $5 \times 10^{-5} \text{ M}$  4-Et<sub>3</sub>P<sup>+</sup> bipyridine in  $0.33 \text{ M Na}_2\text{SO}_4/0.0275 \text{ M NaHSO}_4$  shows a similar strong triplet absorption spectrum with a maxima at 375 nm, which decays with a first order rate constant of  $23 \pm 2 \times 10^2 \text{ sec}^{-1}$ . On saturating the solution with oxygen, the transient drops

sharply in intensity and the decay rate is too fast for the transient to be photographed. This indicates that the transient arises from a triplet state.

Flash photolysis of  $1 \times 10^{-4}$  M 4-NO<sub>2</sub> bipyridine in 0.33M Na<sub>2</sub>SO<sub>4</sub>/0.0275M NaHSO<sub>4</sub> in 20% EtOH-H<sub>2</sub>O mixture gives two overlapping transient absorption bands. One band, has a maximum at 350 nm while the other band has a maximum at 500 nm. Both bands decay according to first order kinetics, with similar rate constants of  $K = 14.1 \pm 2 \times 10^2 \text{ sec}^{-1}$ . Saturating the solution with oxygen does not affect the transients at all, indicating that both the transients arise from the products of a photochemical reaction which originates in the first excited singlet state. In order to investigate the effect of polarity, flash photolysis was also done on  $1 \times 10^{-4}$  M 4-NO<sub>2</sub> bipyridine in 95% EtOH containing 1M Et<sub>4</sub>N<sup>+</sup>Cl<sup>-</sup>. An extremely long lived transient is observed and the transient spectrum has an absorption maximum at 450 nm. This transient was found to decay according to first order kinetics with a rate constant of  $66.7 \text{ sec}^{-1}$ . The photochemical change induced by the flash appears to be permanent since, on repeated flashing of the same solution, the transient absorbance fails to drop to the base line. On saturating the solution with oxygen, the transient is again observed at 450 nm but it decays with a much faster rate constant of  $K = 13.8 \pm 0.7 \times 10^2 \text{ sec}^{-1}$ . This seems to indicate that the transient arises from a reaction originating from a triplet level. The energy level diagram as

reported by Harriman and shown below may be used to explain the results of the flash photolysis experiments (67).



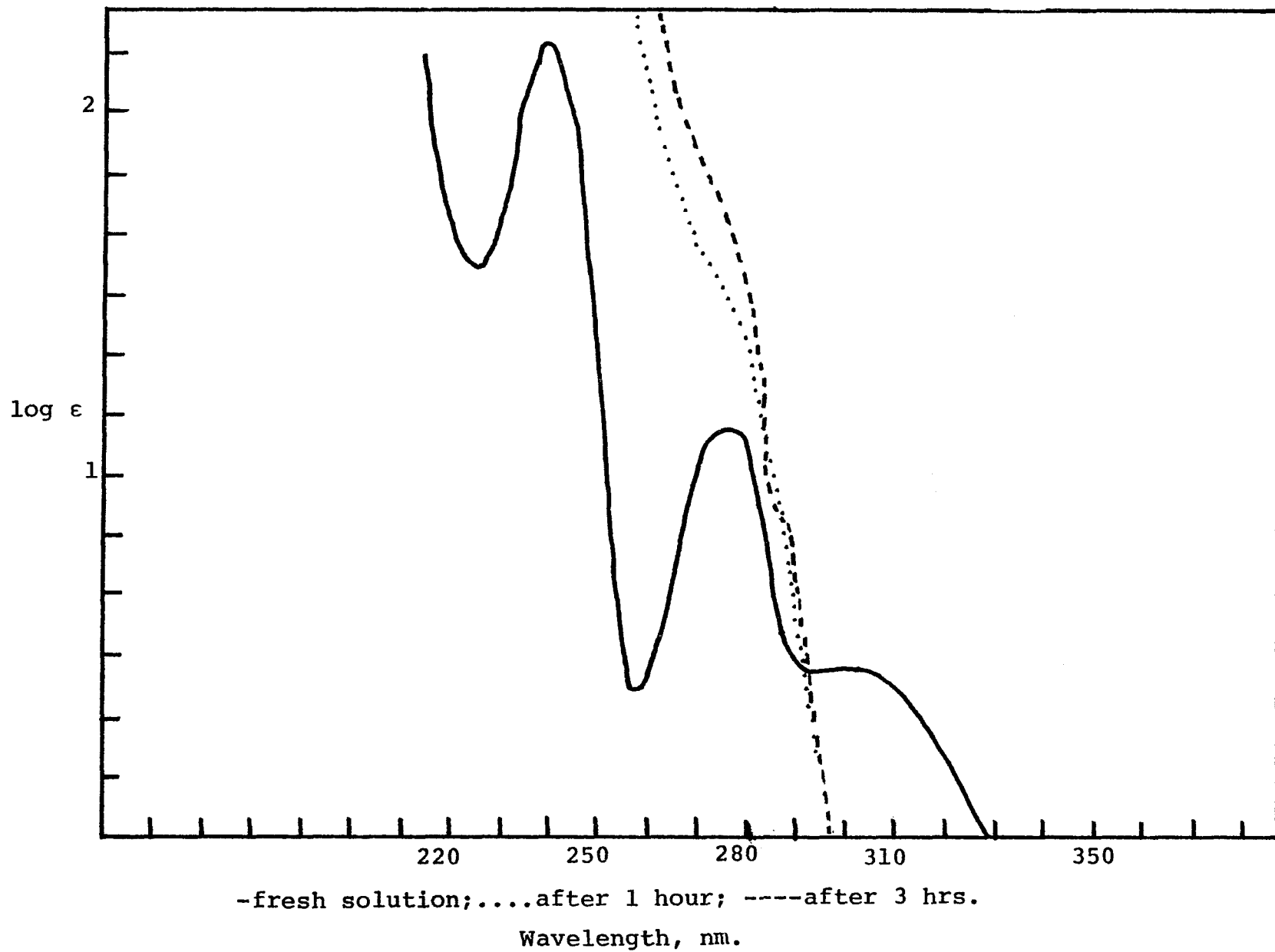
Energy Level Diagram for the Excited States of 2,2'-Bipyridine in Water.

In the flash photolysis of 2,2'-bipyridine and 4-Et<sub>3</sub>P<sup>+</sup>-bipyridine, the transient absorption observed corresponds to the transition from a triplet  $\pi, \pi^*$  state to the triplet  $n, \pi^*$  state. In the case of 4-NO<sub>2</sub> bipyridine in 20% EtOH, the  $^1(\pi, \pi^*)$  state is believed to be sufficiently lowered, such that all excited state reaction takes place from this state and hence is not affected by oxygen. However in a much less polar solvent like 95% EtOH, the  $^3(n, \pi^*)$  is lowered much more than  $^1(\pi, \pi^*)$ , and it is from this state that the reaction takes place and we see an effect of oxygen. Continuous photolysis experiments further confirm the fact that the reaction takes place from two different

excited state levels in the two solvents. Figure 21 and 22 clearly shows that the effect of white light on the spectra of 4-NO<sub>2</sub> bipyridine is substantially different in the two solvents although the spectra are very much the same before irradiation. We are led to believe that the products are different in the two solvents and it arises because of reaction from two different excited states.

Continuous photolysis experiments were also done with 2,2'-bipyridine and 4-Et<sub>3</sub>P<sup>+</sup> bipyridine, and the spectral changes obtained upon irradiation are shown in figure 23 and 24. We have not attempted to identify the products in these continuous photolysis experiments. However, from the nature of the spectral changes, it appears that the final product is probably pyridine N-oxide, as shown in figure 25.

Figure 21

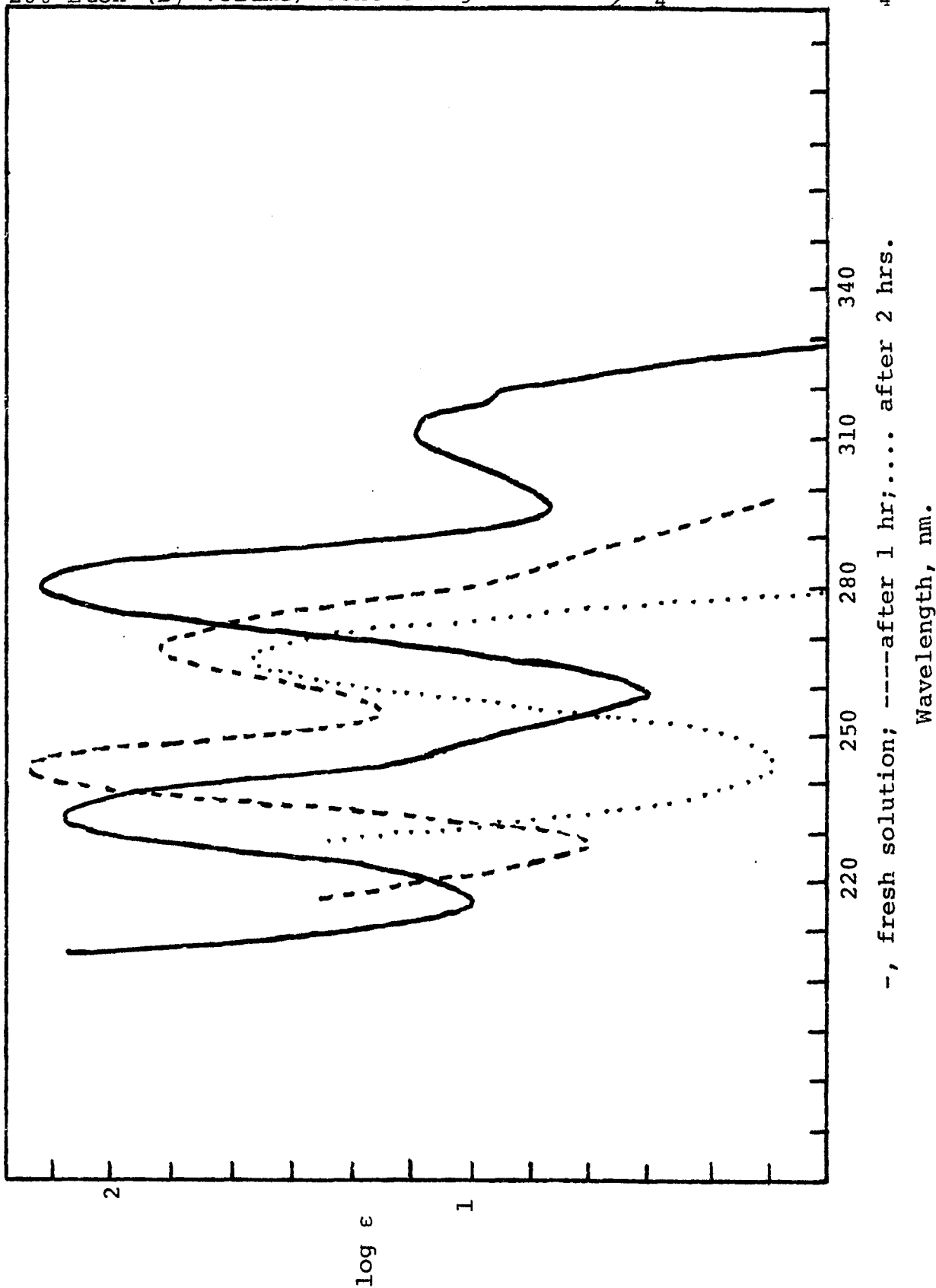


Spectral change in continuous photolysis of 4-NO<sub>2</sub>bpy in  
95% EtOH containing 1M Et<sub>4</sub>N<sup>+</sup>Cl<sup>-</sup>

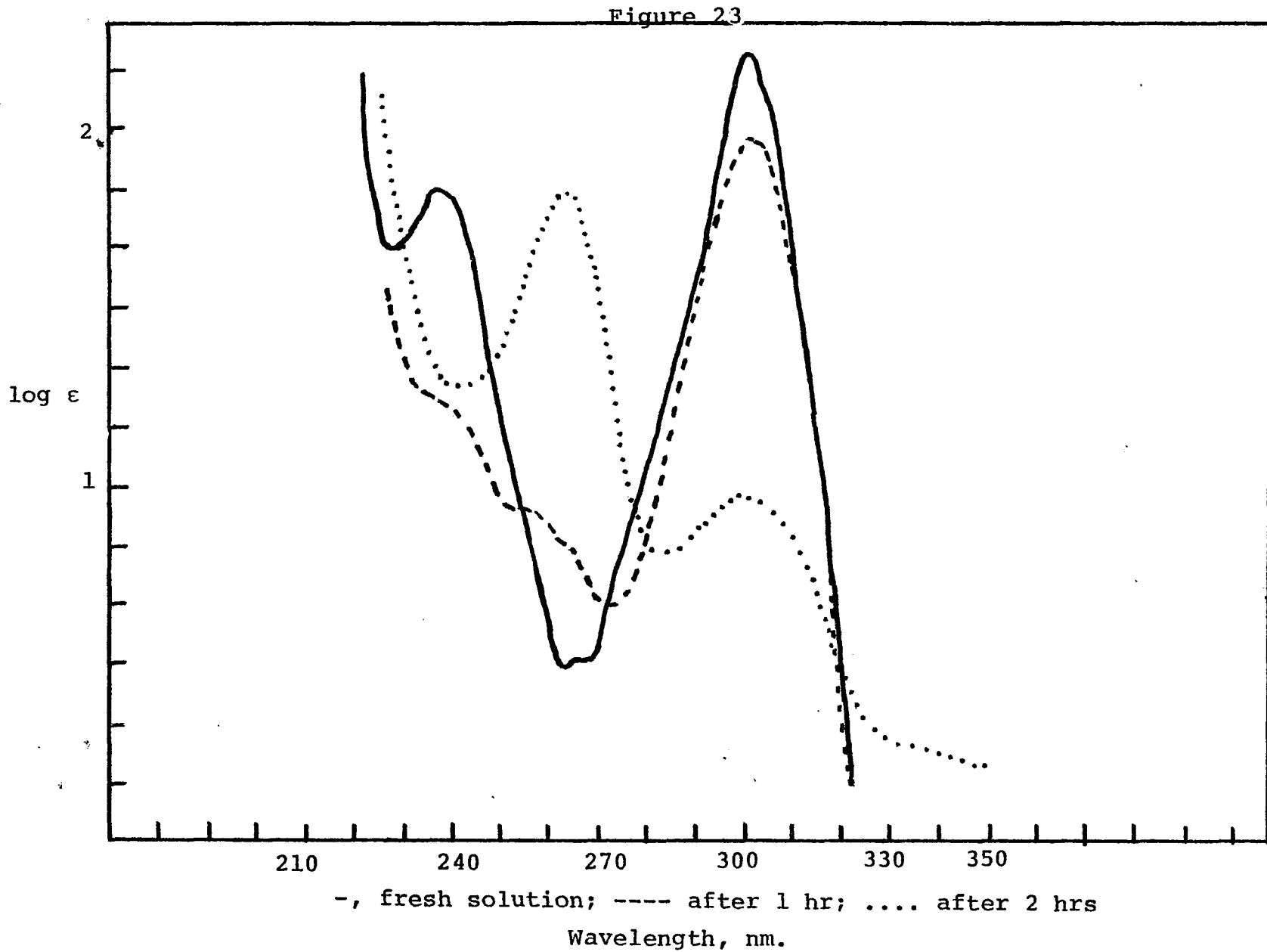
(99)

Spectral change in continuous photolysis of 4-NO<sub>2</sub>bpy in 20% EtOH (by volume) containing 0.33M Na<sub>2</sub>SO<sub>4</sub>/0.0275M NaHSO<sub>4</sub>

Figure 22



Spectral change in continuous photolysis of 2,2'-bipyridine  
in aqueous 0.33M Na<sub>2</sub>SO<sub>4</sub>/0.0275M NaHSO<sub>4</sub>



Spectral change in continuous photolysis of  $4Et_3P^+bpy$  in aqueous  $0.33M Na_2SO_4 / 0.0275M NaHSO_4$

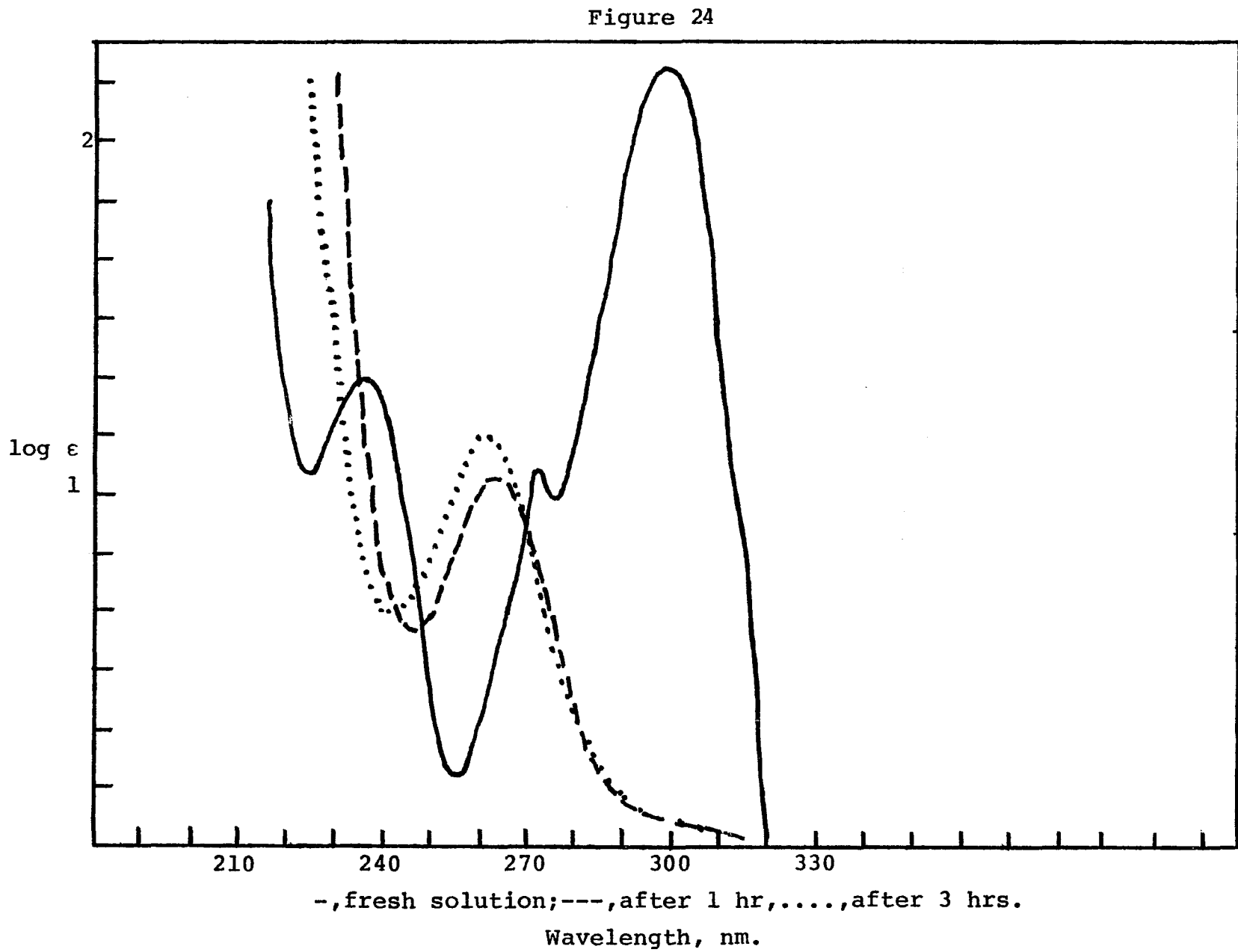
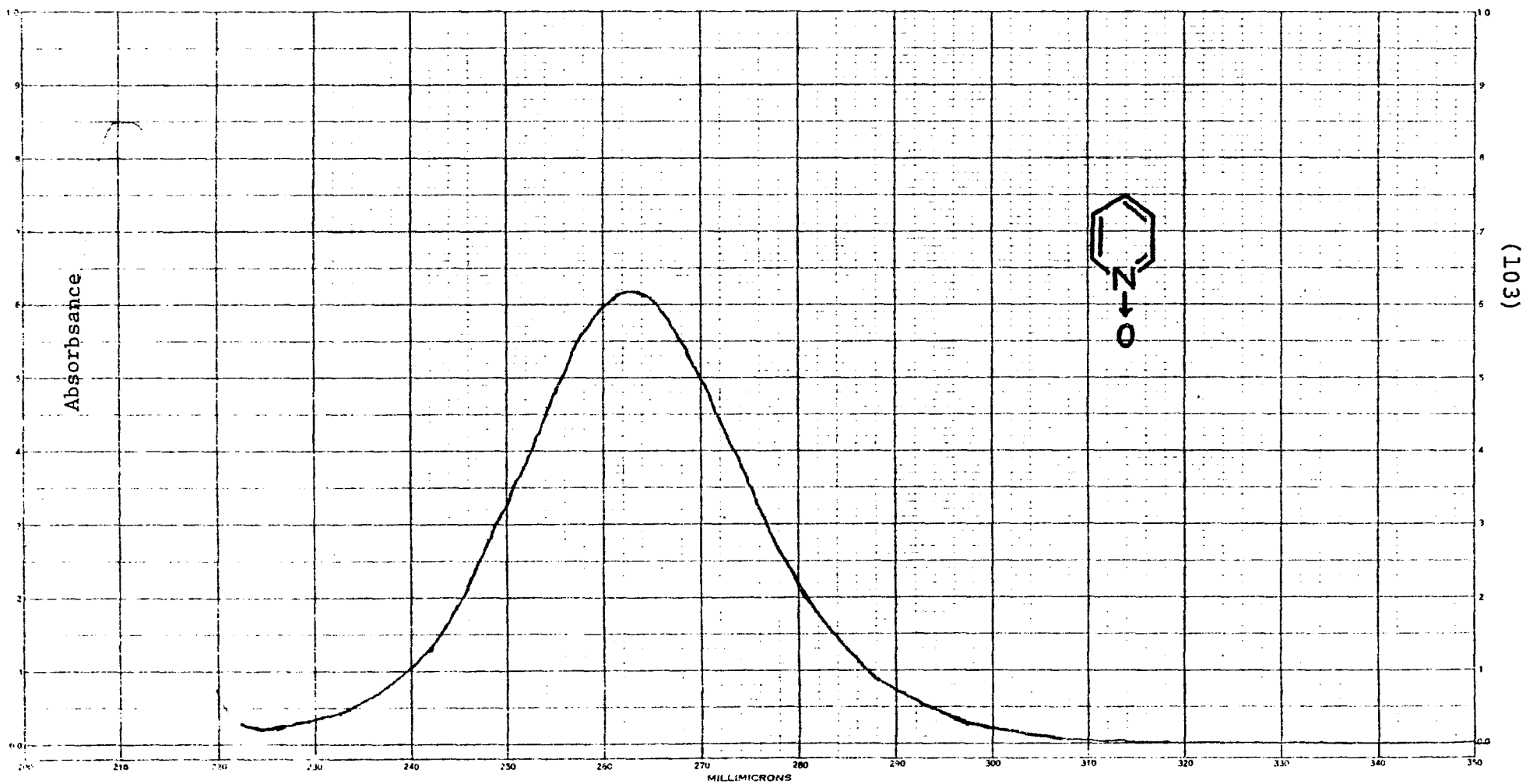


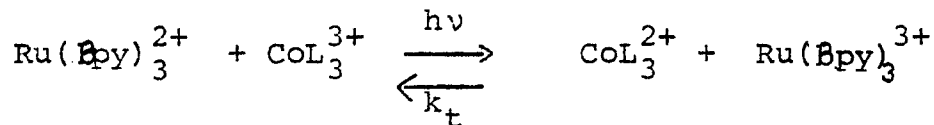
Figure 25

U.V. Spectrum of Pyridine N-oxide



Conclusion

Previous experiments in this laboratory have shown that quenching of  $\text{Ru}(\text{bpy})_3^{2+}$  by  $\text{CoL}_3^{3+}$ , where L denotes 2,2'-bipyridine or 1,10-phenanthroline, proceeds via an electron transfer mechanism



The experiments described above are an extension of these previous studies, in which the effect of strong electron withdrawing groups has been probed.

As described in part I of this thesis, both the absorption spectra and the redox potentials of the Ru(II) complexes are quite sensitive to the electron withdrawing substituents  $\text{NO}_2$  and  $\text{P}^+\text{Et}_3$  on the ligand periphery. These differences give rise to differences in the reaction driving force and, in a manner which reflects this variation in driving force, the rates of the electron transfer reactions. Variation of the driving force, however, is not necessarily indicative of the detailed path of electron transfer. Previous studies of the thermal redox chemistry, particularly that of the cobalt polypyridine complexes, have led to the suggestion of a transient intermediate in which the transferred electron resides in the ligand  $\pi^*$  system. A priori, strong electron withdrawing substituents might be expected to stabilize and increase the lifetime of this intermediate. Consequently, another aspect of these

experiments was to take advantage of the time resolution of the flash photolysis technique to determine if this intermediate could be detected in the photoredox chemistry of  $\text{Ru}(\text{Bpy})_3^{2+}$  and  $\text{Ru}(\text{Et}_3\text{P}^+ \text{Bpy})_3^{5+}$ .

Evidence for the stabilization of the  $\pi^*$  system of the free and complexed ligand was obtained from emission spectroscopy. Room temperature emission spectra of 2,2'-bipyridine,  $4\text{Et}_3\text{P}^+-2,2'$ -bipyridine, and  $4,4'$ -di $\text{Et}_3\text{P}^+-2,2'$ -bipyridine listed in Table X were obtained in 0.33M  $\text{Na}_2\text{SO}_4/0.0275\text{M NaHSO}_4$ . With each species, the emission was not quenched by oxygen and were attributed to fluorescence. The emission spectra of these free ligands at liq  $\text{N}_2$  temperature in 4:1 EtOH-MeOH glass are also listed in Table X and indicate that substitution by electron withdrawing  $\text{Et}_3\text{P}^+$  groups causes a lowering in energy of the singlet energy levels of the bipyridine system. Since the emission observed at 77°k is essentially identical to that observed at room temperature, the structured low temperature emission is assigned to a fluorescent emission. No phosphorescent emission was detectable at either temperature, but the shift of the triplet energy is expected to roughly parallel the red shift of the fluorescent emission. No emission is observed for 4- $\text{NO}_2$  bipyridine at room temperature or liq  $\text{N}_2$  temperature in 4:1 EtOH-MeOH glass. The room temperature emission spectra of the Ru(II) complexes of 2,2'-bipyridine and  $4\text{Et}_3\text{P}^+-2,2'$ -bipyridine taken in 0.33M  $\text{Na}_2\text{SO}_4/0.0275\text{M NaHSO}_4$  (fig. 8 and 9), indicate that the electron with-

drawing  $\text{Et}_3\text{P}^+$  group has the same effect of lowering the energy of the metal to ligand charge transfer state of the  $\pi$  complex as the  $\pi^*$  levels in the free ligands. A similar red shift was found in 4:1 EtOH-MeOH glasses at 77°k. Although a similar kind of emission was expected for the  $\text{Ru}(\text{NO}_2\text{Bpy})_3^{2+}$  complex, we were surprised to obtain a peculiar solvent dependence. The  $\text{Ru}(\text{NO}_2\text{Bpy})_3^{2+}$  did not exist at all at room temperature in 0.33M  $\text{Na}_2\text{SO}_4/0.0275\text{M NaHSO}_4$  and no emission was observed at 77°k in 4:1 EtOH-MeOH glass. A fresh solution of  $\text{Ru}(\text{NO}_2\text{Bpy})_3^{2+}$  in 95% EtOH (containing 1M  $\text{Et}_4\text{N}^+\text{Cl}^-$ ) was nonluminescent, but on storing the solution a new luminescence peak appears at 650 nm, and grows in intensity with time. This change in luminescence characteristics of  $\text{Ru}(\text{NO}_2\text{Bpy})_3^{2+}$  in this medium is accompanied by a corresponding change in its absorption spectra as shown in figures 11 and 12. This suggests that the new luminescence is derived from a different species. From the observed changes in the absorption spectra (vide infra) and the dependence on the EtOH content of the solvent, the new luminescent species is thought to be  $\text{Ru}(\text{OEt-Bpy})_3^{2+}$ .

In our attempt to investigate the effect of electron withdrawing substituents on the rates of electron transfer reactions, we studied the quenching of  $\text{Ru}(\text{Bpy})_3^{2+*}$  with 4- $\text{NO}_2$  bipyridine and 4- $\text{Et}_3\text{P}^+$  bipyridine. As indicated by the rate constants summarized in Table XI, the rate of quenching of  $\text{*Ru}(\text{Bpy})_3^{2+}$  by the free ligands increases with

drawing  $\text{Et}_3\text{P}^+$  group has the same effect of lowering the energy of the metal to ligand charge transfer state of the  $\pi^*$  complex as the  $\pi^*$  levels in the free ligands. A similar red shift was found in 4:1 EtOH-MeOH glasses at 77°k. Although a similar kind of emission was expected for the  $\text{Ru}(\text{NO}_2\text{Bpy})_3^{2+}$  complex, we were surprised to obtain a peculiar solvent dependence. The  $\text{Ru}(\text{NO}_2\text{Bpy})_3^{2+}$  did not exist at all at room temperature in 0.33M  $\text{Na}_2\text{SO}_4/0.0275\text{M NaHSO}_4$  and no emission was observed at 77°k in 4:1 EtOH-MeOH glass. A fresh solution of  $\text{Ru}(\text{NO}_2\text{Bpy})_3^{2+}$  in 95% EtOH (containing 1M  $\text{Et}_4\text{N}^+\text{Cl}^-$ ) was nonluminescent, but on storing the solution a new luminescence peak appears at 650 nm, and grows in intensity with time. This change in luminescence characteristics of  $\text{Ru}(\text{NO}_2\text{Bpy})_3^{2+}$  in this medium is accompanied by a corresponding change in its absorption spectra as shown in figures 11 and 12. This suggests that the new luminescence is derived from a different species. From the observed changes in the absorption spectra (vide infra) and the dependence on the EtOH content of the solvent, the new luminescent species is thought to be  $\text{Ru}(\text{OEt-Bpy})_3^{2+}$ .

In our attempt to investigate the effect of electron withdrawing substituents on the rates of electron transfer reactions, we studied the quenching of  $\text{Ru}(\text{Bpy})_3^{2+}$  with 4- $\text{NO}_2$  bipyridine and 4- $\text{Et}_3\text{P}^+$  bipyridine. As indicated by the rate constants summarized in Table XI, the rate of quenching of  $^*\text{Ru}(\text{Bpy})_3^{2+}$  by the free ligands increases with

increasing electron withdrawing constant of the substituent ( $\sigma^-$  for  $\text{Me}_3\text{P}^+ = 1.02$  and  $\sigma^-$  for  $\text{NO}_2 = 1.27$ ). This dependence of the quenching rate on the substituent and, in turn on the reduction potential of the free ligand, suggests that the quenching proceeds via an electron transfer mechanism, i.e.,



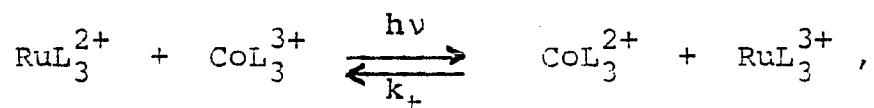
In order to study the rate of the reverse reaction, we carried out flash photolysis experiments on these systems monitoring the transient absorption at 675 nm corresponding to that of  $\text{Ru}(\text{bpy})_3^{3+}$ . But no transient could be seen at 675 nm indicating that the reverse reaction was too fast to observe. However, a transient absorption was observed around 500 nm whose origin was uncertain. In an attempt to investigate the origin of this transient, we carried out flash photolysis experiments on the free ligands by themselves.

Flash photolysis of 2,2'-bipyridine and  $4\text{Et}_3\text{P}^+-2,2'$ -bipyridine in 0.33M  $\text{Na}_2\text{SO}_4/0.0275\text{M NaHSO}_4$  yields transient absorbances at 350 and 375 nm respectively. Both absorbances are quenched by  $\text{O}_2$  and are attributed to triplet-triplet absorptions of the respective compounds. In the absence of  $\text{O}_2$ , the triplet-triplet absorbances of 2,2'-bipyridine and  $4\text{Et}_3\text{P}^+-2,2'$ -bipyridine decay via first order kinetics, with rate constants of  $22 \pm 5 \times 10^2 \text{ sec}^{-1}$  and  $23 \pm 2 \times 10^2 \text{ sec}^{-1}$  respectively.

Flash photolysis of 4-NO<sub>2</sub>-2,2'-bipyridine in a 20% EtOH-H<sub>2</sub>O mixture containing 0.33M Na<sub>2</sub>SO<sub>4</sub>/0.0275M NaHSO<sub>4</sub> yields transient absorption bands at 350 nm and 500 nm which decay by first order kinetics with  $k = 14.1 \pm 2 \times 10^2 \text{ sec}^{-1}$ . Since these transient absorbances are not affected by O<sub>2</sub> bubbling, they are attributed to the products of a photochemical reaction which originates in the first excited singlet state. In 95% EtOH containing 1M Et<sub>4</sub>N<sup>+</sup>Cl<sup>-</sup>, the flash photolytic behavior of 4-NO<sub>2</sub>-2,2'-bipyridine is considerably different. In this solvent, a single long lived transient with an absorption maximum at 450 nm is observed. This transient decays via a first order process with a rate constant of  $k = 66.7 \text{ sec}^{-1}$ . On saturation with O<sub>2</sub>, however, the decay rate increases to  $k = 13.8 \pm 0.7 \times 10^2 \text{ sec}^{-1}$ . This O<sub>2</sub> dependence suggests a reaction originating from a triplet level. The difference in flash photolysis results of 4-NO<sub>2</sub>-2,2'-bipyridine in 20% EtOH and 95% EtOH is thought to be due to a photochemical reaction taking place from different energy states; in 20% EtOH, the reaction originates in a singlet energy level while a triplet energy level is involved in 95% EtOH. This conclusion is supported by continuous photolysis experiments on 4-NO<sub>2</sub>-2,2'-bipyridine in the two different solvents. As indicated by figures 21 and 22, photolysis of the compound leads to different spectral changes. However, the spectral changes observed are the same when 2,2'-bipyridine, 4Et<sub>3</sub>P<sup>+</sup>-2,2'-bipyridine and 4-NO<sub>2</sub> 2,2'-bipyridine were photolyzed in

20% EtOH-H<sub>2</sub>O containing 0.33M Na<sub>2</sub>SO<sub>4</sub>/0.0275M NaHSO<sub>4</sub>. No attempt was made to characterize the products because of the relatively small amounts used in the experiments. The spectral features however, are similar to pyridine N-oxide and suggest this species as the final product.

In an extension of our work on the effect of strong electron withdrawing substituents, we carried out quenching and flash photolytic study of the reaction,



where L = bpy, 4-NO<sub>2</sub> bpy or 4ET<sub>3</sub>P<sup>+</sup>bpy.

When the electron withdrawing group is attached to the ligand of the photoreductant as in Ru(Et<sub>3</sub>P<sup>+</sup>Bpy)<sub>3</sub><sup>5+</sup>, the rate of electron transfer with Co(Bpy)<sub>3</sub><sup>3+</sup> decreased in an expected way from that of Ru(Bpy)<sub>3</sub><sup>2+</sup> and the rate of the back electron transfer went up as would be expected. However, contrary to our expectation, when the electron withdrawing substituent is on the oxidizing quencher as in Co(NO<sub>2</sub>Bpy)<sub>3</sub><sup>3+</sup>, the rate of quenching with Ru(Bpy)<sub>3</sub><sup>2+</sup> goes down from that of Co(Bpy)<sub>3</sub><sup>3+</sup>. This seems to indicate that the electron transfer is metal centered and is not taking place through the ligand π\* system of Co(NO<sub>2</sub>Bpy)<sub>3</sub><sup>3+</sup> which would have definitely caused an enhancement of rate.

References

- (1) Drew, H. D. K. J. Chem. Soc. 1932, 2328.
- (2) Villa, J. Inorg. Chem. 1973, 12, 2054.
- (3) Quagliano, J. V.; Summers, J. T.; Kida, S.; Vallarino L. M. Inorg. Chem. 1964, 3, 1557.
- (4) Goedken, V. L.; Vallarino, L. M.; Quagliano, J. V. Inorg. Chem. 1971, 10, 2682.
- (5) Koloday, R. A.; Morris, T. L.; Taylor, R. C. J. Chem. Soc. Dalton Trans. 1973, 328.
- (6) Dahloff, W. V.; Dick, T. E.; Nelson, S. M. I. Chem. Soc. A. 1969, 2919.
- (7) Weiner, M. A.; Schwartz, P. Inorg. Chem. 1975, 14, 1714.
- (8) Colton, F. A.; Wilkinson, G. "Advanced Inorganic Chemistry". 3rd Ed., John Wiley and Sons, New York, N.Y. 1972, Chapt. 22.
- (9) Lappert, M. F.; Pedley, T. B.; Wilkins, B. T.; Stelzer, O; Unger, E. J. Chem. Soc. Dalton. Trans. 1975, 1207.
- (10) Cotton, F. A.; Kraihanzel, C. S. Inorg. Chem. 1963, 2, 533.
- (11) Graham, W. A. G. Inorg. Chem. 1963, 7, 315.
- (12) Brown, T. L.; Darensbourg, D. J. Inorg. Chem. 1963, 7, 959.
- (13) Dennenberg, R. J.; Darensbourg, D. J. Inorg. Chem. 1972, 11, 72.
- (14) Keiter, R. L.; Shah, D. P. Inorg. Chem. 1972, 11, 191.
- (15) Taylor, R. C.; Keiter, R. L.; Cary, L. W. Inorg. Chem. 1974, 13, 1928.
- (16) Connor, J. A.; Day, J. P.; Jones, E. M.; McEwen, G. K. J. Chem. Soc. Dalton Trans. 1973, 347.
- (17) Jones, R. A.; Roney, B. D. J. Chem. Soc. B 1967, 106.
- (18) Maerker, G.; Case, F. H. J. Am. Chem. Soc. 1958, 80, 2745.

- (19) Ireland, J. F.; Wyatt, P. A. H. *Adv. Phys. Org. Chem.* 1976, 12, 131.
- (20) Hoffman, M. Z.; Henry, M. S. *J. Am. Chem. Soc.* 1977, 99, 5201.
- (21) Castellano, S.; Gunther, H.; Ebersole, S. J. *Phys. Chem.* 1965, 69, 4166.
- (22) Saji, T; Aoyagui, S. J. *Electroanal. Chem. Interfacial Electrochem.* 1975, 58, 401.
- (23) Anderson, C. P.; Salmon, D. J.; Young, R. C.; Meyer, T. J. *J. Am. Chem. Soc.* 1977, 99, 1980.
- (24) Dubois, D. W.; Iwamoto, R. T.; Kleinberg, J. *Inorg. Nucl. Chem. Lett.* 1970, 6, 53.
- (25) Reynolds, W. L. *Inorg. Chem.* 1966, 5, 931.
- (26) Reynolds, W. L.; Mohon, C. *Inorg. Chem.* 1967, 6, 1927.
- (27) Bryant, G. M.; Ferguson, J. E.; Powell, H. K. J. *Aust. J. Chem.* 1971, 24, 257.
- (28) Lytle, F. E.; Hercules, D. M. *J. Am. Chem. Soc.* 1969, 91, 253.
- (29) Meyer, T. J. *J. Am. Chem. Soc.* 1975, 97, 3039
- (30) Ferguson, J. E.; Harris, G. M. *J. Chem. Soc. A* 1966, 1293.
- (31) Bard, A. J.; Tokel-Takvoryan, N. E.; Hemingway, R. E. *J. Am. Chem. Soc.* 1973, 95, 6582.
- (32) Malouf, G.; Ford, P. C. *J. Am. Soc.* 1977, 99, 7213.
- (33) Figard, J. E.; Peterson, J. D. *Inorg. Chem.* 1978, 17, 1059.
- (34) Templeton, J. L. *J. Am. Chem. Soc.* 1979, 101 4906.
- (35) Ford, P. C.; Peterson, J. D.; Huitze, R. E. *Coord. Ch. Chem. Rev.* 1974 14, 67.
- (36) Bolt, R. W.; Dowden, B. F.; Eaborn, C. J. *Chem. Soc.* 1965, 4994.
- (37a) Taft, R. W.; Price, E.; Fox, I. R.; Lewis, I. C.; Anderson, K. K.; Davis, G. T. *J. Am. Chem. Soc.* 1963, 83, 709.

- (37b) Taft, R. W.; Price, E.; Fox, I. R.; Lewis, T. C.; Anderson, K. K.; Davis, G. T. J. Am. Chem. Soc. 1963, 85, 3146.
- (38) Johnson, A. V.; Jones, H. L. J. Am. Chem. Soc. 1968, 90, 5232.
- (39) Jaffe, H. H. Chem. Rev. 1953, 53, 191.
- (40) Schiemenz, G. P. Angiu, Chem. Int. Ed. Engl. 1966, 5, 129.
- (41) Tsvetkov, E. N.; Lobonov, D. I.; Kabochnik, M. I. J. Gen. Chem. U.S.S.R. 1972, 42, 761.
- (42a) Malouf, G.; Ford, P. C. J. Am. Chem. Soc. 1974, 96, 601.
- (42b) Malouf, G.; Ford, P. C. J. Am. Chem. Soc. 1977, 99, 7213.
- (43) Birks, J. B. "Photophysics of Aromatic Molecules" Wiley, Interscience, New York, N.Y. 1970.
- (44) Balzani, V.; Moggi, L.; Manfrin, M. F.; Bolletta, F.; Laurence, G. S. Coord. Chem. Rev. 1975, 15, 321 and references therein.
- (45) Demas, J. N.; Adamson, A. W. J. Am. Chem. Soc. 1971, 93, 1800.
- (46) Wrighton, M.; Markham, J. J. Phys. Chem. 1973, 77, 3042.
- (47) Binet, P. J.; Goldberg, E. L.; Forster, L. S. J. Phys. Chem. 1968, 72, 3017.
- (48) Balzani, V.; Sabbatini, N.; Seandola, M. A. J. Phys. Chem. 1974, 78, 541.
- (49) Balzani, V.; Laurence, G. S. Inorg. Chem. 1974, 13,
- (50) Bock, C. R.; Meyer, T. J.; Whitte, D. G. J. Am. Chem. Soc. 1974, 96, 4710.
- (51) Sutin, N.; Lin, C. T.; Bottcher, W.; Chen, M.; Creutz, C. J. Am. Chem. Soc. 1976, 98, 6536.
- (52) Lin, C. T.; Sutin, N. J. Phys. Chem. 1976, 80 97.
- (53) Porter, G. "Technique of Organic Chemistry". A. Weissberger, Ed., Interscience, New York, N.Y. 1963, Part II, Vol VIII, p. 1055.

- (54) Linschitz, H.; Sarkanen, K. J. Am. Chem. Soc. 1958  
80, 4826.
- (55) Sutin, N.; Navon, G. Inorg. Chem. 1974, 13, 2159.
- (56) Gafney, H. D.; Adamson, A. W. J. Am. Chem. Soc. 1972,  
94, 8238.
- (57) Demas, J. N.; Adamson, A. W. J. Am. Chem. Soc. 1973,  
95, 5159.
- (58) Sutin, N.; Lin, C. T. J. Am. Chem. Soc. 1975, 97,  
3543.
- (59) Sutin, N.; Creutz, C. Proc. Nat. Acad. Sci. U.S.A.  
1975, 72, 2858.
- (60a) Palmer, R. C.; Piper, T. S. Inorg. Chem. 1966, 5,  
864.
- (60b) Przystas, T. J.; Sutin, N. J. Am. Chem. Soc. 1973,  
95, 5545.
- (61) Kitson, E. Anal. Chem. 1950, 22, 664.
- (62) Crosby, G. A.; Hager, G. D. J. Am. Chem. Soc.  
1975, 97, 7031.
- (63) Harrigan, R. W.; Hager, G. D.; Crosby, G. A. Chem.  
Phys. Lett. 1973, 21, 487.
- (64) Balzani, V.; Carassiti, V. "Photochemistry of  
Coordination Compounds". Academic Press, N.Y. 1970.
- (65) Mayer, T. J.; Kenne, F. R.; Young, R. C. J. Am.  
Chem. Soc. 1977, 99, 2468.
- (66) Mayer, T. J. Bock, C. R.; Connor, J. A.; Gutierrez,  
A. R.; Whitten, D. G.; Sullivan, B. P.; Nagle, J. K.  
J. Am. Chem. Soc. 1979, 101, 4815.
- (67) Harriman, A. J. Photochem. 1978, 8, 205.